AN EXAMINATION OF POSSIBLE REVERSIBLE COMBUSTION AT HIGH TEMPERATURES AND PRESSURES FOR A RECIPROCATING ENGINE

A Thesis

by

KAUSHIK TANVIR PATRAWALA

Submitted to the Office of Graduate Studies of
Texas A&M University
in partial fulfillment of the requirements for the degree of

MASTER OF SCIENCE

May 2007

Major Subject: Mechanical Engineering

AN EXAMINATION OF POSSIBLE REVERSIBLE COMBUSTION AT HIGH TEMPERATURES AND PRESSURES FOR A RECIPROCATING ENGINE

A Thesis

by

KAUSHIK TANVIR PATRAWALA

Submitted to the Office of Graduate Studies of
Texas A&M University
in partial fulfillment of the requirements for the degree of

MASTER OF SCIENCE

Approved by:

Chair of Committee,	Jerald A. Caton
Committee Members,	Nagamangala K. Anand
	Jorge L. Alvarado
Head of Department,	Dennis O'Neal

May 2007

Major Subject: Mechanical Engineering

ABSTRACT

An Examination of Possible Reversible Combustion at High Temperatures and Pressures for a Reciprocating Engine. (May 2007)

Kaushik Tanvir Patrawala, Dipl., Shri Bhagubhai Mafatlal Polyte, India; B.E., University of Bombay (Mumbai), India

Chair of Advisory Committee: Dr. Jerald A. Caton

Conventional combustion processes are known to be highly irreversible processes. The potential to obtain useful work from the fuel is degraded during the combustion process. For example, for a reciprocating internal combustion engine, about 20% or more of the potential work from the fuel is destroyed during the combustion process. This potential work is known as availability (a thermodynamic property). The motivation for the current work was to develop a conceptual model of a set of processes related to reciprocating engines that would eliminate this destruction of availability. One conceptual model, proposed by Keenan, suggested that a preselected set of "reactants" could be compressed (at constant composition) to a high temperature and pressure. At this high temperature and pressure, the "reactants" would be in chemical equilibrium. At this point, the "reactants" would be expanded back to the original volume. The expansion process would consist of a "shifting" chemical equilibrium such that the composition during expansion would continue to change. At the end of the compression and expansion, net work would be available without destroying any of the work potential of the fuel. The purpose of the current work was to develop a quantitative model of this concept, and to use the model in a series of computations to examine the effects of temperature, pressure, and other parameters on the work production capability of the concept.

The concept was studied for eight different fuels for various conditions. In general, the net work output increased as the temperature, pressure and compression ratio increased. For low compression temperatures and pressures, the concept resulted in a small amount of net work produced without destroying any fuel availability. For sufficiently high compression pressure and temperature (e.g., 10 MPa and 6000 K, respectively), however, the thermal efficiency was ~28% for isooctane and was ~40% for hydrogen and methane, for air as the oxidant, an equivalence ratio of 1.0, and a compression ratio of 18. Although the temperatures and pressures considered are well beyond practical values for the materials and designs of today, the general result of the study is that conditions can be identified to eliminate the combustion irreversibility.

DEDICATION

To my parents, Tanvir R. Patrawala and Anju T. Patrawala

ACKNOWLEDGEMENTS

I offer my profound gratitude to my committee chair, Dr. Jerald Caton for giving me this opportunity to work under his guidance in a professional environment. I sincerely thank him for the confidence shown in me and helping from time to time. At times when things seemed to be impossible, he motivated me and guided me towards new directions. He is responsible for sharpening my thinking process and honing my reasoning ability. His time and effort has resulted in the successful completion of my thesis.

I am deeply grateful to Dr. N. K. Anand for readily agreeing to be an active member of my committee, out of his busy work schedule. He is responsible for a smooth start of my career at Texas A&M. I would like to thank him for his invaluable guidance.

I would also like to express my sincere thanks to Dr. Jorge Alvarado for his cooperation, support and his ever helping hand.

My innermost gratitude goes to my family members for their patience, love and encouragement that they have shown over the years of my student life, without which, I would not have been able to accomplish my educational goals.

This work was supported in part by the U. S. Department of Energy through the National Energy Technology Laboratory (NETL), Morgantown, WV. The contents of this paper, however, do not necessarily reflect the opinions or views of the sponsors.

TABLE OF CONTENTS

Page

LIST OF FIGURES

FIGURE Page

FIGURE Page

FIGURE Page

FIGURE Page

FIGURE Page

FIGURE Page

FIGURE Page

FIGURE Page

NOMENCLATURE

A_{total}	Total availability of system
$A_{thermo-mech}$	Thermo-mechanical availability of system
A_{chem}	Chemical availability
A_{abs}	Absolute availability
A	Availability
U	Internal energy of system
T	Temperature
S	Entropy of system
P	Pressure
V	Volume
A_{react}	Reactive availability of mixture
A_{diff}	Diffusion availability
n	Number of moles
ΔG	Change in Gibbs energy associated with a reaction
$\bar{R}$	Universal gas constant
$A_{destroyed}$	Availability destroyed
A_{start}	Availability of a system at beginning of a process
A_{end}	Availability of a system at end of a process
A_{heat}	Availability due to heat transfer
A_{work}	Availability due to work transfer
r_{DAC}	Percentage availability destroyed
W_u	Useful work developed by system
$A_{initial}$	Initial availability of mixture
A_{final}	Final availability of mixture
$(F:A)$	Stoichiometric fuel air ratio
M	Molecular weight
$(F:A)_{actual}$	Actual fuel air ratio

H	Enthalpy of system
a_1	Coefficient 1 for least square polynomial fit for determining thermodynamic properties
a_2	Coefficient 2 for least square polynomial fit for determining thermodynamic properties
a_3	Coefficient 3 for least square polynomial fit for determining thermodynamic properties
a_4	Coefficient 4 for least square polynomial fit for determining thermodynamic properties
a_5	Coefficient 5 for least square polynomial fit for determining thermodynamic properties
a_6	Coefficient 6 for least square polynomial fit for determining thermodynamic properties
a_7	Coefficient 7 for least square polynomial fit for determining thermodynamic properties
b_1	Coefficient 8 for least square polynomial fit for determining thermodynamic properties
b_2	Coefficient 9 for least square polynomial fit for determining thermodynamic properties
$\bar{h}_i$	Enthalpy of species k
$\bar{u}_i$	Internal energy of species k
x_i	Mole fraction of species k
$W_{\max}$	Maximum work developed by system
E	Energy of system
N	Number of reservoirs
Q	Heat transfer across system boundary
W	Work transfer across system boundary
I	Irreversibility of system
LHV_{fuel}	Lower heating value of fuel
ΔH	Change in enthalpy
h_f	Change in enthalpy of formation associated with a reaction

Greek symbols

ϕ	Equivalence ratio
η	Efficiency of system

Superscripts

0	Restricted dead state conditions
k	Average ratio of specific heats

Subscripts

0	Reference (atmospheric) conditions
i	Species index
o	Oxidant
f	Fuel
cv	Control volume of system
R	Reservoir
j	Reservoir index

I. INTRODUCTION

To extract energy from fossil fuels, combustion processes are employed. Combustion processes are basically made up of complex chemical reactions which occur when fossil fuel and oxidants are mixed. The outcome of the reactions can be release or absorption of energy. If the energy is released, it is used for further processes, as in internal combustion engines. The amount of energy released/absorbed depends upon the conditions in which the combustion reaction is conducted.

The combustion process finds wide range of applications in many practical devices and industrial systems such as gas turbines (in aircraft engines), internal combustion engines (diesel and spark ignition engines) and other industrial process. This method of obtaining energy is used by almost every person, directly or indirectly, in his/her everyday life. One of the reasons for such heavy dependence on fossil fuels for extraction of energy is due to the availability of adequate internal combustion engine technology that helps easy use of this energy. However, because of the depleting fossil fuel reserves, the price of the fossil fuels is increasing. This calls for the effective use of the fossil fuel and the efficient design of the internal combustion engines that use the fossil fuel.

Combustion processes are highly irreversible. The potential to obtain useful work, at the end of the combustion of the fossil fuel, is always less than the input fuel energy. This loss of work potential is the result of the irreversibilities accompanied with the combustion process [1]. In some cases, like that of a reciprocating internal combustion engine, the potential work losses due to combustion are as high as 25%. The motivation for the current work is to develop a conceptual model of a set of processes related to reciprocating engines that would eliminate this loss of work potential and to use the model in a series of computations to examine the effects of temperature, pressure, equivalence ratio and other parameters on the work production capability of the conceptual model.

Energy

Energy may be considered to have different qualities or grades. An example of high grade energy is mechanical work and that of low grade energy is thermal energy. Most of the high grade energy (in the form of mechanical work) is obtained from fuels, through the use of heat engines. The complete conversion of energy into work is impossible according to the second law of thermodynamics. That part of the energy which can be converted into work is referred to as availability (or exergy).

This thesis follows the style and format of Energy.

Dead State

If the state of a system is different to that of its surroundings, there exists an opportunity for producing work [2, 3]. However, when the system undergoes changes to reach its surroundings, this opportunity (for producing work) diminishes, and it ceases to exist when the two are in equilibrium with each other. When the system is in equilibrium with its surroundings, it must be at the same pressure and temperature as that of its surroundings. It must also have the same chemical composition as that of its surroundings, i.e., there should not be any potential chemical reaction or mass transfer between the system and its surroundings. This state of the system is called the *dead state*. If the system is in temperature and pressure equilibrium, but not in chemical equilibrium with its surroundings, then this state of the system is known as the *restricted dead state*. The restricted dead state is usually taken as that of the atmosphere at a temperature of 298.15 K and a pressure of 1.01325 bar [4], however the composition may not be the same as that of the atmosphere.

Availability

Whenever useful work is obtained during a process in which a finite system undergoes a change of a state, the process terminates when the system has reached the dead state [2, 3]. For example, an air engine operating with compressed air taken from the cylinder will continue to deliver work till the pressure of the air in the cylinder becomes equal to that of its surroundings. The heat released during an exothermic combustion process, used as the high temperature source of the heat engine, will deliver work until the temperature of the source becomes equal to that of the surroundings.

The availability of a given system is defined as the maximum useful work that is obtainable in a process in which the system comes to equilibrium with its surroundings. Availability is thus a composite property depending on the state of both, the system and its surroundings. It is a direct consequence of the second law of thermodynamics [3-6]. It should be well understood that terms total energy and availability are different, the latter being the subset of the former. No system can perform work greater than its availability without violation of the second law.

The total availability of a system consists of two major components,

$$A_{total} = A_{thermo-mech} + A_{chem} \tag{1.1}$$

where $A_{thermo-mech}$ is the thermo-mechanical availability and A_{chem} is the chemical availability. $A_{thermo-mech}$ is due to the pressure and temperature of the system. It can be further split into,

$$A_{thermo-mech} = A_{abs} - A^0 \tag{1.2}$$

where A_{abs} is the absolute availability and A^0 is the availability of the restricted dead state. The absolute availability of the system accounts for the total amount of energy available when the system undergoes thermo-mechanical equilibrium from the existing state to the zero datum. However, no system reaches zero datum, and can only reach the state of the surroundings, so it is necessary to define the availability of the dead state. Mathematically, absolute and dead state availability are defined as,

$$A_{abs} = U - T_0 \cdot S + P_0 \cdot V \tag{1.3}$$

$$A^0 = U^0 - T_0 \cdot S^0 + P_0 \cdot V^0 \tag{1.4}$$

The equations (1.3) and (1.4) are applicable to the closed system only. Availability for the open system can be found elsewhere [7]. In this study only closed volume systems will be examined.

The chemical availability of the system can be further split into,

$$A_{chem} = A_{react} + A_{diff} \tag{1.5}$$

where A_{react} is the reactive availability and A_{diff} is the diffusive availability. The reactive availability accounts for the availability that can be extracted when all the species of the system are converted to that of the surroundings through chemical reactions. The diffusive availability consists of the availability that is due to conversion of partial pressure of the species in the system to that of the species in surroundings. The reactive availability and the diffusive availability in general give the chemical potential of the system.

$$A_{react} = \sum_{i=1}^{n} n_i \cdot \left(\Delta G_i^0\right) \tag{1.6}$$

$$A_{diff} = \sum_{i=1}^{n} n_i \cdot \bar{R} \cdot T \cdot \ln\left(\frac{P_i}{P_{i,o}}\right) \tag{1.7}$$

where ΔG_i^0 is value of change in Gibbs free energy. These values are available in appendix IV. Some of the values were taken from [8] while others were calculated using [9]. P_i is the partial pressure of the i^{th} specie and $P_{i,o}$ is the partial pressure of the i^{th} specie at reference conditions.

$$P_i = n_i \cdot P \tag{1.8}$$

$$P_{i,o} = n_i \cdot P_0 \tag{1.9}$$

Thus the total availability of the closed system is given by,

$$A_{total} = A_{abs} - A^0 + A_{react} + A_{diff} \tag{1.10}$$

$$A_{total} = \left(U - U^0\right) - T_0\left(S - S^0\right) + P_0\left(V - V^0\right) + \sum_{i=1}^{n} n_i \cdot \left(\Delta G_i^0\right) + \sum_{i=1}^{n} n_i \cdot \bar{R} \cdot T \cdot \ln\left(\frac{P_i}{P_{i,o}}\right) \tag{1.11}$$

In some previous work, the chemical availability term has been neglected. As shown by Chavannavar [8], the contribution of this term may be significant, and so for better accuracy, it is included in this study.

The availability destroyed and the percentage destruction of availability can be calculated as,

$$A_{destroyed} = A_{start} - A_{end} + A_{heat} + A_{work} \tag{1.12}$$

$$r_{DAC} = \left(\frac{A_{start} - A_{end} + A_{heat} + A_{work}}{A_{start}}\right) \times 100 \tag{1.13}$$

where A_{start} is the initial availability of the system, A_{end} is the availability of the system at the end of a process, A_{heat} is the availability due to heat transfer in or out of the system, A_{work} is the availability due to work developed or consumed by the system, $A_{destroyed}$ is the availability destroyed due to any process in the system and r_{DAC} is the percentage availability destroyed [4].

The availability analysis helps us to understand the upper limit of efficiency of the system. It also helps in designing new thermal systems, reducing inefficiency of existing systems and improving overall system economics.

Objective

The objective of this study was to develop a model for hypothetical combustion processes which eliminate the irreversibility of the combustion process and allow maximum utilization of the fuel. To achieve the objective, a model was developed, which was designed to work in such a way that the availability destruction was completely eliminated from the combustion process. The model was then used for a range of thermodynamic conditions.

II. LITERATURE REVIEW

Previous Work

Significant work has been done based on the second law with the goals of understanding the thermodynamic irreversibility in the combustion process. Many years ago, one such work was done by Keenan [10]. In his literature, he proposed the concept of reversible combustion process. He stated that, when the temperature of the reactant mixture is increased, the equilibrium shifts and so the tendency of the reactants to react diminishes. At very high temperature, a state can be achieved where the reactants remain in equilibrium state without formation of products and hence there is practically no irreversible combustion reaction.

The concept by Keenan [10] was further extended by Obert [11, 12]. He stated that equilibrium conditions at very high temperature can be achieved by compressing the reactant mixture isentropically. The compression is to be completed in such a way that the reactant species are not allowed to react. When the equilibrium state is reached, the mixture is expanded slowly and isentropically, allowing the mixture molecules to react and form products. These sequences of processes of chemical reactions were referred by him as reversible.

With respect to applications, a number of studies have been completed using the second law of thermodynamics to analyze internal combustion engines. Caton [13] provides a review of past studies which used the second law to investigate internal combustion engines. He commented on some major findings that were published earlier and provided quantitative insight. He also included a brief review of the general characteristics of availability, and the destruction of availability because of heat transfer and combustion processes. The work by Caton showed that, in general, the percentage destruction in availability reduced monotonically as the combustion temperatures increased.

Dunbar and Lior [1] studied the basic combustion process by dividing it into several, small hypothetical processes. The study was conducted for hydrogen (H_2) and methane (CH_4) as fuels and atmospheric air as oxidant. Various hypothetical models were developed. Each model was divided into small chambers to precisely understand the nature of the combustion process proceeding at each step. The combustion process was conducted adiabatically and at constant pressure. Further, the combustion process was separated into: a diffusion process, a chemical reaction, an internal energy transfer process and a mixing process.

The work by Dunbar and Lior quantifies the entire entropy generation process and estimates the entropy contributed by each sub-process listed above. Simplifications were made in the study to get useful and important results without the use of complex mathematical analysis.

Dunbar and Lior concluded that, in general, for a combustion process, the major contribution of the availability destruction is from the internal thermal energy transfer between the molecules of the mixture. They also concluded that availability destruction can be reduced by conducting the combustion reaction at high temperatures, which may not be practical with presently available materials technology.

Lutz et al. [14] have conducted an analysis to compare the efficiency of a Carnot engine and a fuel cell both operating at the same conditions. By deriving the expressions, they showed that the efficiency of the Carnot engine is the same as that of the fuel cell when the Carnot engine is driven by the same combustion reaction as that of the fuel cell. They illustrated their concept using numerical examples for hydrogen and methane.

The work completed by Lutz et al. is based on an assumption that enthalpy and entropy changes are not dependent upon the temperature. This assumption, however, was proved to be reasonable by evaluating hydrogen-oxygen reaction. The work also proposed the fact that for chemical reactions involving positive entropy change, the maximum fuel cell efficiency is 100% and not more when proper heat transfer was taken into consideration.

The work by Lutz et al. also clearly explains the difference between the *adiabatic flame temperature* and the *combustion temperature*. They defined the combustion temperature as the temperature at which the reaction becomes “reversible”, i.e. the reaction can proceed in either direction. In their work, they have evaluated combustion and adiabatic temperatures along with fuel cell efficiencies for common fuels like hydrogen, methane and methanol.

To further improve the understanding about irreversibility from combustion, a study was conducted by Daw et al. [15]. They considered the equilibrium dissociation of the reaction products at high temperatures, in contrast to the complete products considered by Lutz et al. [14]. They introduced a hypothetical counter-flow preheating process for constant pressure combustion considering the products in equilibrium.

Daw et al. [15] concluded that by using such an advanced hypothetical isobaric combustion process which involved preheating of fuel and air, it should be possible to reduce irreversibility in the combustion process to some extent. The reduction in irreversibility was observed due to combustion taking place near chemical equilibrium as a result of which the temperature gradients were small and so the irreversibility due to thermal energy exchange was less. However, the irreversibility due to mixing process cannot be eliminated by this approach.

Richter and Knoche [16] also worked on ways to conduct chemical reactions reversibly. They pointed out that entropy production due to irreversibility can be reduced if the chemical reaction is conducted at very high temperature so that the chemical reaction is near thermal equilibrium. They noted, however, that the present material technology is not sufficient to sustain

these high temperatures. They therefore proposed another innovative way of reducing thermodynamic irreversibility.

Richter and Knoche found that if the combustion process is conducted such that the direct contact of the fuel and oxidant is prevented and instead intermediate chemical reactions are employed, then the availability destruction will be lower and consequently more work can be extracted from a work producing device. They selected metal oxides to conduct these intermediate low temperature endothermic reactions with the fuel. This concept was demonstrated analytically, and its actual practical application needs to be examined.

Work completed by Caton [4] provides useful insight about the destruction of availability when the combustion process occurs adiabatically in a closed volume. He examined the effects of temperature, pressure and equivalence ratio on availability considering frozen and equilibrium products of combustion. He concluded that at higher temperatures (above 2000 K), the effect of dissociation is significant and so availability is higher for products in equilibrium than when frozen. Also, as the combustion temperature increased, destruction of availability decreased, but never reached zero even for unrealistic temperatures of about 6000 K.

For rich mixtures, Caton concluded that due to higher chemical energy, availability is higher; which further increased with temperature. With reasonable assumptions, his work can be directly applied to internal combustion engines.

Another study was completed by Chavannavar [8] to approach reversible combustion. He extended the analysis done by Lutz et al. [14] by considering dissociation of species at high temperature and products in equilibrium as against complete product analysis done earlier [14]. The combustion process was restricted to isobaric, constant temperature conditions. The combustion temperature was found for as many as eight fuels, where change in Gibbs free energy is zero.

Chavannavar concluded that conducting combustion process near the combustion temperature can reduce the irreversibility to some extent as the transition from reactant mixture to equilibrium products is easier, both being similar in nature. However, irreversibility in combustion process due to irreversible mixing processes still exists.

Hassanzadeh and Mansouri [17] compared and contrasted their work with the work completed by Lutz et al. [14]. They stated that although the efficiencies of combustion engine and fuel cell are limited by the second law of thermodynamics, the maximum thermal efficiencies of the two systems are different. This difference is due to the involvement of irreversibility of combustion processes in the combustion engine. They commented that the use of a combustor reactor, as suggested by [14], in place of the high temperature heat reservoir, in the heat engine, is inappropriate as the combustion reactor is associated with irreversible chemical reactions.

They also proposed that for accurate results, chemical equilibrium criteria should be used as against complete products for the process that involve chemical reactions as done by Lutz et al.

Motivations

As described above, several availability analyses using the second law were completed in the past few decades with the goals to reduce the generation of entropy and to improve the availability from the combustion process. Some of the analyses were general in nature while some were applicable to internal combustion engines. Some were for constant volume conditions and constant pressure conditions, while others were for constant temperature conditions. For all the analyses, one common problem was addressed: reducing the irreversibility of the combustion processes.

Combustion processes are found to be inherently irreversible in nature. The irreversibility present in combustion is due to: thermal energy transfer, diffusion and mixing processes between the particles of mixture [1]. This irreversibility can be reduced by using proper strategies developed by the various authors [1, 4, 13-17]. However, no such strategy, or condition that is reported, that can completely eliminate irreversibility. Hence, the question of completely reversible combustion needs to be answered.

The current study is directed towards achieving the combustion process with zero destruction in availability. The study aims at developing a model consisting of hypothetical processes that can preheat the reactants to the equilibrium temperatures and pressures, without internal mixing of the molecules of the reactant mixture. Once this state is achieved, the reactant mixture is brought to the original state, by reversing the process direction to follow the most stable path of equilibrium. This leads to the development of work from the fuel energy, without availability loss and hence, this theoretical model can be termed as “reversible combustion”.

This concept of reversible combustion was evolved a few decades back and its literature can be found elsewhere [10, 11]. Here, the aim is to quantify this information and expand the concept into a model consisting of hypothetical processes, using reasonable approximations.

Preview of Remaining Sections

The following sections of this thesis outline the development of the model of hypothetical processes, the results obtained from the analyses of the model and the discussions and comparisons thereof.

Section III, Description of Model, deals with the development of the model to attain reversible combustion by making use of the concept proposed by Keenan [10] and Obert [11, 12].

Section IV, Implications to Reciprocating Engine, describes why and how the developed model is related to a reciprocating internal combustion engine.

Next, section V, Development of the Computer Program, describes the computer program that was developed to represent the model of hypothetical processes. It also outlines the equations used to calculate thermodynamic properties and lists the reasonable assumptions made in development of the code.

Section VI, Results and Discussion, presents the results of the parametric study. Work output and efficiency are provided as functions of operating parameters. The parameters include as fuel, oxidant, temperature, pressure, equivalence ratio and compression ratio.

Finally, section VII, Summary and Conclusion, summarizes the work reported on this reversible combustion concept, and provides conclusions.

III. DESCRIPTION OF MODEL

Concept

An early reference to the concept of reversible combustion is stated by Keenan [10]. He mentioned that a system has the ability to do work if it is not in thermodynamic equilibrium with the surroundings. However, when the system is brought to thermodynamic equilibrium with the surroundings, the work gained due to this process is always less than the maximum possible. He represented this by means of a simple equation.

$$W_u = A_{initial} - A_{final} \tag{3.1}$$

where, W represents the useful work, A represents availability and the subscripts u, $initial$, $final$ stand for terms: useful, initial and final respectively.

Loss of work is due to the inherent irreversibilities in any process that involves conversion of energy to useful work. Losses are also seen in the combustion process. Moreover, reasons for these losses [1] in combustion processes are due to thermal energy exchange between the species, diffusion and irreversible mixing of particles. To avoid any losses due to the reasons mentioned above, the reactant mixture needs to be brought to a state, which is required for the extraction of the energy, without any reactions between the reactants. Once this state is achieved, the mixture can be brought back to the state of the surroundings by means effecting work developing/consuming device and a heat exchanger that follows the path of most stable states [10].

The above concept was further explored by Obert [11]. He commented that without regard for the Carnot process, the combustion engine can deliver the maximum amount of work if all of the processes, including the combustion process, are conducted reversibly. For reversible combustion to take place, he stated that, initially the reactant mixture should be compressed isentropically to high temperatures till the point where the constituents are in equilibrium with each other, so no products are formed. The compression should be done in such a way that either it is too swift so that reaction between reactant particles is avoided or it may be assumed that some type of “negative” catalyst is present that prohibits such reactions. After the required state of equilibrium is reached, the mixture can be expanded slowly and isentropically. During expansion, the pressure and the temperature decrease, and the species are allowed to equilibrate themselves, resulting in more number of species which creates more

opportunities to extract work. In these constant entropy processes, the chemical reaction can be said to occur reversibly.

Current Model

The current study aims at using the above mentioned concept to develop a model of hypothetical processes that works in accordance to the concept suggested by Keenan [10] and Obert [11,12]. Again, this concept requires that the reactants be brought to a required higher temperature where they are in stable form, without reacting internally to reach the state. Even when preheating is used to increase the temperature of reactants, reactions among the reactant species are bound to occur. As mentioned above, a “negative” catalyst may be used to avoid these reactions among the reactant species. The current study is directed towards quantifying the results for such a process. The model of the hypothetical processes developed for this concept, is described in the next few lines of this section.

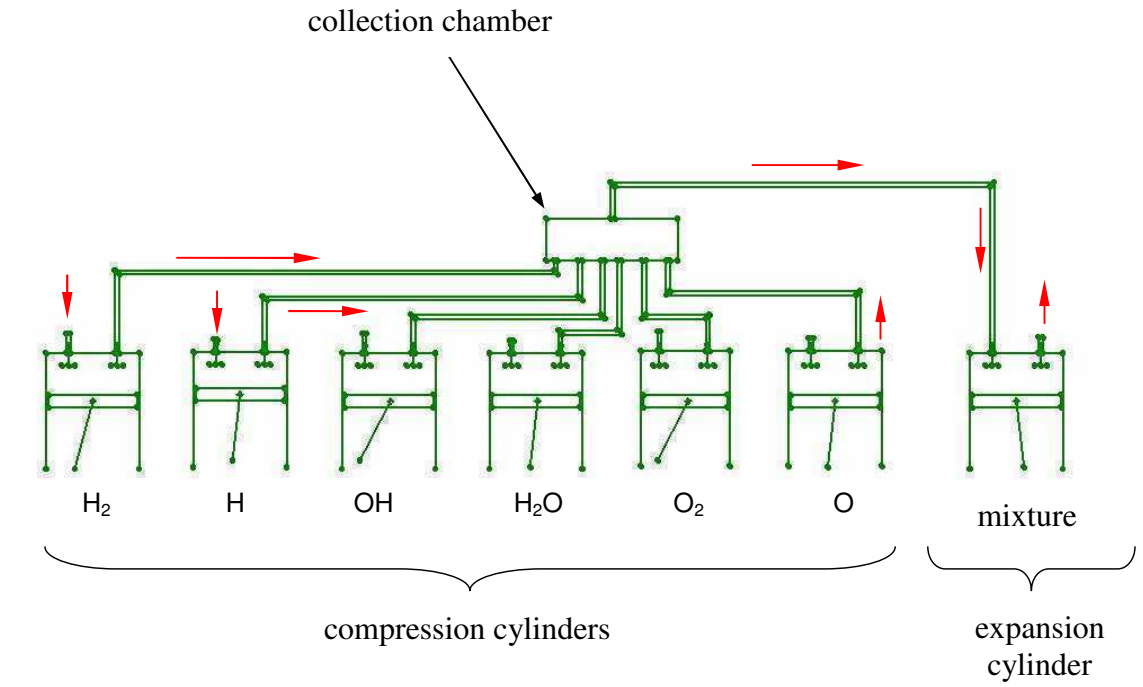

Fig. 1. Construction and working of the reversible combustion model of hypothetical processes.

The model consists of several piston cylinder assemblies as shown in fig. 1. The high temperatures that are required to attain state of equilibrium are obtained by using compression cylinders while the work is extracted by using expansion cylinder. The collection chamber only collects the output of the compression cylinders. There is no chemical reaction taking place in the collection chamber and it is assumed that the collection process is instantaneous.

The model can be explained better by using a specific case. Consider that hydrogen is used as the fuel and pure oxygen as the oxidant for the combustion process. This case is specially selected since hydrogen and oxygen have less species on dissociation. Other cases with other fuels and air will be considered in the subsequent sections. In general, when hydrogen and oxygen are mixed and heated to high temperature, the mixture will dissociate and only six major species can be formed, namely, H_2, H, H_2O, OH, O, and O_2. Now, keeping this in mind, six compression cylinders are taken and each is introduced with the desired quantity of each of the species. The desired quantity is just the amount of each of the species that will exist at equilibrium, at the final (specified) temperature and pressure. When these species are individually compressed isentropically in the compression cylinders, and are then collected in the collection chamber, the final mixture of the species are already in equilibrium and they do not react. Due to absence of reaction, there is no entropy generation due to the collection of the species, and so the entropy of the mixture at the exit of the collection chamber is same as that at the entrance.

The desired quantity of each of the species to be introduced in each of the compression cylinders along with their respective temperature and pressure is calculated using the computer program (explained in the next section). The collection process is instantaneous which is followed by the expansion process. As the mixture is expanded, it is allowed to equilibrate at each stage of expansion in such a way that expansion is isentropic. As the expansion proceeds, more and more species are formed. The expansion of greater number of species causes production of work.

The net work gain from the system is the difference between the work extracted during the expansion process and the work consumed during the compression of species in the compression cylinder. Some energy also leaves the system in the form of exhaust gas. This energy can be tapped by suitable turbo compounding technology so that it is not wasted. Here, the goal is only to conduct the combustion process reversibly. The mathematics behind work calculation is presented in the next section.

Fig. 2 shows the variation of the pressure as a function of volume for the proposed processes. The process 1-3 is the isentropic compression of the frozen species in the different compression cylinders. The process 3-4 is the isentropic expansion of the species in equilibrium.

The reason for following the peculiar numbering scheme (1, 3 and 4 instead of 1, 2 and 3) will be explained later.

At state 1, the different amounts of the individual species calculated by the computer program developed enter the different compression cylinders. In the process 1-3, the compression of the species takes place. During this process the pressure and so the temperature of the species increases. The pressure at the end of compression, at state 3, is termed as the *compression pressure* while the temperature at state 3 is referred to as the *compression temperature*. At the end of compression, the species are mixed instantaneously. The collection is presented by point 3 on the pressure-volume (P-V) diagram. As the mixture is expanded in the process 3-4, the pressure of the mixture decreases while the volume increases. The expansion is continues till the original volume at the beginning of expansion is reached.

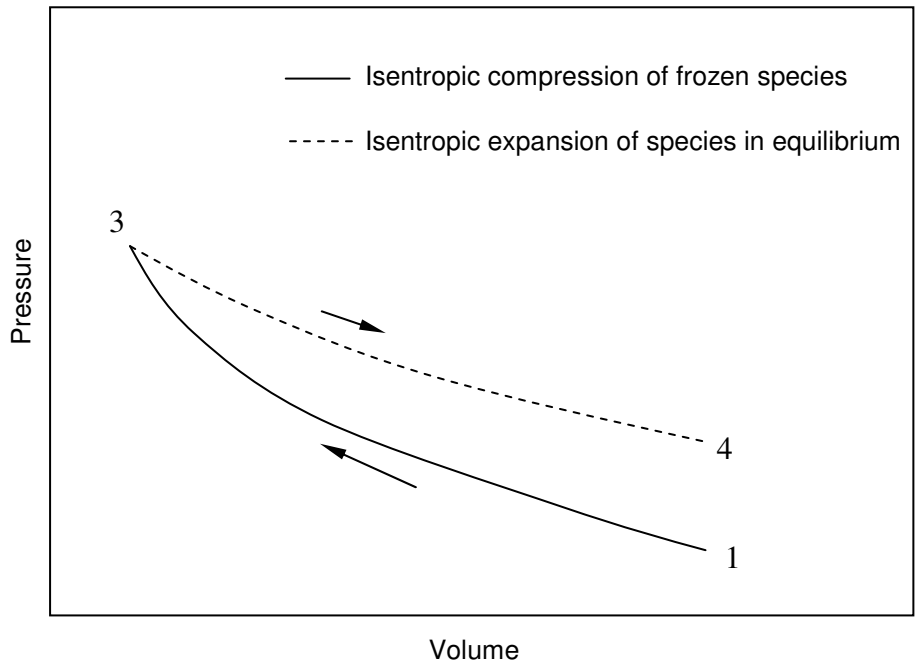

Fig. 2. Variation of pressure as a function of volume for the model of the hypothetical processes.

The area under the curve for any process on the P-V diagram, represents the work transfer due to that process. In fig. 2, the area under the curve 1-3 represents the work consumed by the model in the compression of the species, while the area under the curve 3-4 represents the work produced by the model during the expansion of the species. Thus, the area between the expansion and the compression curves represents the net work. The area between the curves is the result of the deviation of the two curves after point 3 for higher volumes. This deviation is due to the difference in states of the species at which both the processes take place. The species in the process 1-3 are frozen and are not allowed to react with each other, while in the process 3-4, the species are allowed to react and equilibrate themselves.

In this model, the cylinders, piping and collection chamber are assumed to be perfectly insulated and so there is no heat loss to the surroundings, and the expansion and the compression processes are isentropic. The number of compression cylinders used may not be restricted to six, and this number will depend upon the fuel-oxidant selected. For example, if isooctane is used as the fuel and air as the oxidant, then far more number of species may be formed upon dissociation at high temperature, and thus a greater number of compression cylinders may be needed.

Thus, by using this model, the irreversibility of the combustion process is avoided since theoretically there is no direct combustion reaction taking place. Whenever the species see each other at the end of the compression, in the collection chamber, they are in the state where their tendency to react has already disappeared, the mixture being in the equilibrium state. Also, there is no thermal energy exchange between the species in the collection chamber as all the species enter the chamber at same temperature. Species are not able to react prior to the collection as they are compressed in different cylinders. During the isentropic expansion of the mixture in the single cylinder, the mole fraction of the various species keeps on changing, so as to keep the mixture in the equilibrium state, thus increasing the number of products, which is the key to generation of work in this model.

It should be noted that process 1-3 in fig. 2 shows the combined P-V relation during compression of various species in different cylinders. For more information refer appendix VI.

To simplify the above concept, it may be visualized that the compression and expansion are taking place in a single cylinder with an anti-catalyst present during compression and no such catalyst during expansion. Presence of anti-catalyst prevents the reaction between the species and also prevents the thermal energy exchange between them.

Again, as this concept allows the elimination of the direct combustion process itself, the destruction of availability is zero, and the process can be said to be “reversible”.

IV. IMPLICATIONS TO RECIPROCATING ENGINE

Reciprocating internal combustion engines are those in which the combustion processes occur inside the reciprocating piston-cylinder arrangements. There are two principal types of reciprocating internal combustion engines: the spark-ignition (SI) engine and the compression ignition (CI) engine. The essential difference in the two types of the engines is the method by which the combustion process is initiated.

In an SI engine, fuel and air mixture are ignited by means of a spark plug while in a CI engine the high compression of gases causes the ignition of the fuel after it is injected. After the ignition, the combustion reactions begin. The release of chemical energy causes the piston to reciprocate, thus, producing work. The work from the piston-cylinder is always less than the input energy, i.e., the fuel energy. One of the reasons, for this loss of work, is irreversibilities in the combustion reactions. As stated earlier, the irreversibility is due to thermal energy exchange between the molecules of the combustion mixture, diffusion and irreversible mixing of combustion species.

Standard Air Cycle Analysis

The detailed study of the actual SI and CI engines is difficult. This is because a detailed study needs to take into account many features. These features include the effects of irreversibilities due to friction, pressure and temperature gradients within the system, heat transfer between the cylinder walls and the cylinder gases, irreversibilities due to combustion and heat loss to the surroundings. To avoid these complexities, elementary study of the internal combustion engine can be conducted by employing air-standard analyses.

The assumptions made for air-standard analyses are-

- the working fluid of the engine is modeled as an ideal gas
- the combustion process in actual engine is replaced by a heat transfer process
- there are no intake and exhaust processes
- the processes are internally reversible

The standard air cycles are of two major types: the Otto cycle and the diesel cycle. The difference in the two cycles is only due to the way in which the heat addition process takes place.

Figs. 3 and 4 show the Otto cycle on the pressure-volume (P-V) and the temperature-entropy (T-S) diagrams, respectively.

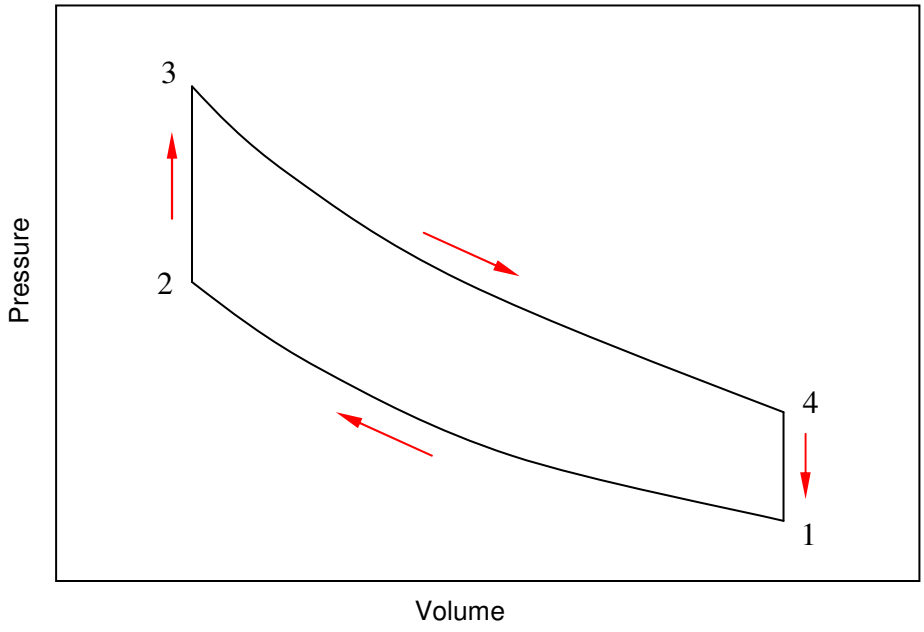

Fig. 3. Pressure-volume diagram of the air standard Otto cycle.

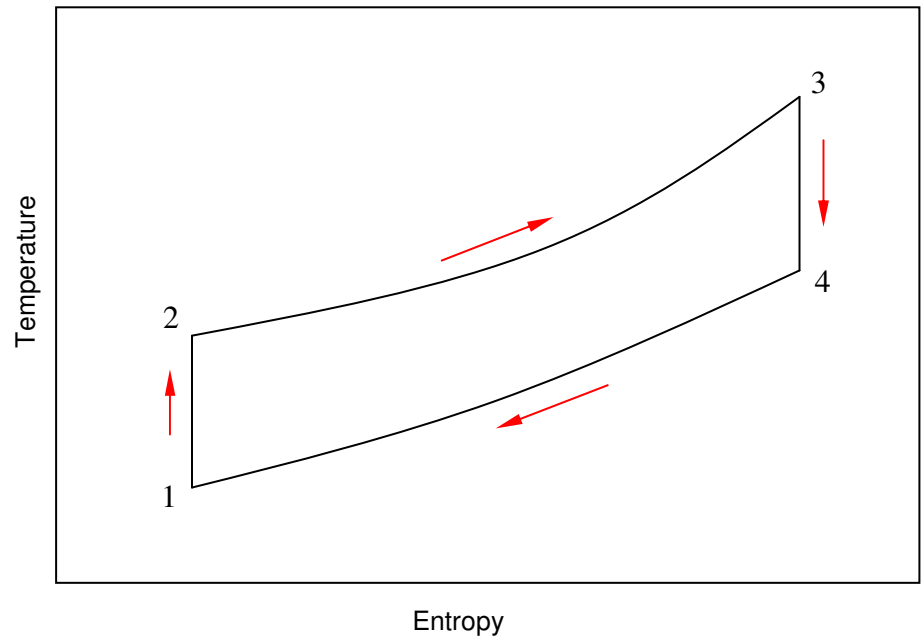

Fig. 4. Temperature-entropy diagram of the air standard Otto cycle.

For the case of the Otto cycle, process 1-2 is the isentropic compression process of the air mixture, process 2-3 is a constant volume heat addition to the air from external source, process 3-4 is the isentropic expansion process and process 4-1 is the heat rejection from the air to the surroundings.

Figs. 5 and 6 show the air standard Diesel cycle on the P-V and T-S diagrams respectively. The working of the Diesel cycle is similar to that of the Otto cycle except for the heat addition process 2-3. The heat addition process in the Diesel engine is conducted at constant pressure.

For both the cycles, the enclosed area 1-2-3-4 on the P-V diagram can be interpreted as the net work output while the area enclosed on the T-S diagram represents the net heat added to the system. In the temperature-entropy diagrams for the Otto and the Diesel cycles (fig. 4 and 6), it can be seen that due to heat addition 2-3, the entropy of the cycle increases. The entropy generation gives rise to the irreversibilities.

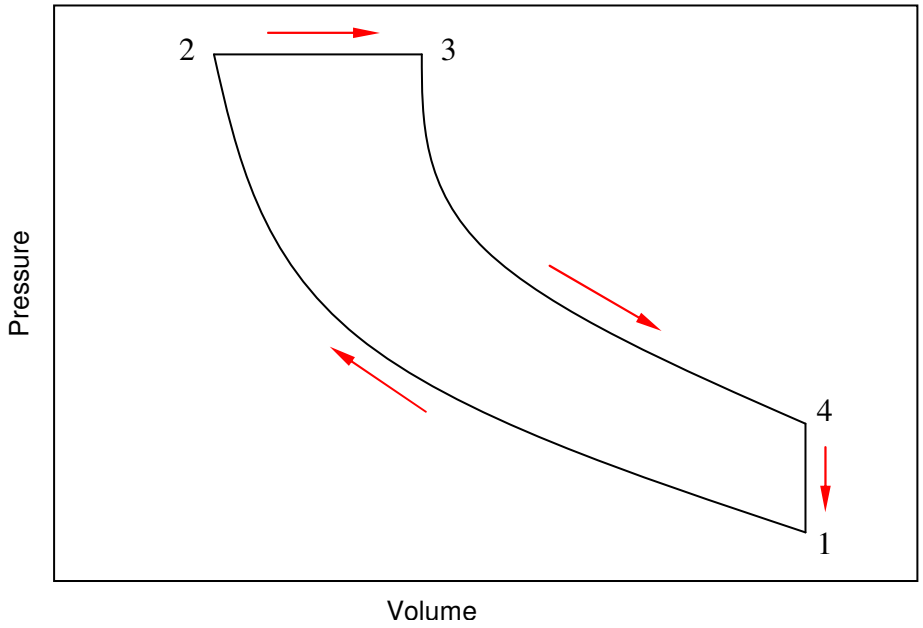

Fig. 5. Pressure-volume diagram of the air standard Diesel cycle.

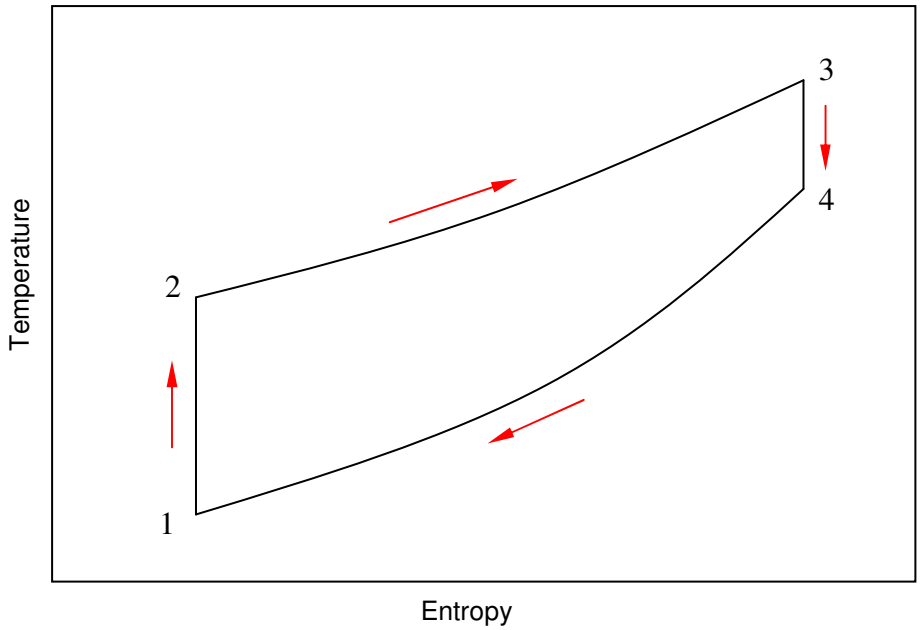

Fig. 6. Temperature-entropy diagram of the air standard Diesel cycle.

If the actual reciprocating internal combustion engine is to be compared with the standard air cycles, then for the above figures, 1-2 will be the compression process, 2-3 will be the combustion process (initiated by means of spark for the case of an SI engine and by injection of fuel into the hot air for the case of a CI engine), process 3-4 will be expansion of the combustion gases to extract work, i.e., the power stroke and process 4-1 will be the heat rejection process at constant volume.

However, as discussed earlier, for the actual reciprocating internal combustion engine, many losses may be identified. These losses can be prevented only if,

1. the internal combustion engine is completely insulated and is frictionless, so that there is no heat loss from the system to the surrounding and also no loss of work because of friction.
2. the compression of the mixture is conducted without mixing of the molecules of the mixture, so that there is no irreversibility due to mixing and also no heat exchange between the molecules, as they are not in contact with each other, and
3. the combustion process is conducted reversibly

For the current work, point 1 listed above is the assumption made in this study as the focus of this work is on the combustion processes and not on the mechanical aspect of the engine. The compression of the mixture without the mixing of its molecules can be imagined to be possible by the use of an anti-catalyst. So, only the other possibility of conducting combustion with zero irreversibility needs to be verified. This can be done by means of an availability analysis.

Availability Analysis of a Combustion Process

As described in the literature review, the combustion irreversibilities are minimized if the combustion processes are conducted at very high temperatures [4, 8]. To examine the reversibility of combustion processes, an availability analysis [8], was completed for a range of reactant temperatures at three reactant pressures and for three equivalence ratios.

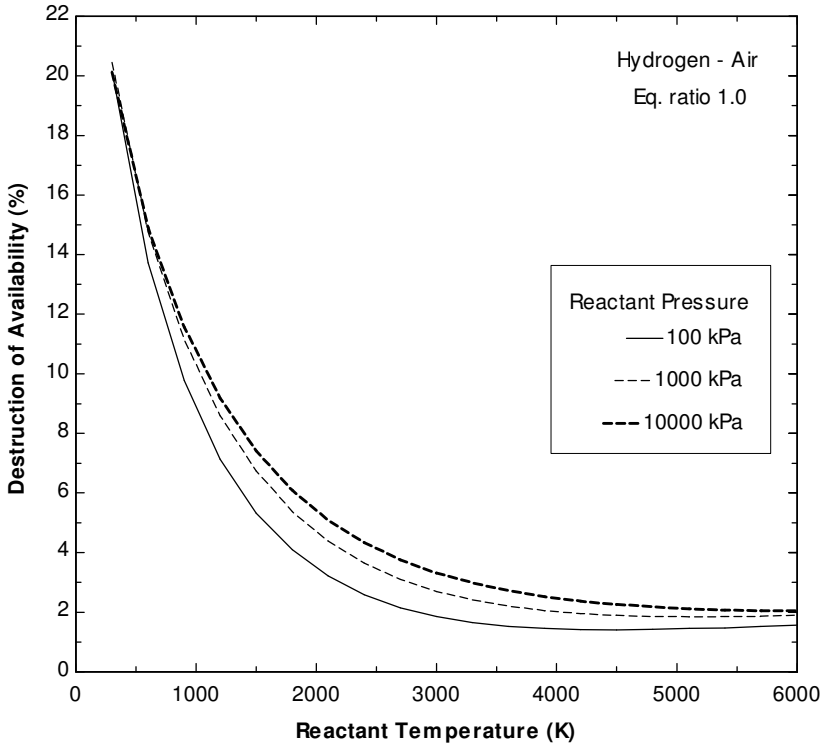

Fig. 7. Percentage destruction of availability as a function of reactant temperature for three reactant pressures for constant volume combustion.

Fig. 7 shows the variation of the destruction of availability for hydrogen, for three reactant pressures (100 kPa, 1000 kPa and 10000 kPa) as a function of reactant temperature. For low temperatures, the destruction of availability is high (~20%) and is approximately the same for all three pressures. The availability destruction reduces as the reactant temperature increases. The reactant pressure has modest effects on the availability destruction. Precisely, availability destruction for lower reactant pressures (100 kPa) is lowest (~2%) at the highest reactant temperature.

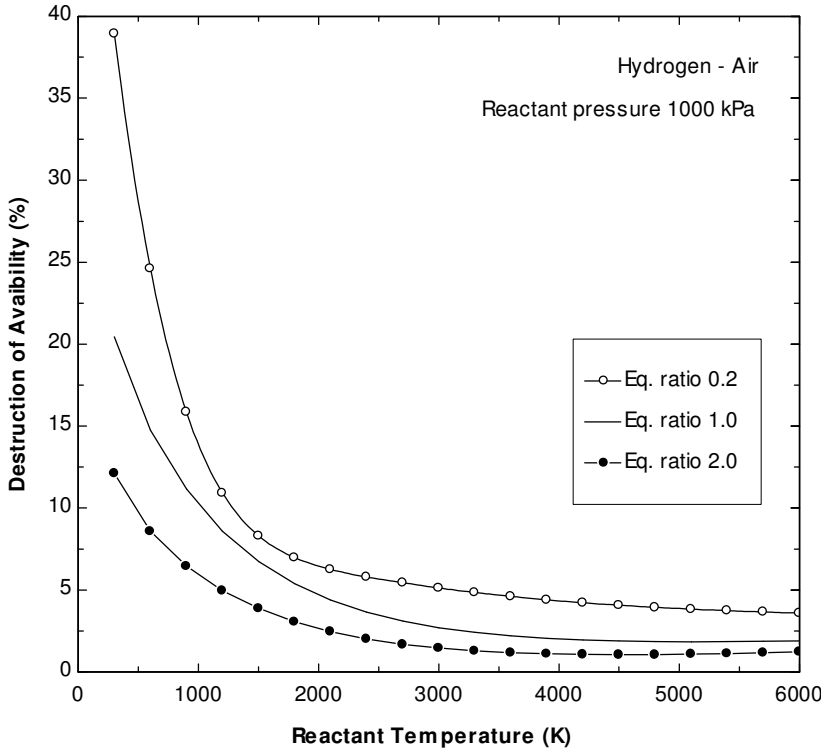

Fig. 8. Percentage destruction of availability as a function of reactant temperature for constant volume combustion for three equivalence ratios.

Fig. 8 shows the destruction of availability for constant volume combustion for three equivalence ratios (0.2, 1.0 and 2.0) as a function of reactant temperature. The destruction of availability, corresponding to 300 K, is highest for an equivalence ratio of 0.2 and lowest for an equivalence ratio of 2.0. Initially, the destruction of availability decreases rapidly as the reactant

temperature increases. At higher temperatures (greater than 2000 K) the decrease in availability destruction is gradual and is about 2.0 to 3.5% for all the equivalence ratios.

Fig. 9 shows the destruction of availability for isooctane fuel, for constant volume combustion processes at different pressures, as a function of reactant temperature. The availability destruction is similar to that for hydrogen fuel (fig. 8). At the lower temperatures and lower pressures, the availability destruction is high (about 22 – 25%). The significance of pressure variation becomes almost nil for high temperatures leading to convergence of availability destruction curves at 6000 K. The value for availability destruction for 6000 K is ~3.5%.

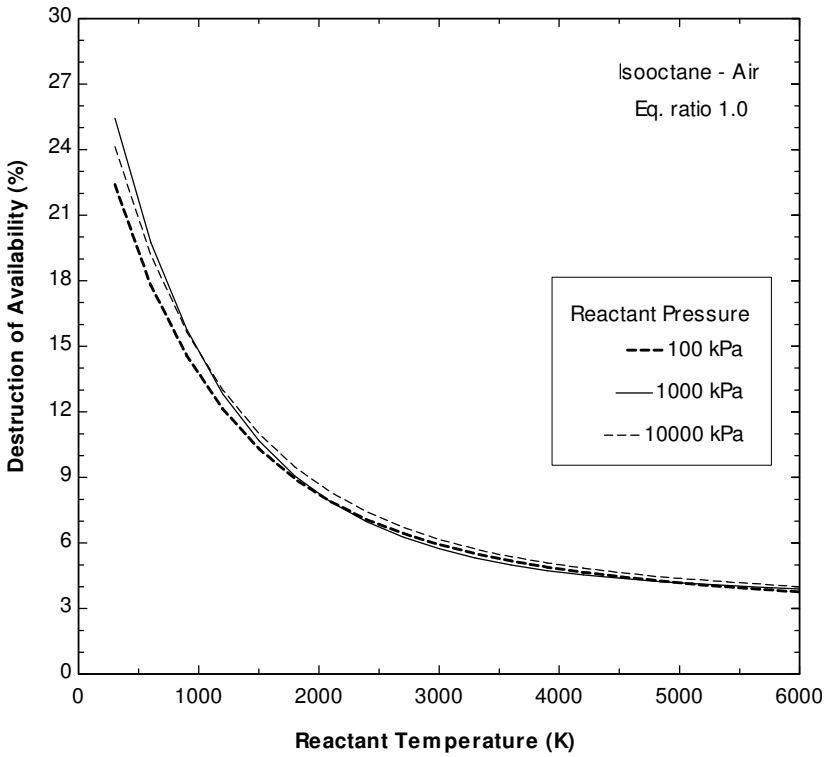

Fig. 9. Percentage destruction of availability as a function of reactant temperature for three reactant pressures for constant volume combustion.

Fig. 10 shows the availability destruction variation for isooctane, for equivalence ratios ranging from 0.2 to 2.0. Again, for lower equivalence ratio, the availability destruction is

maximum and for rich mixture (equivalence ratio 2.0), the availability destruction is lesser. The availability destruction values further decrease as the reactant temperature increases. The reversal of trend at about 1500 K, for lean and stoichiometric mixtures, is due to the fact that the reactive availability for mixture at equivalence ratio 0.2 is very small as compared to thermo-mechanical availability at higher temperatures. The lowest availability destruction at 6000 K is about 4.0%. The results at higher temperatures are similar to those found for hydrogen fuel.

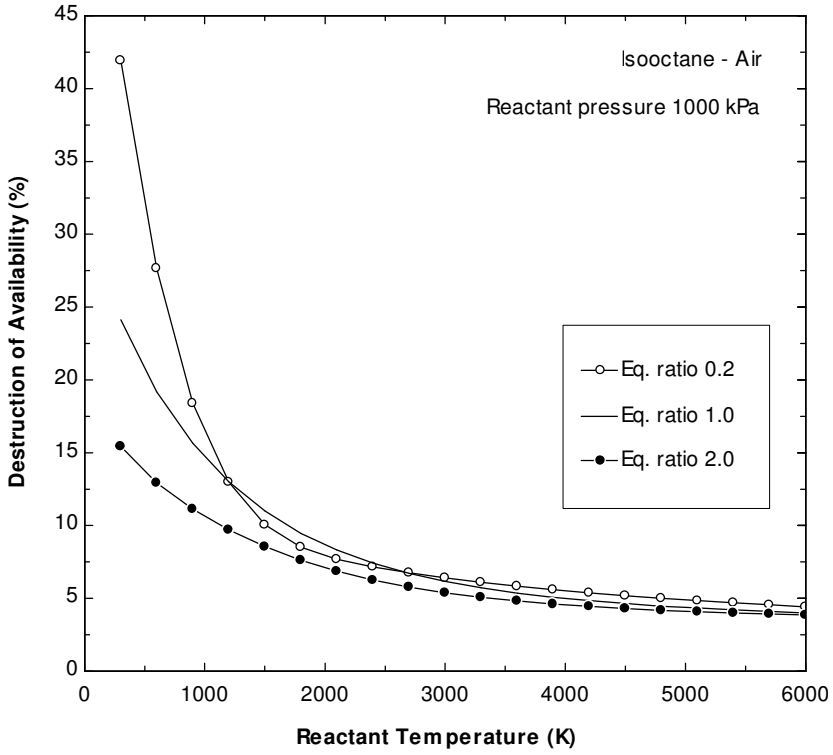

Fig. 10. Percentage destruction of availability as a function of reactant temperature for constant volume combustion for three equivalence ratios.

The above study was restricted to hydrogen and isooctane as fuels. The detailed parametric analysis can be found elsewhere [4, 8]. The analysis reveals the fact that even at very high temperatures that cannot be handled by present materials technology, the availability destruction was very low but never zero. Hence, it may not be possible to conduct combustion

reaction reversibly using high temperatures. Thus, a conceptual model that can substitute the irreversible constituent of combustion process was developed, as describe in the earlier section.

Applications to Reciprocating Engines

The current model helps in achieving the objective of reversible combustion, without the thermal energy exchange and premixing of the combustion species. The model, though theoretical, can be related to actual reciprocating engines.

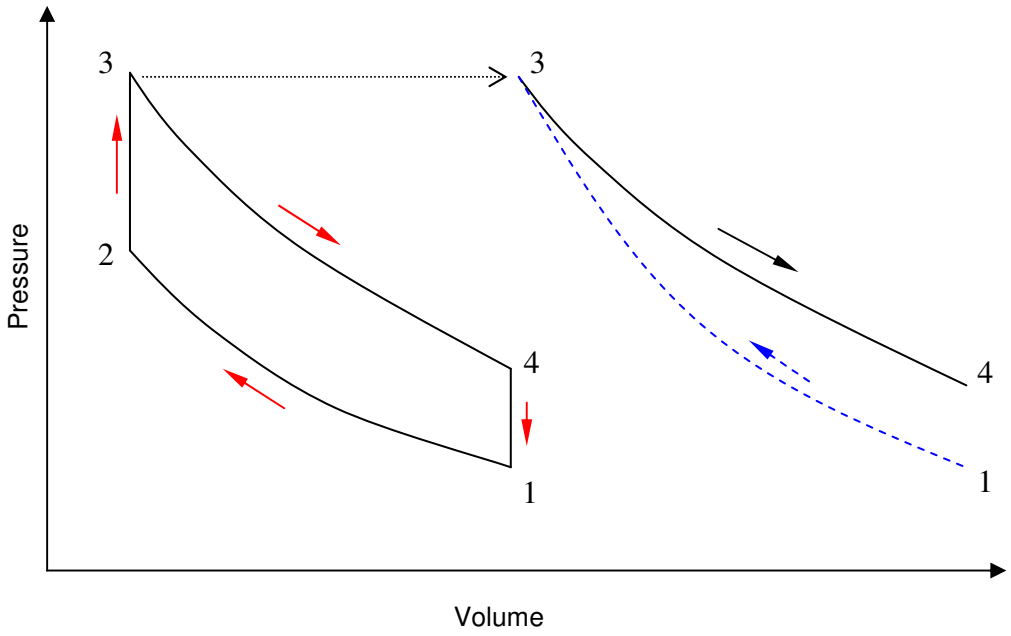

Fig. 11. Pressure-volume diagram of the model of hypothetical processes and the air standard Otto cycle.

When the working of the model is compared with the Otto cycle and the Diesel cycle, on P-V diagram, in figures 11 and 12, it is represented by the processes 1-3-4 (process 1-3 is shown by a dotted line). In this model, the processes 1-2 and 2-3, of the air standard cycles, are represented by one process (1-3). The compression of the different species of the mixture are conducted in different cylinders, as a result of which there is no irreversible mixing and also no heat transfer between the species, each specie being compressed individually and separately.

The process 2-3 is completely eliminated. Due to the complete elimination of the combustion process, the processes for this model are described using a peculiar numbering scheme (1-3-4) which indicates the absence of irreversible combustion.

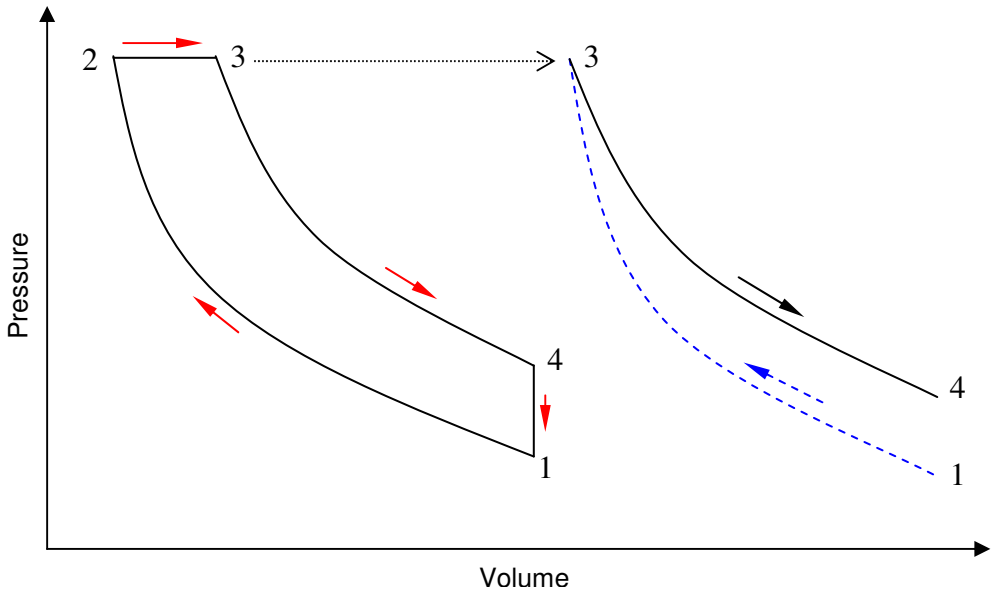

Fig. 12. Pressure-volume diagram of the model of hypothetical processes and the air standard Diesel cycle.

When the species are compressed in the compression cylinders to state 3, their tendency to react diminishes, as state 3 is the state of thermodynamic equilibrium, pre-selected by means of a computer program developed (will be explained in next section). As a result of this, state (3) required to extract energy from the fuel is achieved without combustion process and hence there is no irreversibility associated with the combustion process in this model of hypothetical processes.

V. DEVELOPMENT OF THE COMPUTER PROGRAM

This section discusses how the thermodynamic properties, the availability and the work were calculated. A major feature of these calculations was the use of the NASA Lewis polynomial fits to the thermodynamic properties [9, 19].

Structure of the Program

Fig. 13 shows the structure of the computer program developed to analyze the model under different operating conditions

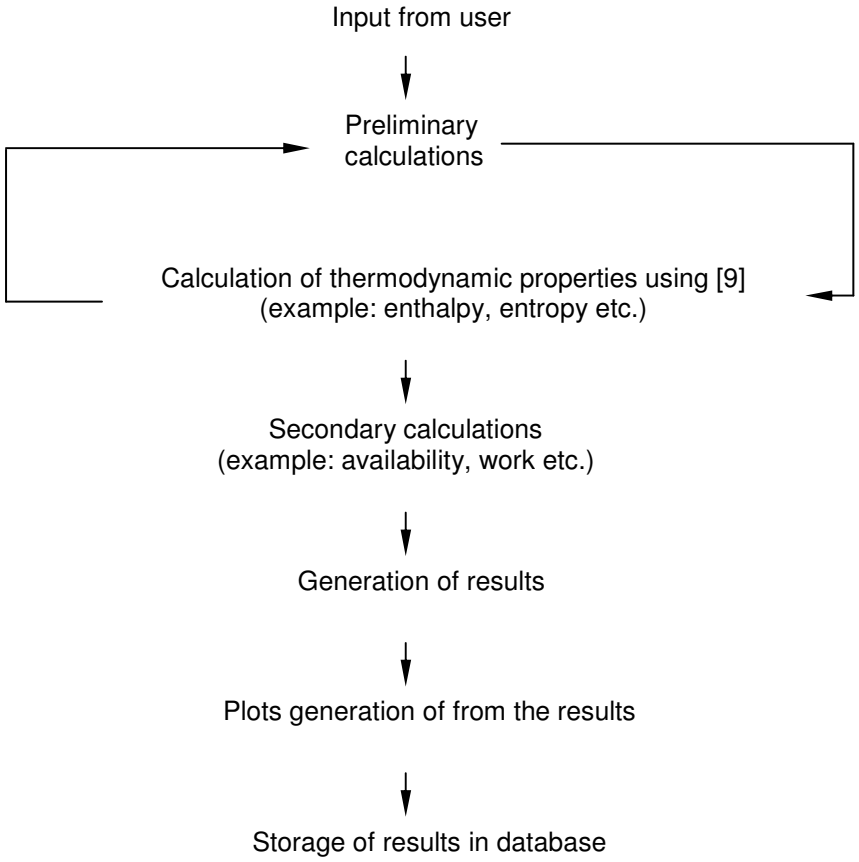

Fig. 13. Structure of the computer program developed to calculate the thermodynamic properties of the fuel-air mixture for the model of the hypothetical processes.

The computer program was developed to represent the model of hypothetical processes, described earlier. It was designed such that user only needs to provide some primary initial data like, type of fuel, oxidant, compression ratio, compression pressure and temperature and the conditions of the restricted dead state. Once this is done, the program executes all the necessary calculations.

Assumptions

The major assumptions used in the analysis of the model are:

1. Gases follow ideal gas behavior.
2. Collection chamber, reciprocating engines and their contents make up a thermodynamic system.
3. The system is perfectly insulated and is frictionless.
4. Gases in the system had enough time to attain equilibrium conditions.
5. The thermodynamic properties such as temperatures, pressures etc. are spatially uniform at each and every stage of the process.
6. Gases mix instantaneously in the collection chamber.
7. The thermodynamic properties are calculated using standard algorithms [9, 19].

Development of Program

The computer program was developed to handle eight different fuels:

- Hydrogen
- Acetylene
- Methane
- Propane
- Isooctane
- Methanol
- Ethanol
- Benzene

The oxidants that can be used are: pure oxygen and air. Here, standard composition of air was used [4] which can be found in appendix I.

After supplying the initial data, primary calculations [8] are conducted. Firstly, the number of moles in the reactant mixture is found using the Ideal gas law

$$PV = n\bar{R}T \tag{5.1}$$

where P is pressure, V is volume and T is temperature, of the system under consideration. $\bar{R}$ is the universal gas constant and n is the number of moles in the system. The value for $\bar{R}$ is taken as 8.314 $\frac{kPa - m^3}{kmole - K}$.

The total number of moles found, is further used to find number of moles of fuel and number of moles of oxidant using stoichiometric equations. Once the moles of fuel and oxidant are known, the fuel air ratio is found as below.

$$(F:A) = \frac{n_f . M_f}{n_o . M_o} \tag{5.2}$$

where n_f is the number of moles of fuel and n_o is the number of moles of oxidant. M_f and M_o stand for molecular weight of fuel and oxidant respectively. The fuel air ratio found above is for the stoichiometric balance and if the equivalence ratio is other than unity, then actual fuel air ratio needs to be calculated.

$$(F:A)_{actual} = (F:A) \cdot \phi \tag{5.3}$$

where ϕ is equivalence ratio.

The results from the above equations are used to calculate thermodynamic properties using NASA Lewis polynomial, developed by Gordon and McBride [9]. The literature about interfacing of the data input file and the code of polynomial fits is presented by Zehe et al. [19]. It may also be useful to refer literature by Caton [4] and Chavannavar [8] to find more detailed explanation regarding primary calculations.

Thermodynamic properties like enthalpy, entropy, internal energy and composition of reactant mixture were calculated using NASA Lewis polynomial fit. The latest “7+2” coefficients as calculated in [8] were used to calculate the thermodynamic properties. These coefficients are listed in appendix III and can also be found on website [18]. The equations [19] used to calculate thermodynamic properties, enthalpy and entropy using these coefficients are:

$$H = \left(- a_1 \cdot T^{-2} + a_2 \cdot T^{-1} \cdot \ln(T) + a_3 + a_4 \cdot \frac{T}{2} + a_5 \cdot \frac{T^2}{3} + a_6 \cdot \frac{T^3}{4} + a_7 \cdot \frac{T^4}{5} + \frac{b_1}{T} \right) \cdot \bar{R} \cdot T$$

....(5.4)

$$S = \left(- a_1 \cdot \frac{T^{-2}}{2} - a_2 \cdot T^{-1} + a_3 \cdot \ln(T) + a_4 \cdot T + a_5 \cdot \frac{T^2}{2} + a_6 \cdot \frac{T^3}{3} + a_7 \cdot \frac{T^4}{4} + b_2 \right) \cdot \bar{R} \qquad (5.5)$$

where H is enthalpy and S is entropy of the mixture. Other equations used to calculate enthalpy, entropy and internal energy were,

$$H = \sum_{i=1}^{n} n_i \cdot \bar{h_i} \qquad (5.6)$$

$$U = \sum_{i=1}^{n} n_i \cdot \bar{u_i} \qquad (5.7)$$

$$S = \sum_{i=1}^{n} n_i \cdot \left(S^0 - R \cdot \bar{\ln}(x_i) \right) \qquad (5.8)$$

where x_i denotes mole fraction of the specie and U is internal energy.

After determining reactant mixture properties, product mixture properties are calculated by linking reactants and products by means of the combustion process which can be constant pressure or constant temperature or constant volume. The calculations discussed here are in general for any combustion problem.

For the proposed model discussed earlier, a major challenge was to find the exact composition of mixture at the end of compression process such that upon collection of reactant species, no product is formed. Rigorous programming was done to achieve the target. Initially for the given fuel-oxidant combination, the code calculates the maximum number of species that can be obtained upon dissociation of the fuel-oxidant mixture at high temperature. After finding the number and type of species, the code assumes some predefined amount of each of the species. These species are compressed, by reduction in volume, for a small step size. At the end of compression, all the species are allowed to equilibrate. After equilibrium, the new equilibrium composition is compared with earlier predefined composition and depending upon the differences, the quantity of each of the species is adjusted for a second iteration. The code

undergoes several iterations before finding the exact-required number of moles of each of the species in each compression cylinder.

Once the species come together in the collection chamber they are expanded very slowly and isentropically, again with a small step size, such that at each step they are in equilibrium. This is continued until the mixture has expanded to the original volume.

The species considered in the dissociation at the end of compression stroke are:

- Hydrogen
- Oxygen
- Water
- Nitrogen
- Hydroxyl atom
- Argon
- Nitrogen
- Hydrogen atom
- Oxygen atom
- Nitrogen atom
- Carbon atom
- Carbon 2
- Carbon 3
- Carbon monoxide
- Carbon dioxide
- Methane
- Acetylene
- CH
- Nitrogen oxide
- Nitrogen dioxide

To calculate the work extracted from the system, an availability analysis is necessary. The availability balance equation is given by [3] as,

$$W_{\max} = -d\frac{\left(E_{cv} - T_0 \cdot S_{cv}\right)}{dt} + \sum_{j=1}^{N} Q_{R,j}\left(1 - \frac{T_0}{T_{R,j}}\right) + A_{initial} - A_{final} \tag{5.9}$$

where $W_{\max}$ is the maximum work available from a system if the irreversibility is zero, $Q_{R,j}$ is the heat interaction between the system and a reservoir (*j*), N is the number of heat interactions across the control volume. Subscripts R represents reservoir and CV represents control volume. In the above equation, first and second terms on right hand side are zero because our model is assumed to operate in steady state and is perfectly insulated. Also,

$$W_{\max} = W + I \tag{5.10}$$

where W is the actual work and i is the irreversibility. As discussed, since the irreversibility in the developed model is zero, actual work is same as maximum work. Thus actual work is given by,

$$W = A_{initial} - A_{final} \tag{5.11}$$

$A_{initial}$ and A_{final} are calculated using the equations listed in earlier sections. More discussion about zero irreversibility can be found in upcoming sections. A thermal efficiency of the model may be defined as,

$$\eta = \left(\frac{W}{LHV_{fuel}} \right) \times 100 \tag{5.12}$$

where LHV_{fuel} is the lower heating value of the fuel which can be calculated as in [4],

$$LHV_{fuel} = -(\Delta H)_{P_0,T_0} = \left(\sum_{i=1}^{n} n_i \cdot h_{f,i}^0 \right)_{products} - \left(\sum_{j=1}^{n} n_j \cdot h_{f,j}^0 \right)_{reactants} \tag{5.13}$$

where $(\Delta H)_{P_0,T_0}$ is difference in enthalpy between reactants and products at reference temperature and pressure, h_f^0 is enthalpy of formation at reference conditions. Lower heating values of different fuels are listed in appendix II.

VI. RESULTS AND DISCUSSION

This section presents the results from the study of reversible combustion model that was developed using the concept proposed by Keenan [10]. The results were obtained from the code developed, which makes the use of NASA Lewis polynomials to calculate the thermodynamic properties. The results obtained from the code are presented in the form of plots in this section for better understanding of the trends that this model follows. The code considers the dissociation of species at high temperature for achieving accurate results.

The variables considered in this analysis are:

- Fuel
- Oxidant
- Temperature
- Pressure
- Equivalence ratio
- Compression ratio

The different fuels considered in this analysis are:

- Hydrogen, H_2
- Isooctane, C_8H_{18}
- Acetylene, C_2H_2
- Methane, CH_4
- Propane, C_3H_8
- Methanol, CH_3OH
- Ethanol, C_2H_5OH
- Benzene, C_6H_6

The oxidants used for the combustion processes are:

- Pure oxygen
- Air i.e. standard wet atmosphere (appendix I)

The range for which analysis is conducted:

- Temperature: 500 K – 6000 K
- Pressure: 1000 kPa – 20000 kPa
- Equivalence ratio: 0.2 – 2.0
- Compression ratio: 4 – 24

As listed above, the analysis was done for fairly large ranges of parameters. The upper limits considered were unrealistically high (6000 K, 20000 kPa, and equivalence ratio 2.0) and are unlikely to occur in the practical systems. However, such analysis provides useful insight about the work and efficiency trends followed by the model of hypothetical processes. It helps better selection of the most optimum condition under which this model should be used for more work extraction and higher efficiency.

This section is divided into two main subsections – the base case study and the parametric study. The first subsection illustrates the results for the selected base case and the variations in base case. The base case selected for the study was:

- fuel: isooctane
- oxidant: air
- compression temperature: 2500 K
- compression pressure: 10000 kPa
- equivalence ratio: 1.0
- compression ratio: 18

The base case was selected in such a way that it lies in between the analysis range, stated above, and also closely represents the conditions that are used in practice. For example, isooctane is often used to model actual SI engine fuels and atmospheric air is used as the oxidant. High compression ratios of 18 are common for Diesel engines where the compression pressures are as high as 10000 kPa and even higher in some cases.

The base case study includes the following sub-sections:

- Effects of compression temperature in combination with high compression pressure
  - illustrates the base case
  - illustrates the base case, but at higher compression temperature (6000 K)
  - illustrates the base case, but for range of compression temperatures (0-6000 K)
- Effects of compression temperature in combination with low compression pressure
  - illustrates the base case, but for range of compression temperatures (0-6000 K) and lower compression pressure (1000 kPa)
- Effects of compression temperature in combination with rich mixture
  - illustrates the base case, but for range of compression temperatures (0-6000 K) and rich reactant mixture (equivalence ratio 2.0)
- Effects of compression temperature in combination with lean mixture
  - illustrates the base case, but for range of compression temperatures (0-6000 K) and lean reactant mixture (equivalence ratio 0.2)
- Effects of compression temperature in combination with high compression ratio

  - illustrates the base case, but for range of compression temperatures (0-6000 K) and high compression ratio (compression ratio 24)
- Effects of compression temperature in combination with high compression ratio
  - illustrates the base case, but for range of compression temperatures (0-6000 K) and lower compression ratio (compression ratio 4)
- Effects of compression temperature in combination with oxygen as oxidant
  - illustrates the base case, but for range of compression temperatures (0-6000 K) and oxygen as oxidant.

The second subsection, which is the last subsection, presents the parametric study which illustrates the behavior of the model when used under different thermodynamic conditions and with different fuels. The parametric study also discusses the effects of compression pressures, equivalence ratios and compression ratios for the entire range of temperatures. Several combinations of thermodynamic properties were considered, in search of efficient fuel and feasible thermodynamic condition that can develop more work. However, both the subsections discuss only peculiar cases of study, while the other similar results can be found in appendix V.

Base Case Study

For the base case, the reversible combustion model uses isooctane as fuel and air as oxidant. To study the effects of pressure, temperature, equivalence ratio and compression ratio, each of these parameters of the base case will be varied through out this section while keeping the others constant to analyze the efficiency trends of the model.

Effects of compression temperature in combination with high compression pressure (10000 kPa)
Part I

In this part of the study, the conditions include a compression temperature of 2500 K, a compression pressure of 10000 kPa, an equivalence ratio of 1.0 and a compression ratio of 18, i.e. at the selected base case conditions.

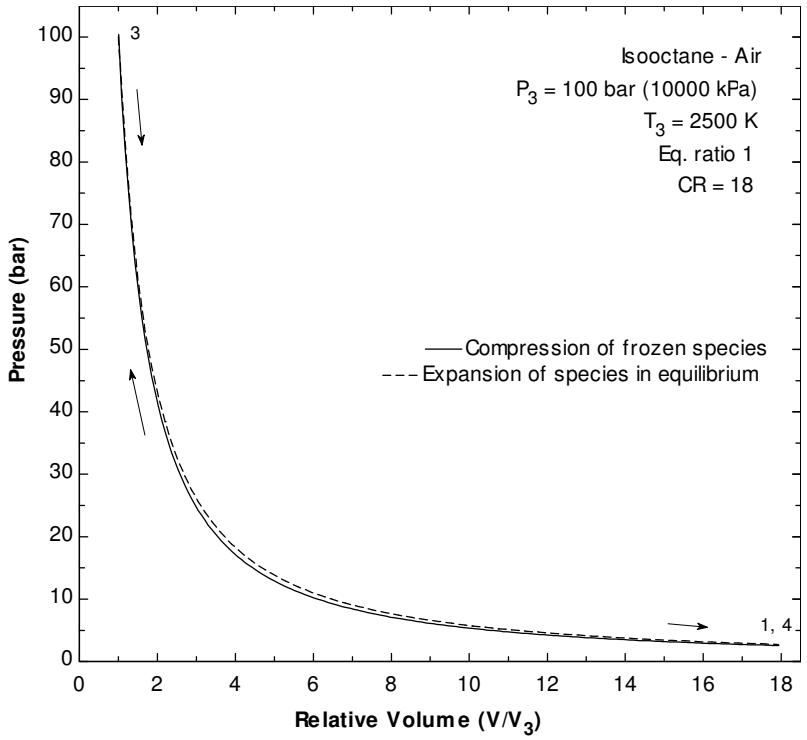

Fig. 14. Variation of pressure as a function of relative volume for isooctane-air at 2500 K compression temperature, 10000 kPa compression pressure, Φ = 1.0 and CR = 18.

Fig. 14 shows the base case processes on a P-V diagram. The processes in the model are numbered by 1-3-4. The process 1-3 is the compression process. The compression is conducted isentropically in different cylinders to avoid any reactions and the irreversible mixing of species. As the compression proceeds from point 1 (relative volume of 18), the volume of gases decreases while the pressure increases exponentially. Increase of pressure leads to higher temperatures. The compression process is continued until the total pressure of all the species reach 10000 kPa and the temperature of the individual species reach 2500 K, which is the compression pressure (P_3) and compression temperature (T_3) for the selected base case. The relative volume of the species at the end of compression is 1 as the compression ratio selected for this case is 18.

At the end of the compression (point 3), the species are taken from the different compression cylinders and are allowed to mix instantaneously in the collection chamber. When the different species come together, the species find themselves in equilibrium and have no tendency to react and form products. This phenomenon of species being in equilibrium at the

end of compression is the result of the compression of the exact amount of species in the compression cylinders at the pre-selected thermodynamic states, combined to form state 1 in fig. 14. This is a key feature of the current study. The state 1 of the species is found iteratively by the use of the code as discussed earlier.

The species in equilibrium, at point 3, are then expanded isentropically to point 4 by increasing the volume. As the volume increases, the pressure exponentially decreases and so also the temperature decreases. The expansion is stopped at the original volume from where the compression was started.

For the selected base case (2500 K, 10000 kPa), it can be seen that the points 1 and 4 coincide. The area under the curve 1-3 represents the work consumed by the model for compressing the species in the compression cylinders while the area below the curve 3-4 is the amount of work developed by the model during the expansion process. The area between the curves 1-3 and 3-4 on the P-V diagram is the difference between the work produced and the work consumed, which is proportional to the net work developed by the current model.

The model is assumed to be perfectly insulated and so there is no heat transfer between the system (model) and the surroundings. Also, since this model contains no actual combustion process, as in contrast to that in the case of the Otto and the Diesel cycle, the losses due to combustion irreversibility are zero. Hence, on the application of the second law availability analysis, it can be seen that the available energy entering the model is the same as the available energy going out of the model, so the model can be said to be operating reversibly.

The generation of work is because of the difference in the path followed by the processes 1-3 and 3-4 on the P-V diagram, which is the result of difference in the conditions under which these processes take place. The process 1-3 is the compression of frozen species in the different cylinders and the process 3-4 in the expansion of species in a single cylinder where they are allowed to react with each other and equilibrate themselves at every infinitely small step of isentropic expansion.

Part II

Part II of the study, discusses the operation of the base case but at a higher temperature (6000 K instead of 2500 K) to examine the behavior of the model at higher temperatures.

Fig. 15 shows the pressure as a function of volume for a compression temperature of 6000 K while the compression pressure, equivalence ratio and compression ratio are kept the same (10000 kPa, 1.0, 18, respectively) as in the previous case, to see the effect of compression temperature on the results.

For compression temperature of 6000 K, the model consists of the similar processes - the isentropic compression of frozen species and the isentropic expansion of the species in equilibrium. As the volume decreases, the pressure increases during compression while for expansion, the pressure decreases as the volume increases. The point 4, which is the end point of the expansion process, is however seen to be above point 1 and no more coincides with point 1, as it did for 2500 K compression temperature. This is due to the larger deviation of the expansion curve (3-4) from the compression curve (1-3). The more the deviation between the curves, the more is the area between the curves and so more work can be developed.

As discussed earlier, the amount of work developed is indicated by the area between the curves. This work is developed by the total mixture and so has the units of “kJ/kg of mixture”. By appropriate calculations, as discussed in the earlier section, the work developed by the fuel can be calculated, which if is divided by the lower heating value of the fuel gives the thermal efficiency. In one of the literatures [6], this efficiency is termed the fuel conversion efficiency.

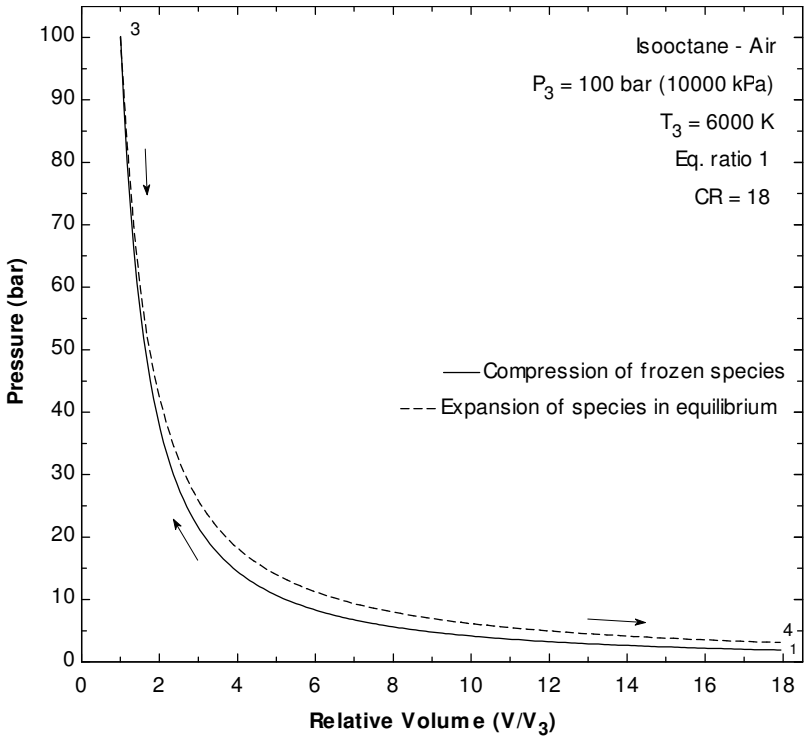

Fig. 15. Variation of pressure as a function of relative volume for isooctane-air at 6000 K compression temperature, 10000 kPa compression pressure, Φ = 1.0 and CR = 18.

Hence, referring to the fig. 15, it can be concluded that higher efficiency can be obtained when the model is allowed to operate at 6000 K as compared to when it is operated at 2500 K compression temperature.

Part III

To determine the nature of the dependence of work and efficiency on the compression temperature, several P-V diagrams were examined. Calculations for work and efficiencies were completed for the compression temperatures ranging from 500 K to 6000 K. The P-V diagrams for most of these cases are presented in appendix V.

Fig. 16 shows the net work (per kg of fuel & per kg of mixture) as functions of compression temperatures (500 K to 6000 K) for the base case parameters.

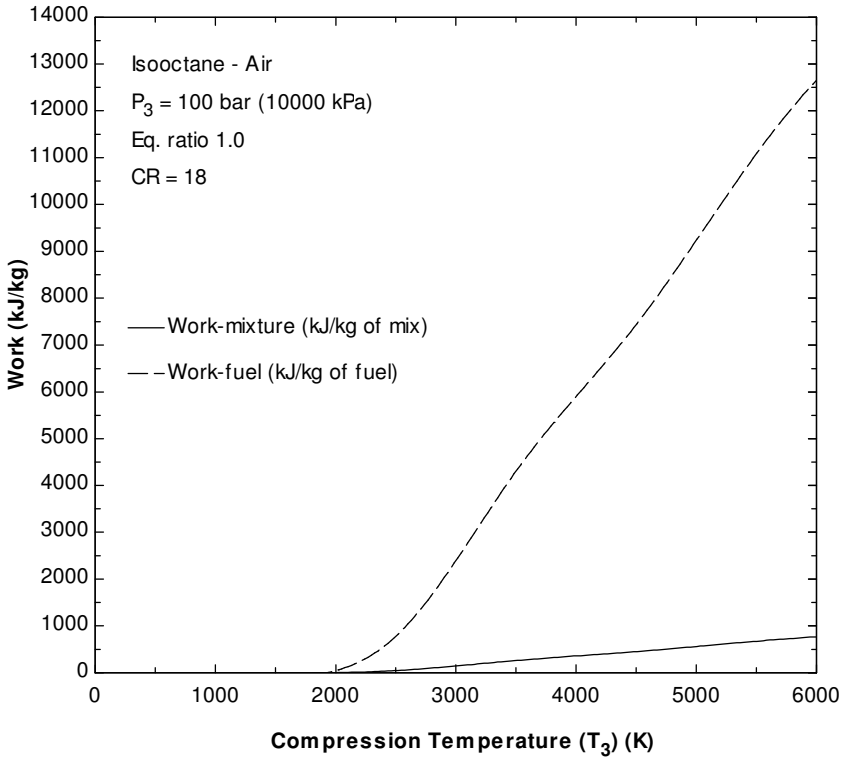

Fig. 16. Work as a function of compression temperature for isooctane-air at 10000 kPa compression pressure, Φ = 1.0 and CR = 18.

The work developed by the mixture increases almost linearly as the temperature increases. It is almost zero until about 2000 K while at 6000 K it is approximately 800 kJ/kg of mixture. As the work developed by the fuel is dependent upon the work by the mixture, it is also zero until about 2000 K compression temperature and is approximately 12600 kJ/kg of fuel at 6000 K.

Fig. 17 shows the variation of efficiency as a function of compression temperature for the same case discussed above, for the range 500 K to 6000 K.

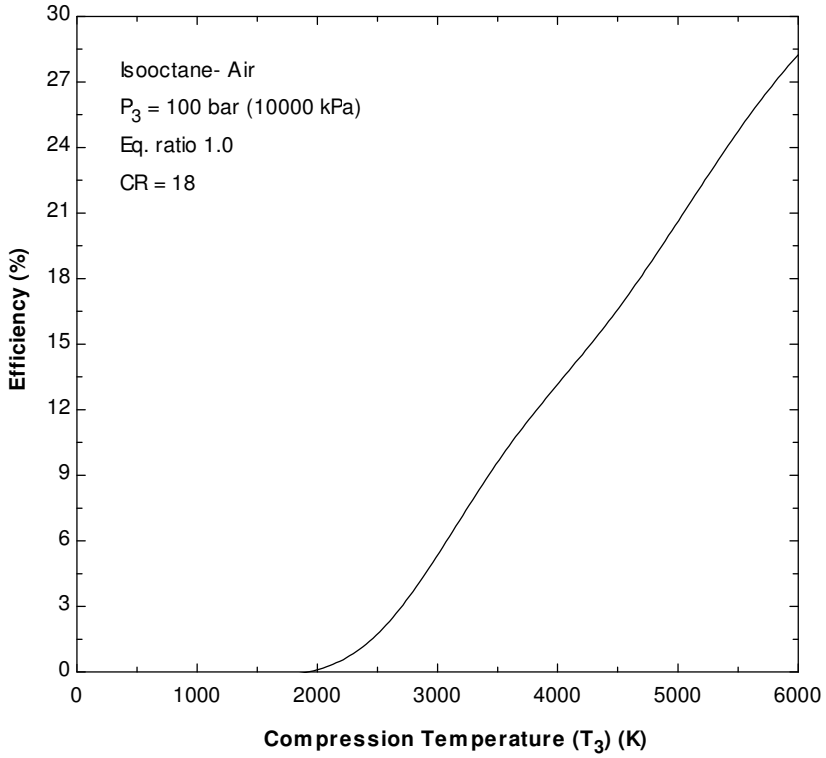

Fig. 17. Percentage efficiency as a function of compression temperature for isooctane-air at 10000 kPa compression pressure, Φ = 1.0 and CR = 18.

The efficiency is proportional to the work produced by the fuel and follows the trend similar to that seen for the work developed by the fuel. Again, until compression temperature of about 2000 K, the efficiency of the model is nearly 0% while for the compression temperatures

greater than 2000 K, the efficiency increases almost monotonically with compression temperature. At 6000 K, the efficiency is highest and is ~28%.

Fig. 17 indicates that compression temperature is an important factor on which the efficiency of the model depends. It is also clear that, for 10000 kPa, the efficiency of the model increases with compression temperature. To understand this increasing efficiency trend for the model, availability variations need to be analyzed.

Fig. 18 shows the effect of temperatures on availabilities (availability at points 1, 3, and 4), again for the same case of isooctane-air combination and 10000 kPa compression pressure.

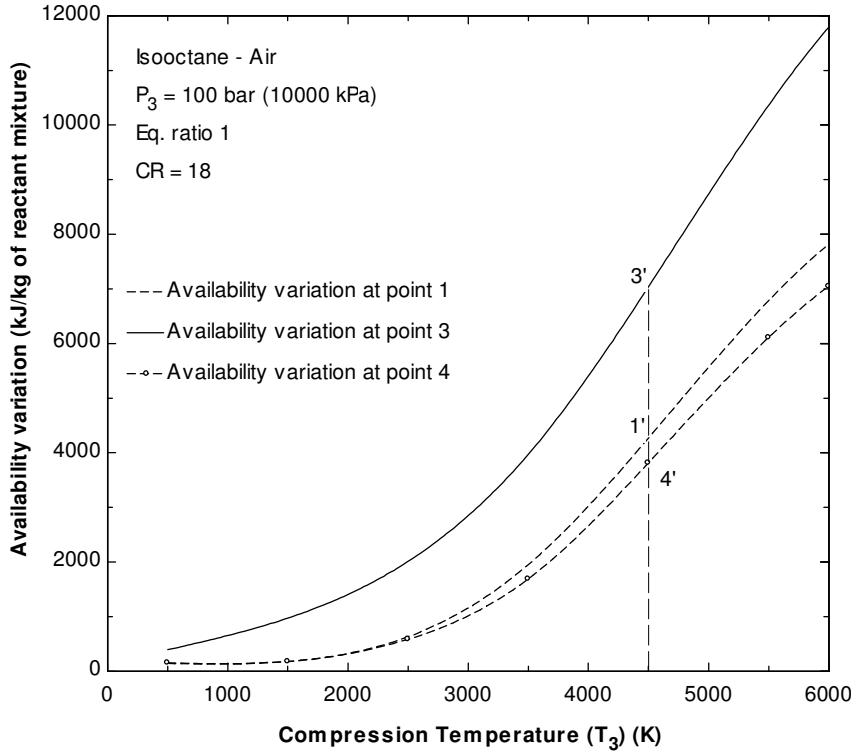

Fig. 18. Availabilities as a function of compression temperature for isooctane-air at 10000 kPa compression pressure, Φ = 1.0 and CR = 18.

The availability at three states of the processes (at the beginning of the compression (point 1), at the end of compression (point 3) and at the end of expansion (point 4)) increases

almost linearly for the higher compression temperatures. This is in consistent with the literature of Caton [4] and Chavannavar [8]. As the temperature of the mixture increases, the thermo-mechanical availability, which is governed by pressure and temperature of the model, increases and so the availabilities at points 1, 3 and 4 increase. At lower temperatures (about 500 K), the thermo-mechanical component of the availability is very small and the difference in the states 1, 3 and 4 are purely due to the chemical availability component of availability.

The increasing availability trends of the states 1, 3 and 4 are similar but not the same. This is due to the differences in which the three states exist in the model for the same amount of mixture mass. At state 3, the species of the mixture are in equilibrium and are at high compression temperature and pressure obtained due to the compression of species. At state 4, again, the species are in equilibrium but the temperature and pressure are lower due to the expansion of the species. At state 1, the temperature and the pressure are low but the species are not in equilibrium, each being placed in different cylinders. As a result, the availability at three points for a particular temperature is different, the availability at point 3 being the highest. The availabilities at 6000 K compression temperature are 7000, 7800 and 11800 kJ/kg of mixture for states 4, 1 and 3 respectively.

The points on the intersection of the vertical dashed line and the three availability variation curves, 1', 3' and 4' are the availabilities at points 1, 3 and 4 respectively of the processes when the compression temperature is 4500 K. The vertical distance between the points 3'–1' represents the work consumed by the model in compressing the species in the compression cylinders. The distance between the points 3'-4' represents the work developed by the model. Thus, the distance between 1' and 4' represents the net work developed by the model. For the considered case, as the compression temperature (T_3) increases, the distance between the points 1 and 4 increases and so the net work and the efficiency of the model increase.

From the above discussion, it is clear that point 3, which is the end of the compression process, plays a major role in work consumption and work extraction calculations. The positions of the points 1 and 4 are dictated by the position of point 3. As the compression temperature increases, more and more species are formed at the end of the compression process due to dissociation and hence more and more extraction of work is possible. This is in line with the literature of Keenan [10] and Obert [11] from which this model was developed.

Fig. 19 shows the variation of the partial pressure of species, as they are expanded isentropically and in equilibrium in the expansion cylinder for the base case (compression temperature 2500 K). The partial pressure of the species is dependent upon the amount of species, so these variations also represent the species variation.

The expansion process 3-4 starts at a pressure of 10000 kPa and at a relative volume of 1. It is presented by a thick continuous line in fig. 19 which represents the total pressure in the expansion cylinder. The expansion continues until the compression ratio of 18 is reached. The curves below the thick line represent the variation of partial pressure of the species as they are expanded in equilibrium in the expansion cylinder. The sum of the partial pressures is the total pressure during expansion.

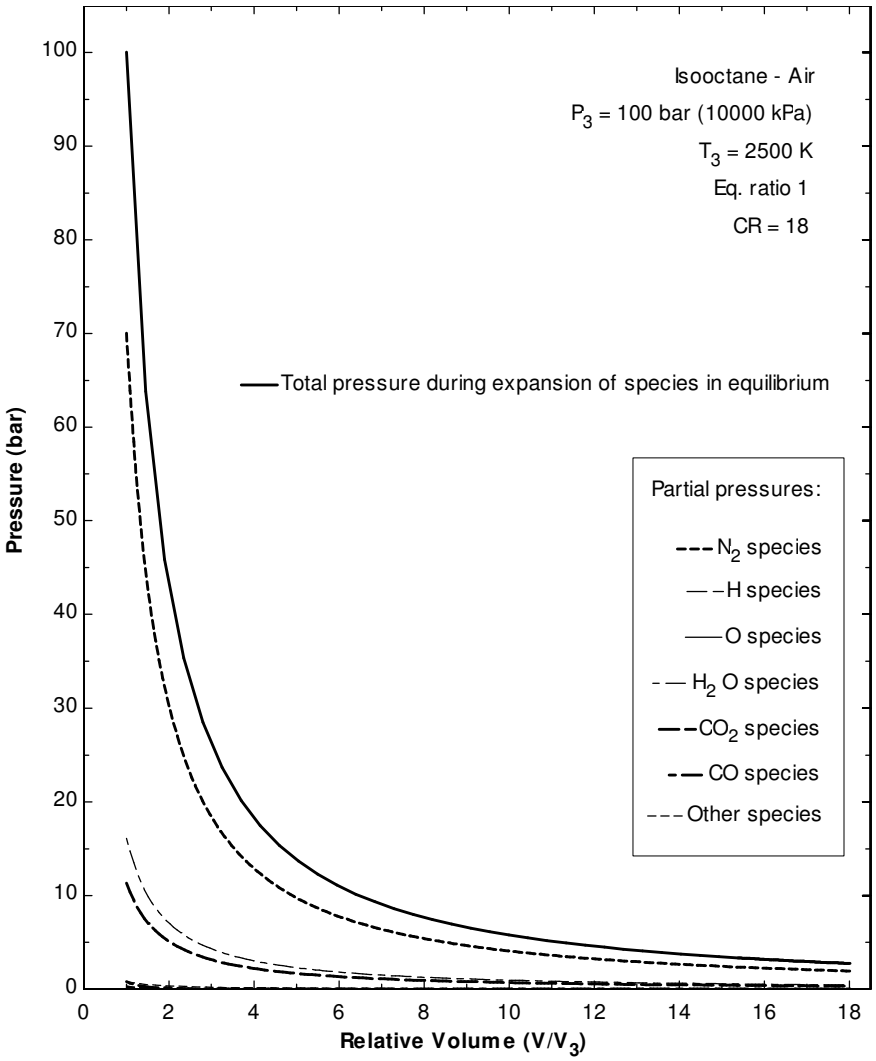

Fig. 19. Partial pressures of the species and the total pressure of the mixture, during isentropic expansion, as a function of relative volume for isooctane-air at 2500 K compression temperature, 10000 kPa compression pressure, Φ = 1.0 and CR = 18.

For a compression temperature of 2500 K, when the relative volume is 1, the number of species formed due to dissociation are very few, namely N_2, H_2O, CO_2 and some other species in small amounts. But for the case of higher compression temperature (6000 K), illustrated in fig. 20, the results are different.

Fig. 20 shows the variation of partial pressures of the species during the expansion process 3-4 when the compression temperature is 6000 K.

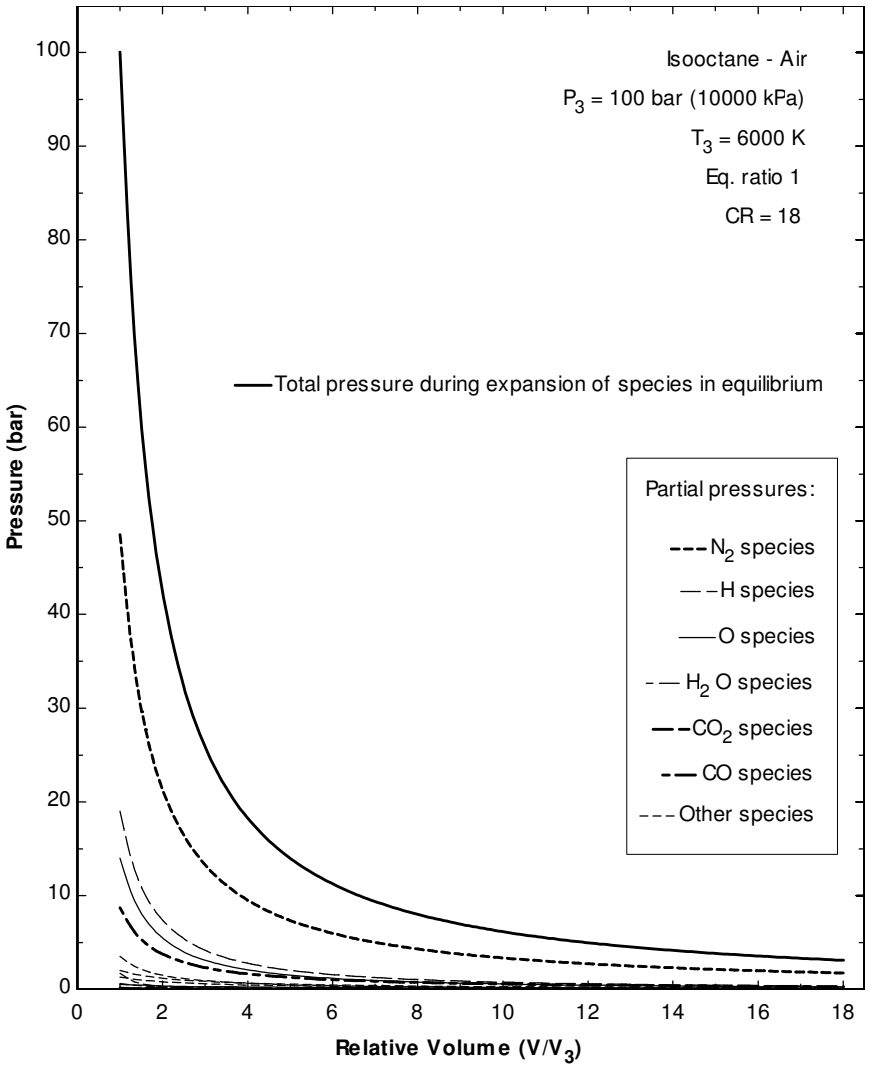

Fig. 20. Partial pressures of the species and the total pressure of the mixture, during isentropic expansion, as a function of relative volume for isooctane-air at 6000 K compression temperature, 10000 kPa compression pressure, Φ = 1.0 and CR = 18.

When the expansion process starts from the same compression pressure (10000 kPa) and same relative volume of 1, as for the earlier case, but at higher compression temperature (6000 K), the number of species formed due to dissociation is more at state 3 as compared to when the compression temperature was 2500 K. This is purely due to the high compression temperature. For such high temperatures more dissociation of species occur, resulting in more number of species.

As per the concept [10] of this model, more number of species is one of the requirements for the work generation. This is because when higher number of species is expanded following the most stable states of equilibrium, the work extraction from the system is possible. The higher the number of species during expansion, the greater is the work produced. Since, in the case of higher compression temperature of 6000 K, the number of species is higher, more work can be extracted than in earlier case of 2500 K.

Hence, for 10000 kPa compression pressure, it can be concluded that as the compression temperature increases, the thermal efficiency increases.

Effects of compression temperature in combination with low compression pressure (1000 kPa)

The compression pressure considered in the above cases was 10000 kPa. To study the effect of compression temperature at lower compression pressures, the model will be analyzed for 1000 kPa compression pressure, in this part of the section.

Fig. 21 shows the variation of pressure as a function of relative volume for a compression temperature of 3500 K. The equivalence ratio and compression ratio are the same (1.0 and 18, respectively) for consistent comparison with the earlier case of 10000 kPa compression pressure.

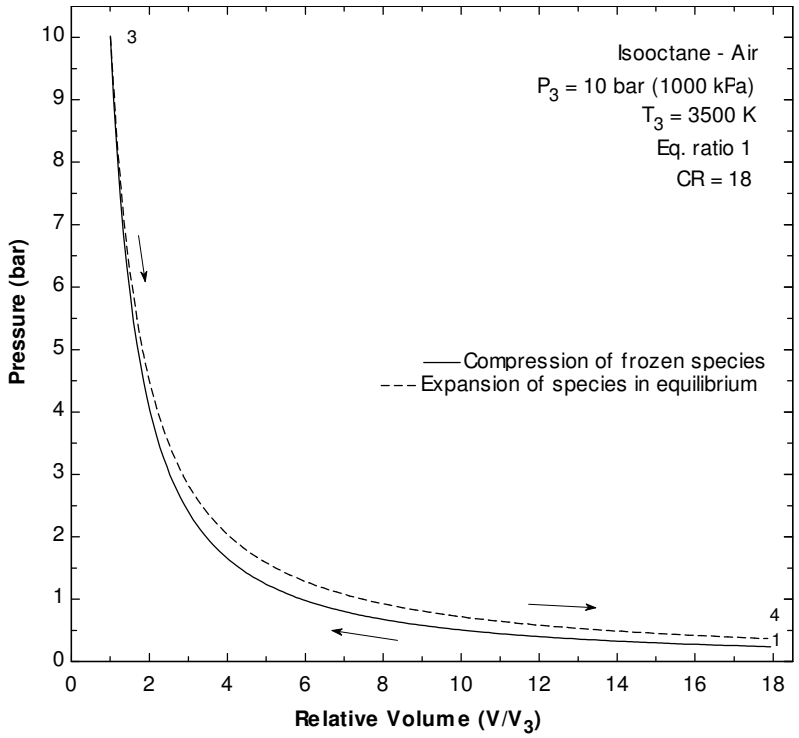

Fig. 21. Variation of pressure as a function of relative volume for isooctane-air at 3500 K compression temperature, 1000 kPa compression pressure, Φ = 1.0 and CR = 18.

The species are compressed in the compression cylinder from a relative volume of 18 (point 1) to a relative volume of 1 (point 3), and are then expanded back to the original relative volume of 18, to extract the work developed by the model. The area between the expansion and the compression curves represents the work developed by the model for 3500 K compression temperature case.

To study the behavior of the model and see the work generation trend for varying temperatures, the model was allowed to operate for a range of compression temperatures (500 K to 6000 K) and a constant compression pressure of 1000 kPa. For each of these compression temperatures, the work by mixture and fuel was calculated, which is presented in fig. 22.

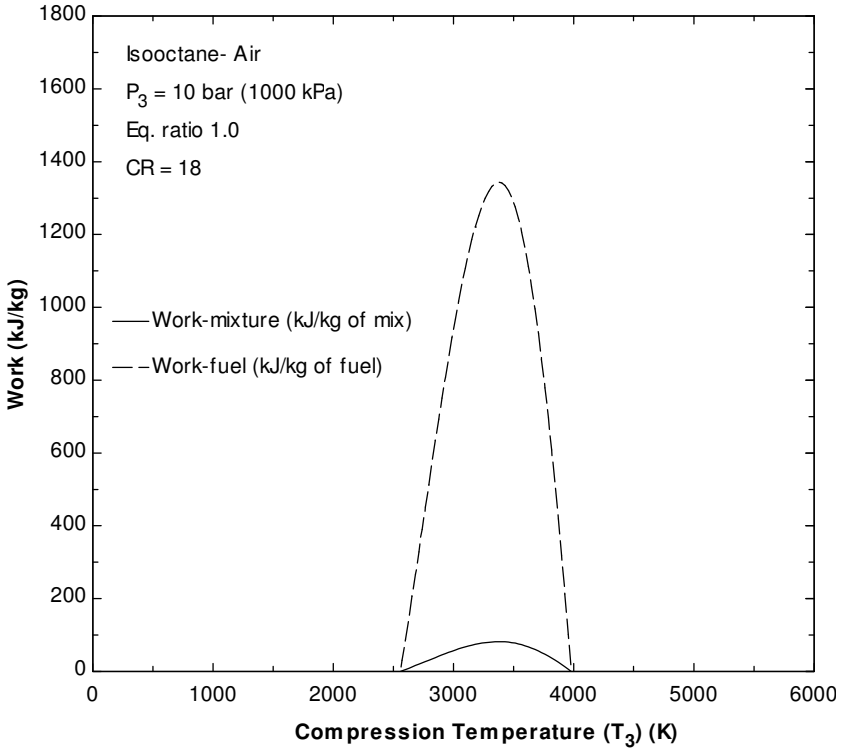

Fig. 22. Work as a function of compression temperature for isooctane-air at 1000 kPa compression pressure, Φ = 1.0 and CR = 18.

Fig. 22 shows the net work for 1000 kPa compression pressure and for a range of compression temperatures. The work is produced only for 2600 K – 4000 K temperature range. This is in contrast to the results discussed for the high compression pressure case (10000 kPa) where the work developed by the model increased monotonically with temperature and was never zero at higher temperatures (4000 K to 6000 K). The maximum work developed here, is 13400 kJ/kg of fuel and the work developed for the case in fig. 21 (3500 K compression temperature) is 12800 kJ/kg of fuel.

Fig. 23 shows the efficiency variation of the model for a range of compression temperatures.

The efficiency of the model is zero from 0 K to ~2600 K compression temperature. It then rapidly increases to reach 3% at 3400 K and later it sharply falls back to zero as temperature is increased to 4000 K. For the temperatures greater than 4000 K, the percentage efficiency is again zero. The efficiency being linear function of the work follows the trend similar

to that followed by fuel work in fig. 22. To better understand the work and efficiency trends, the availability variations are studied.

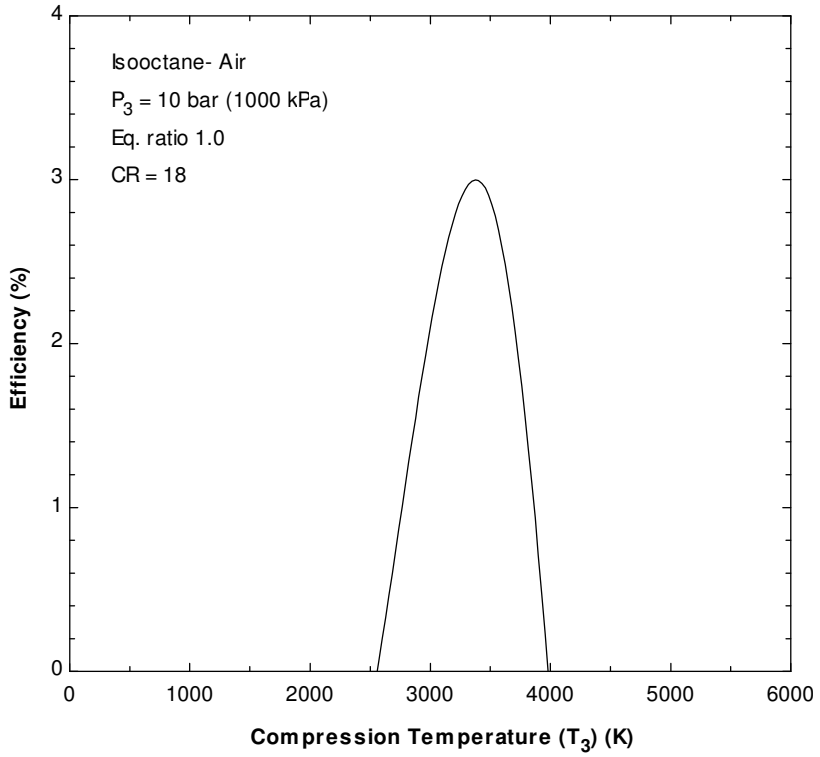

Fig. 23. Percentage efficiency as a function of compression temperature for isooctane-air at 1000 kPa compression pressure, Φ = 1.0 and CR = 18.

Fig. 24 shows the variation of availabilities at state 1, 3 and 4 as a function of compression temperature. As discussed earlier, the vertical distance at any compression temperature, between availability curves for points 3 and 1 represent the work consumed by the model in compression of the species while the distance between curves 3 and 4 represents the work developed by the system. Thus, the net work developed by the system can be found by analyzing the between availability curves for points 1 and 4 for a particular compression temperature. If this difference is positive i.e. the availability at state 1 is greater than that at state 4, the net work is developed by the system. If the availability difference is negative, no net work is developed; in fact some work is consumed by the system for its operation.

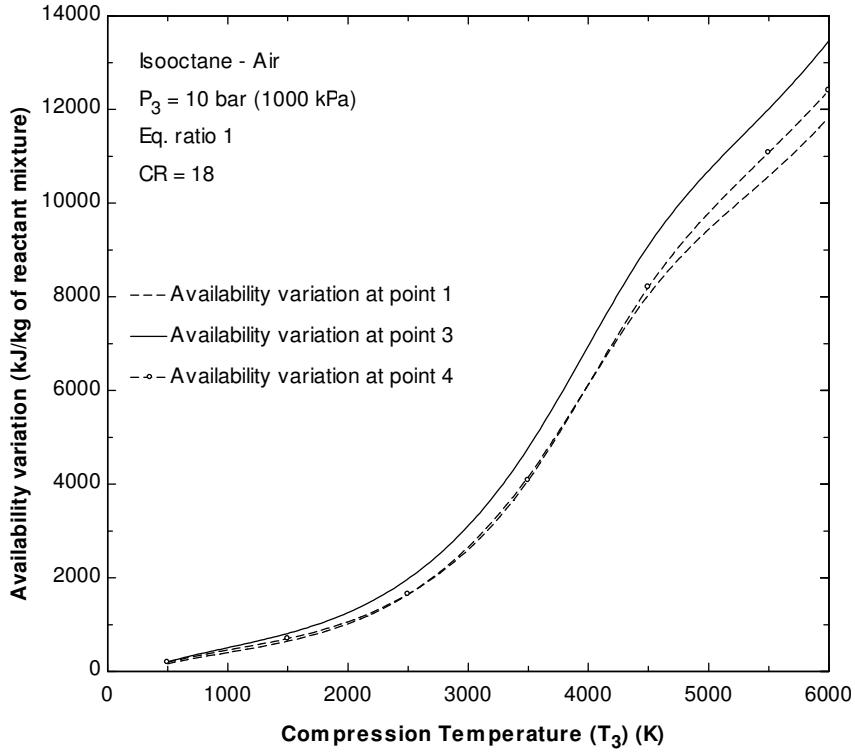

Fig. 24. Availabilities as a function of compression temperature for isooctane-air at 1000 kPa compression pressure, Φ = 1.0 and CR = 18.

The calculations show that, for temperatures 2600 K to 4000 K, the difference between the availability curves at points 1 and 4 are positive, hence some work is delivered by the model (as shown in figs. 22 and 23). While for the other compression temperatures, the difference being negative, work is consumed by the model.

To analyze the reason for zero efficiency, the behavior of the model was examined at compression temperatures of 500 K (compression temperature lower than 3500 K where efficiency was zero) and 6000 K (compression temperature greater than 3500 K where again efficiency was zero) and their corresponding P-V diagrams are shown in figs. 25 and 26.

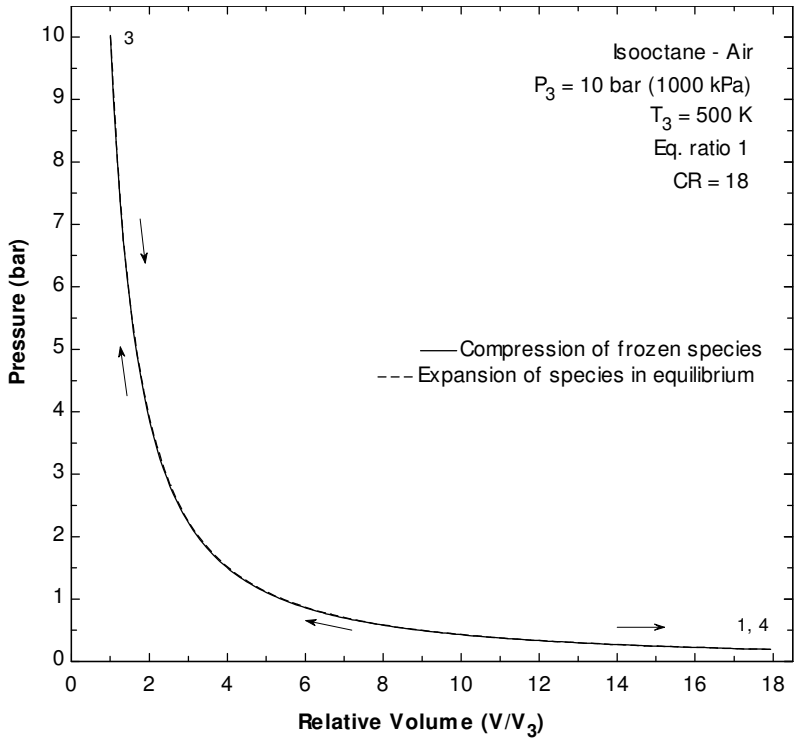

Fig. 25. Variation of pressure as a function of relative volume for isooctane-air at 500 K compression temperature, 1000 kPa compression pressure, Φ = 1.0 and CR = 18.

Fig. 25 shows the behavior of the model on P-V diagram for the compression temperature 500 K. The other parameters - compression pressure, equivalence ratio and compression ratio are held constant as in the earlier case – 1000 kPa, 1.0 and 18 respectively. It can be seen from the figure, that the path followed during the compression process from point 1 to point 3 (1000 kPa compression pressure and 500 K compression temperature) is the same as that followed by the expansion process from point 3 to 4. As a result of this, points 1 and 4 coincide and the area (which represents the work transfer) between the expansion and the compression curves is almost zero. In fact, in some small part of fig. 25, a small amount of negative work is developed (which is not discernible due to the scale of the plot). To study this unusual trend, analysis of the species variation during equilibrium expansion is necessary, which will be illustrated after the examination of P-V diagram for 6000 K compression temperature.

Fig. 26 shows the P-V diagrams for another zero efficiency condition, but this time at compression temperature greater than 3500 K (i.e. at 6000 K). The fig. 26 also shows the superimposed P-V diagram for the compression temperature 3500 K for direct comparison.

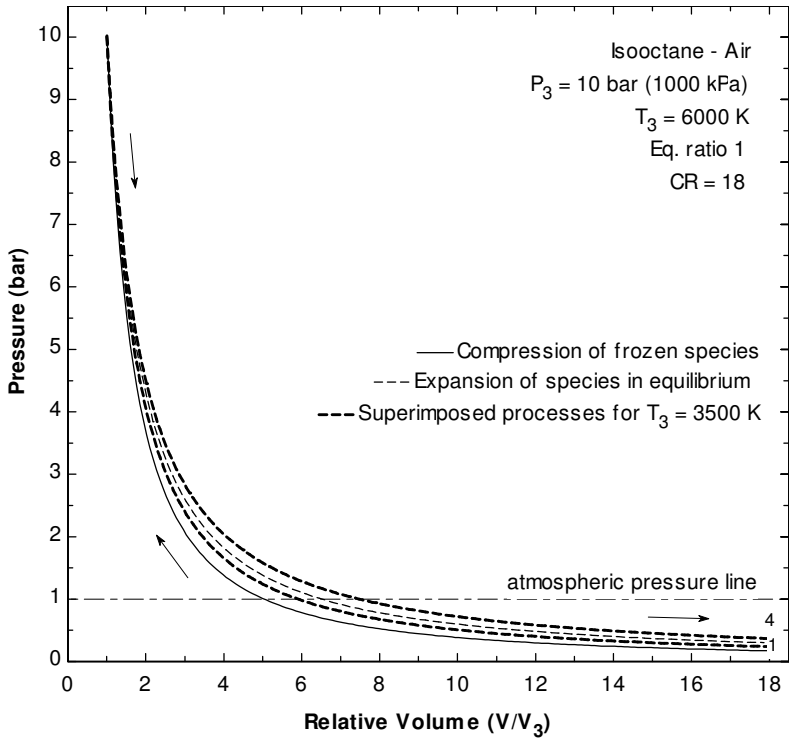

Fig. 26. Variation of pressure as a function of relative volume for isooctane-air at 3500 K and 6000 K compression temperatures, 1000 kPa compression pressure, Φ = 1.0 and CR = 18.

When the species (at 1000 kPa compression pressure and 6000 K compression temperature) are expanded, the pressure at state 4 decreases and goes below the atmospheric pressure. As discussed earlier, the position of points 4 and 1 are dictated by the position of point 3. So, for low compression pressure of 1000 kPa, point 1 is also seen to fall below atmospheric pressure line. As a result of this, the entire P-V diagram shifts downwards, some part being below the atmospheric pressure line. The area between the expansion and the compression curves below atmospheric pressure line indicates the negative work. This negative work is the result of the work (i.e. the pdv work) consumed in displacing the surrounding atmosphere (which is at higher pressure) on the other side of the piston. This results in the loss of work from the net work developed by the model. This loss being higher than the net work developed, the efficiency is zero at 500 K compression temperature.

The negative pdv work is also seen for the operating conditions – 1000 kPa and 3500 K, which is superimposed on the P-V diagram in fig. 26. However, for this case, the area under the

atmospheric pressure line is comparatively smaller, than when the compression temperature was 500 K. This results in comparatively lower loss of work due to the displacement of the surroundings, allowing the model to produce small amount of net work which further results to positive efficiency.

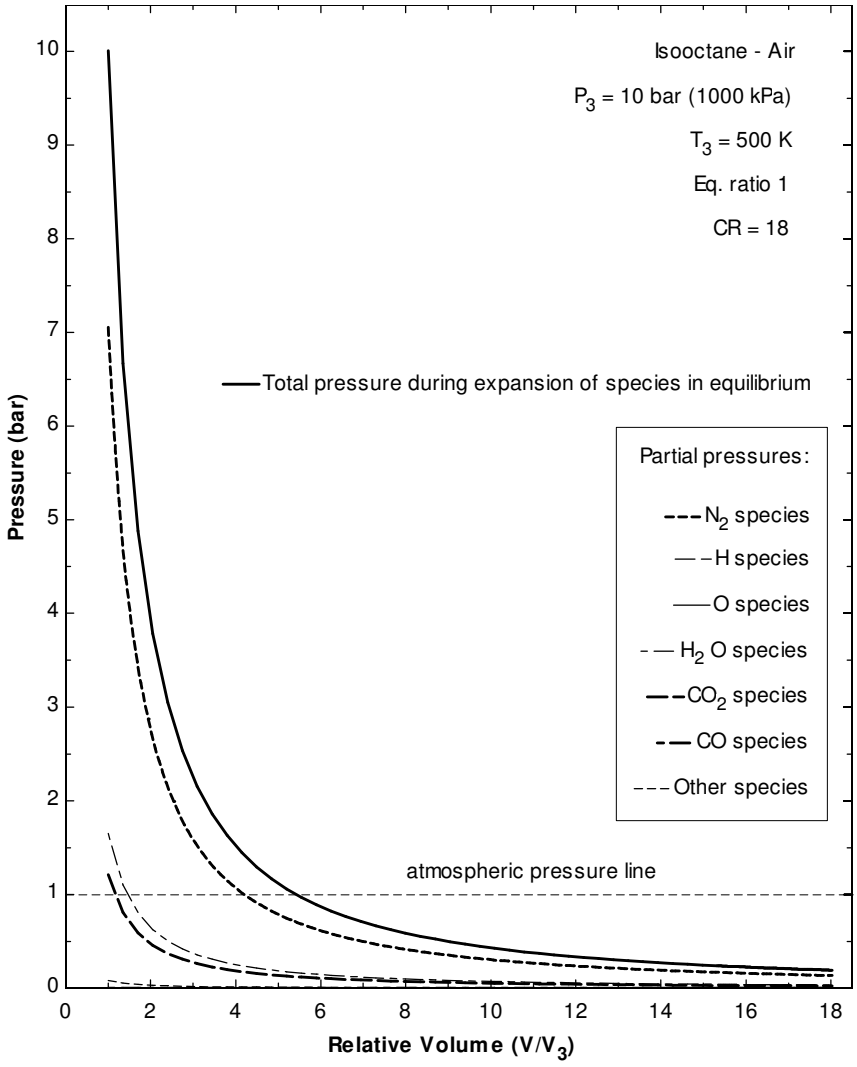

Fig. 27. Partial pressures of the species and the total pressure of the mixture, during isentropic expansion, as a function of relative volume for isooctane-air at 500 K compression temperature, 1000 kPa compression pressure, Φ = 1.0 and CR = 18.

To study the differences in the three typical cases (500 K, 3500 K and 6000 K compression temperatures) selected above, from the view point of species variation, the following study is conducted. This study helps to understand the dependence of the work transfer on the species variation.

Fig. 27 shows the partial pressure variation of the species during the expansion process for 500 K compression temperature. The number of species at point 3, (where the species mix instantaneously at the end of isentropic compression) depends upon the thermodynamic conditions at that state. At 500 K compression temperature, the dissociation of the species is less due to the lower temperature. The major species seen are those of N_2, H_2O CO_2 and small amounts of other species which include argon. The lower number of species leads to development of less work. This is because, for lower dissociation the composition of the species is almost similar during the expansion and the compression processes. As a result, the path followed by both the processes almost coincides with each other and hence no work is developed by the model. This is in conformance to the earlier results which indicated that more species at high temperature (which when expanded along the most stable path) generate more work.

The very small amount work that can be obtained due to few species at state 3 further gets negated by the work done by the surroundings (negative work) as the species are expanded below the atmospheric pressure in the expansion cylinder.

Fig. 28 shows the variation in partial pressure of the species during equilibrium expansion from 1000 kPa pressure when the compression temperature is 3500 K. The number of species formed due to dissociation is higher as compared to when the compression temperature was 500 K. As a result, more work can be obtained and this is in consistency with fig. 22 and 23. In fig 28, the point ‘p’ denotes the condition when the pressure in the expansion cylinder is the same as that of the surrounding atmosphere during expansion.

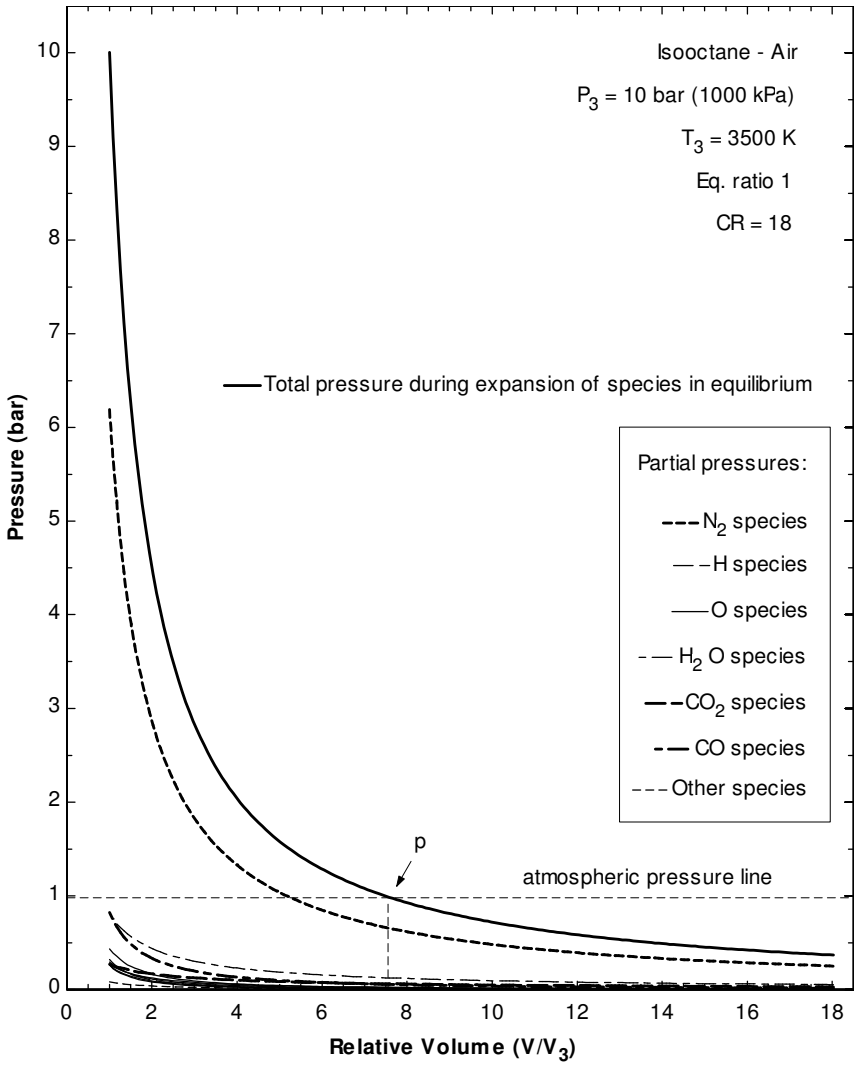

Fig. 28. Partial pressures of the species and the total pressure of the mixture, during isentropic expansion, as a function of relative volume for isooctane-air at 3500 K compression temperature, 1000 kPa compression pressure, Φ = 1.0 and CR = 18.

Fig. 29 shows the variation of species during expansion process when the compression temperature is 6000 K and the compression pressure is 1000 kPa. Due to higher compression temperature the number of species formed upon dissociation is very high. This number is even greater than when the compression temperature was 3500 K, in the earlier case. This is because dissociation is the temperature dependent phenomenon. It increases with temperature. However, in contrast to the earlier case, the work developed decreased for higher dissociation of

species instead of increasing as per the standard explanation of the model's concept followed until this point of study. This is due to lower compression pressure.

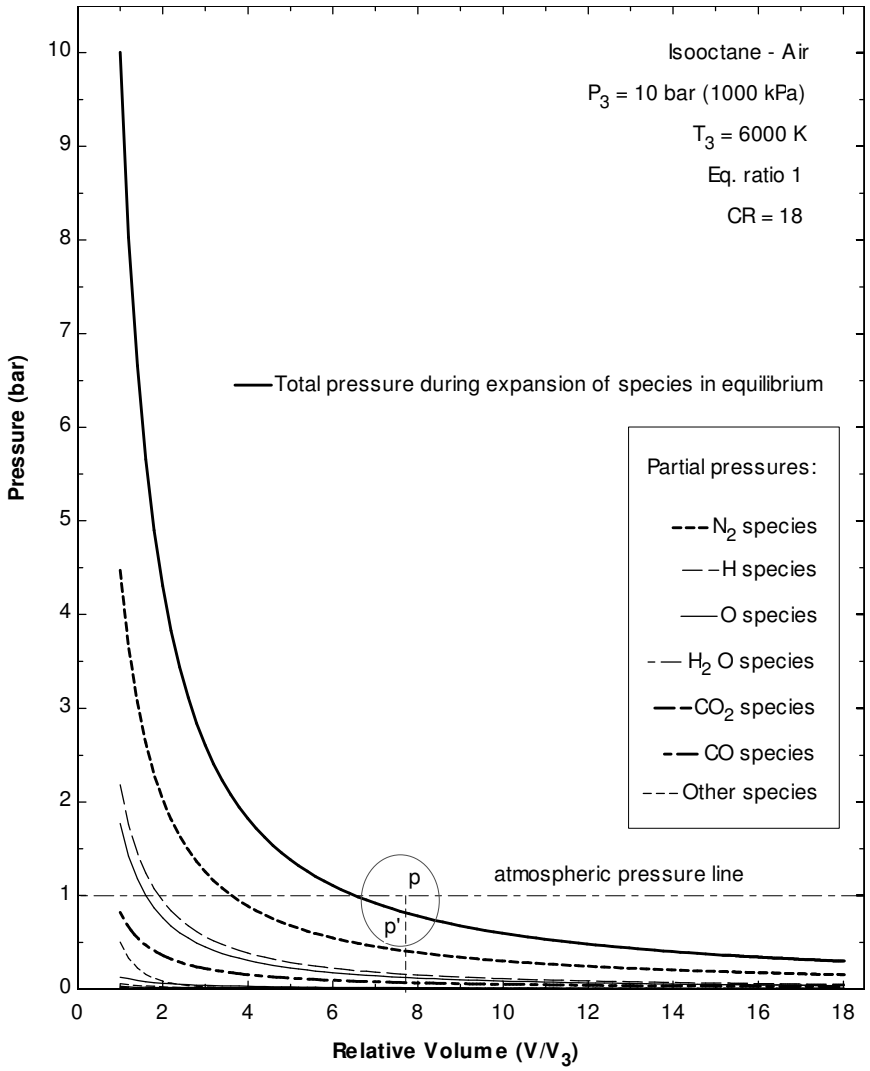

Fig. 29. Partial pressures of the species and the total pressure of the mixture, during isentropic expansion, as a function of relative volume for isooctane-air at 6000 K compression temperature, 1000 kPa compression pressure, Φ = 1.0 and CR = 18.

For 1000 kPa compression pressure and 6000 K compression temperature, the number of species formed is so high that the partial pressure of the individual species is reduced to a

very small value. Expansion of these low pressure species results in the early fall of the total pressure below the atmospheric pressure line as shown in fig. 29. The point ‘p’ which was defined as the point on the expansion curve when cylinder pressure is equal to the atmospheric pressure, for the case of 3500 K compression temperature, is seen to have shifted vertically downwards from p to p’. As a result of this, the work done by the surrounding on the model is more in the case 6000 K compression temperature, leading to zero efficiency.

However, for the case of 10000 kPa compression pressure, which was considered at the beginning of this section, even at higher temperatures, the work developed by the model increased almost linearly with compression temperature. This is because, in that case, the higher temperature was accompanied by the higher compression pressures which suppressed the dissociation, producing less negative work.

Effects of compression temperature in combination with rich mixture (equivalence ratio of 2.0)

The earlier cases of study involved variation in compression pressures for the same temperature range 500 K to 6000 K for stoichiometric mixtures. This part of the study will deal with effects of compression temperature on the efficiency when the mixture is rich in fuel. Except for an equivalence ratio of 2.0, all the other parameters will be the same as defined for the base case, i.e. a compression pressure of 10000 kPa and a compression ratio of 18. The temperature range used for the analysis is again 500 k to 6000 K.

Fig. 30 illustrates the variation of work developed per total mixture mass and per fuel mass. Up to approximately 3200 K, the work developed by the model is zero. This is because of lower dissociation of species which in this case is due to the combined effect of lower temperatures and high pressure (10000 kPa). After 3200 K, as the compression temperature increases, more species are formed due to dissociation and hence more work is developed. The maximum work developed by the mixture is about 800 kJ/kg of mixture and that by the fuel is about 7450 kJ/kg of fuel.

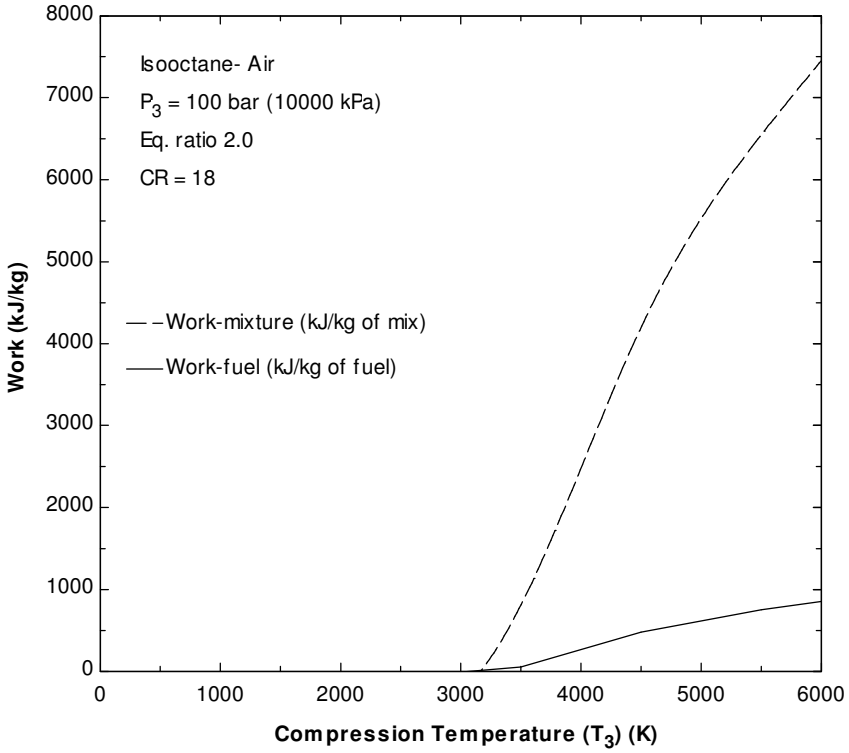

Fig. 30. Work as a function of compression temperature for isooctane-air at 10000 kPa compression pressure, Φ = 2.0 and CR = 18.

Fig. 31 shows the variation of the efficiency as a function of compression temperature. For the temperatures lower than 3200 K, the efficiency is zero, since also the work per total mixture mass and per fuel mass is zero as shown in the fig. 30. Then, as the work increases with temperature due to dissociation of species, the percentage efficiency also increases. The maximum thermal efficiency of the model at 6000 K is ~16.5%.

At higher compression temperatures (4000 K – 6000 K), the problem of excess dissociation, which causes reduction of pressures below atmospheric pressure during expansion (as seen in the earlier case when the compression temperature was 6000 K and compression pressure was 1000 kPa) is avoided because the compression pressure is comparatively high (10000 kPa) for this case. The higher pressure decreases the dissociation at high temperatures.

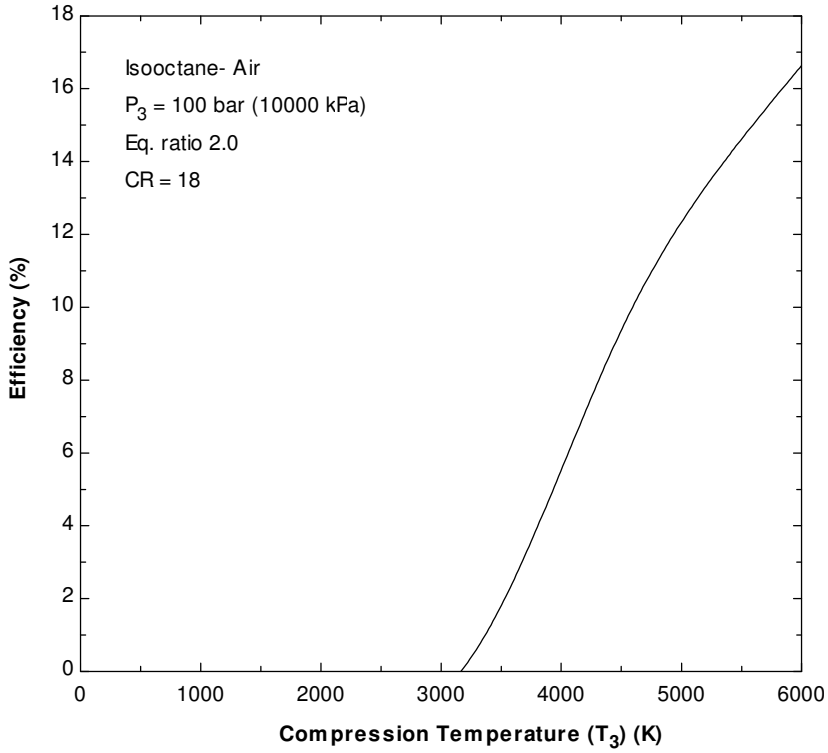

Fig. 31. Percentage efficiency as a function of compression temperature for isooctane-air at 10000 kPa compression pressure, Φ = 2.0 and CR = 18.

Fig. 32 shows the availability variations for a range of compression temperatures. Again, consistent with the work and percentage efficiency trends in the figures 30 and 31 respectively, the difference between the availability curves for points 4 and 1 (which represents the net work developed) increased only after 3200 K. For this case, the work and the percentage efficiency numbers are positive after this point.

For the temperatures below 3200 K, the availability difference is slightly negative, as the availability curve for point 4 is slightly higher than for point 1, resulting in more consumption of work than developed. At 500 K, the availability at point 1 and 4 coincides and hence no work can be extracted.

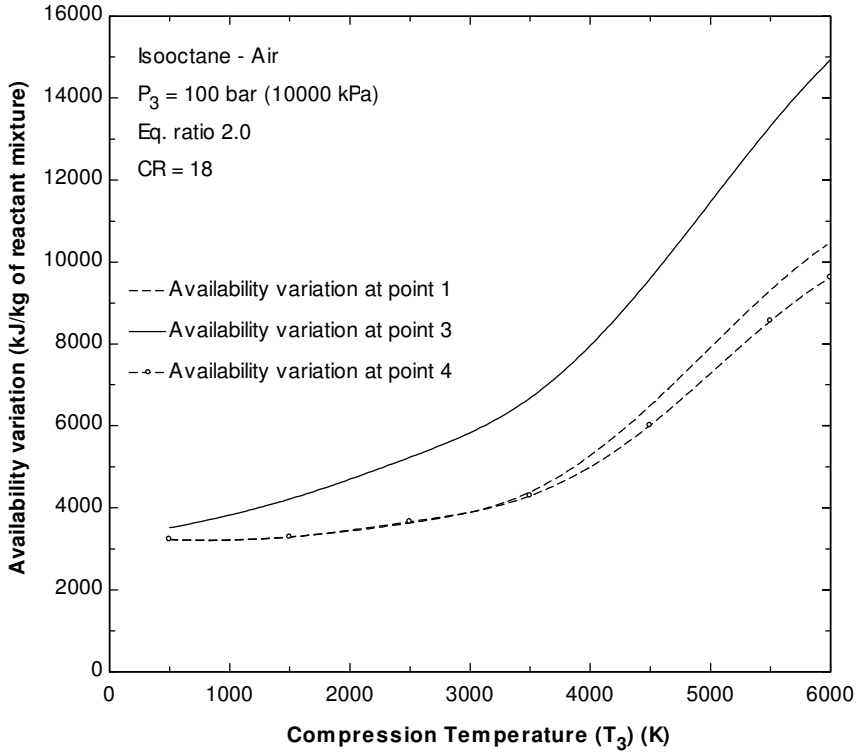

Fig. 32. Availabilities as a function of compression temperature for isooctane-air at 10000 kPa compression pressure, Φ = 2.0 and CR = 18.

Effects of compression temperature in combination with lean mixture (equivalence ratio of 0.2)

This part of the section investigates the effects of using lean mixtures. Fig. 33 shows the variation of the work with the change in compression temperature for mixture with equivalence ratio 0.2. The compression pressure and compression ratio are the same as that used for the earlier case of rich mixture, i.e. 10000 kPa and 18, respectively.

Again, for lower temperatures, no work is developed by the model and further as the compression temperature increases, the work developed also increases. At 6000 K, the work per total mixture mass is about 500 kJ/kg (37000 kJ/kg of fuel). These figures are different than those for the earlier case of rich mixture (equivalence ratio 2.0).

For the case of rich mixture, at 6000 K, the work per unit mass of fuel (7450 kJ/kg) is less than that for the lean case (37000 kJ/kg of fuel). This is because, when the mixture is rich, some of the fuel gets less air, resulting in incomplete utilization of the fuel. However, in the case of the lean mixture, the fuel is utilized fully, because the molecules of fuel get sufficient amount of air that it needs, and hence, the work per unit mass of fuel is higher for lean case. But, when

work per total mixture mass is considered, the rich mixtures (800 kJ/kg) are better than the lean mixtures (500 kJ/kg), at 6000K. This is because, even though there is incomplete utilization of fuel in the case of rich mixture, the work produced is still higher than that produced in lean case, because of the higher chemical availability.

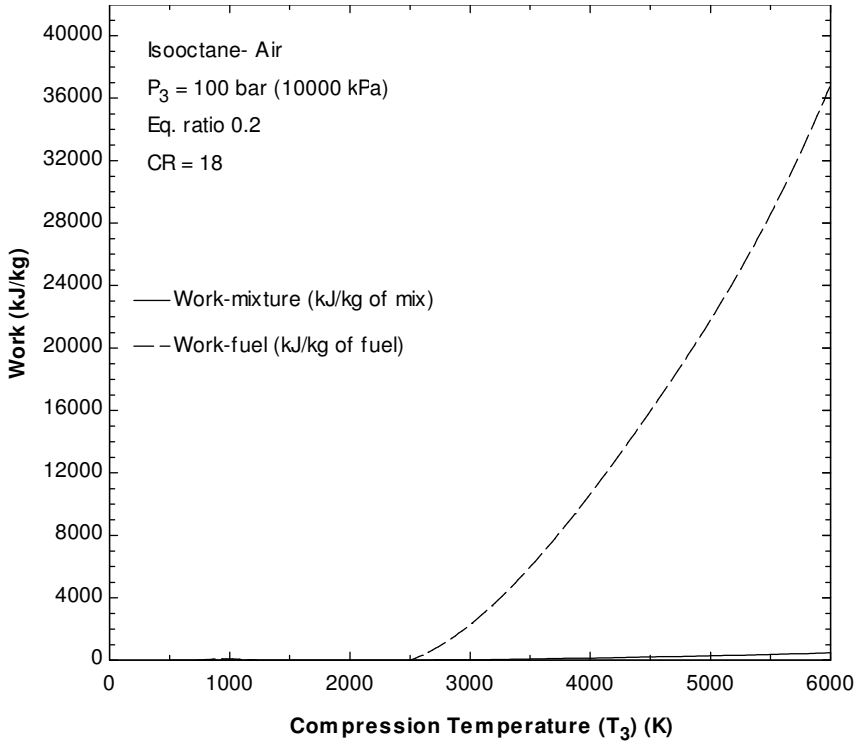

Fig. 33. Work as a function of compression temperature for isooctane-air at 10000 kPa compression pressure, Φ = 0.2 and CR = 18.

Fig. 34 shows the efficiency for the lean case, considered above for 10000 kPa compression pressure, for isooctane-air combination. Again, consistent with fig. 33, the trend followed by the efficiency variation for increasing compression temperatures is similar to that followed by the work developed per fuel mass. As the compression temperature increases, the percentage efficiency also increases. The efficiency of the model at 6000 K is highest and is higher than that noted for the rich mixture.

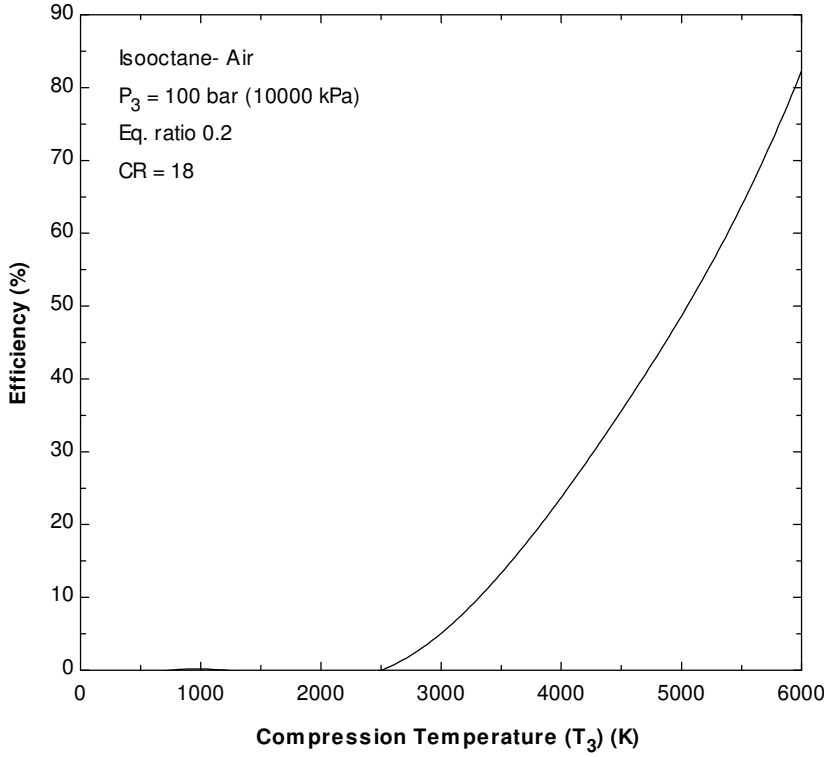

Fig. 34. Percentage efficiency as a function of compression temperature for isooctane-air at 10000 kPa compression pressure, Φ = 0.2 and CR = 18.

Fig. 35 shows the variation of availabilities at three crucial points of the model of hypothetical processes as a function of compression temperature. The availability differences between the curves for point 1 and point 4 increases and so the work generation increases with temperature, as was seen in figs. 33 and 34. However for the present lean case, the values of availability for all three points are lower than that noted for the rich case. This reduction of availability values is due to lesser available chemical energy of the fuel in lean mixture.

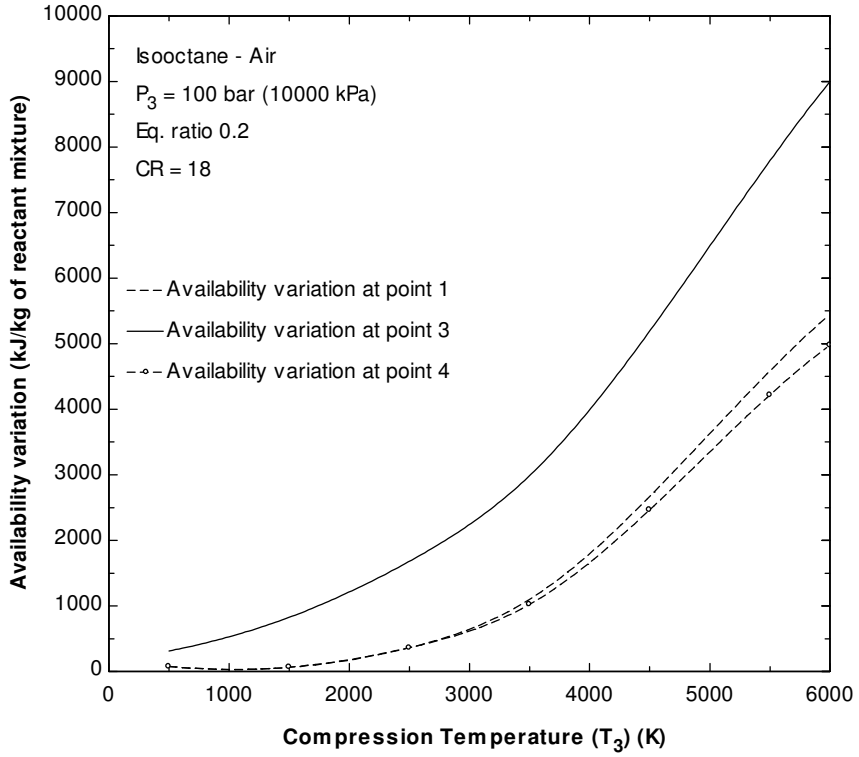

Fig. 35. Availabilities as a function of compression temperature for isooctane-air at 10000 kPa compression pressure, Φ = 0.2 and CR = 18.

As stated earlier and as illustrated in figs. 33, 34 and 35, the efficiency of the model is dependent upon the work done by the fuel, which in turn is directly proportional to the work done by the mixture. The work developed by the mixture is further dependent upon availability variations at points 1, 3 and 4 of the model. So to avoid repetitive discussions, the remaining literature of the thesis will only discuss efficiency trends. The trends for– availability variations, work done by fuel and mixture, can be found in appendix V for peculiar cases.

Effects of compression temperature in combination with high compression ratio (CR = 24)

In this part of the section, the effects of the compression temperature on the efficiency are studied for a higher compression ratio (24) and for a range of temperature (500 K to 6000 K). The other parameters of the base case will be the same as used earlier, i.e. compression pressure 10000 kPa and equivalence ratio 1.0.

Fig. 36 shows the variation of efficiency of the model as a function of temperature. For the initial temperature range (0 to 2000 K), the species are restricted from dissociation because

of high compression pressure (10000 kPa) in combination with lower compression temperatures. However, for temperatures greater than 2000 K, the species slowly starts dissociating and so the work that can be extracted during the expansion process, increases with temperature. The increased work results in increase in efficiency. The maximum efficiency at 6000 K is ~32%.

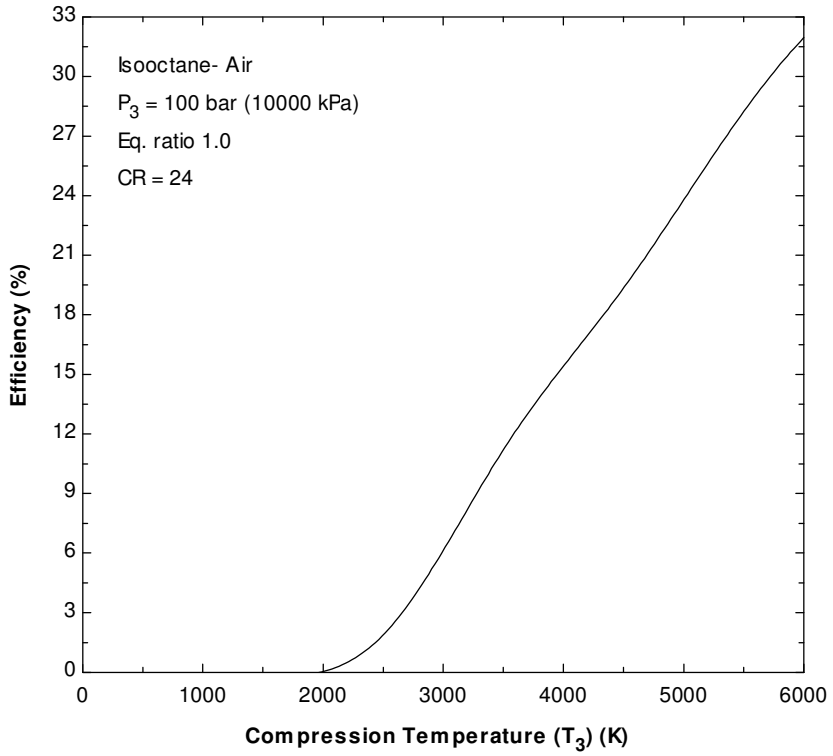

Fig. 36. Percentage efficiency as a function of compression temperature for isooctane-air at 10000 kPa compression pressure, Φ = 1.0 and CR = 24.

Effects of compression temperature in combination with low compression ratio (CR = 4)

In this part of the section, the analysis of the model for a lower compression ratio of 4 is discussed. The other parameters are kept the same as for the earlier case for direct comparison between the two cases.

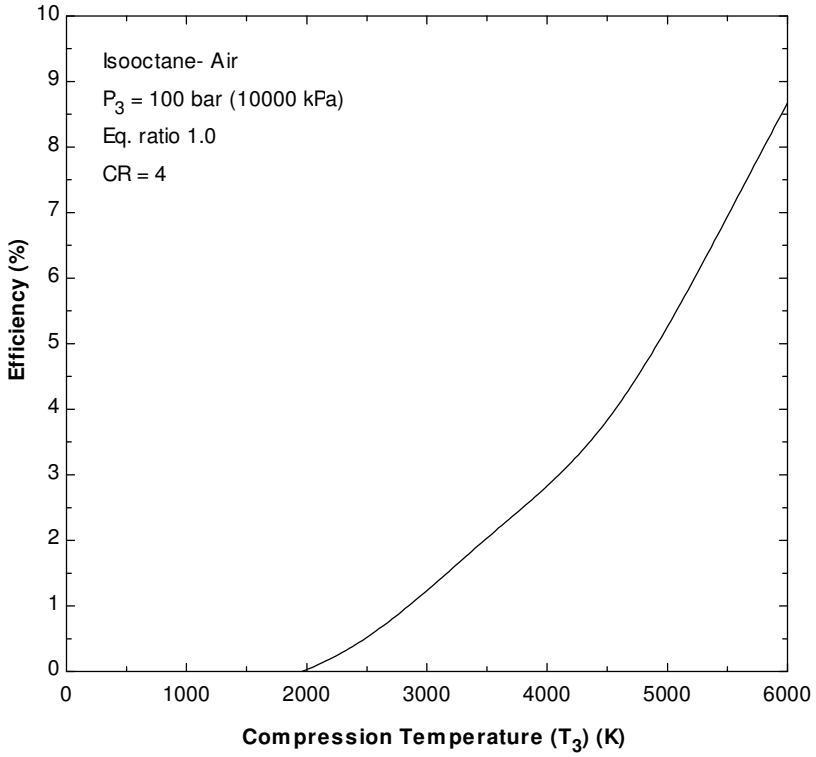

Fig.37. Percentage efficiency as a function of compression temperature for isooctane-air at 10000 kPa compression pressure, Φ = 1.0 and CR = 4.

Fig. 37 shows the efficiency as a function of the compression temperature. Again, until about 2000 K compression temperature, the number of species due to dissociation at point 3 (the end point of the compression process) are not enough to generate much work and so for the temperatures lower than 2000 K, the efficiency is almost nil. Then, as the temperature increases, efficiency of the model also increases.

The maximum efficiency of the model at 6000 K is noted to be about 8.7%. This number is too small in comparison to that seen when the compression ratio was higher (CR = 24) for the earlier case of study. This is because for higher compression ratios, the model has more opportunities for extracting work during expansion due to longer expansion stroke length. Of course, longer expansion strokes also mean longer compression strokes for a given compression ratio. But due to the deviating nature of the curves of expansion and compression, i.e. the point 3 is a common point for both the curves, while points 1 and 4 move apart as the volume increases; more work area on the P-V diagram can be trapped as the compression ratio is increased, resulting in higher net work.

However, from the above discussion, it may be inappropriate to conclude that the efficiency of the model is always proportional to the compression ratio. When the compression ratio is increased for a model operating at a particular compression pressure, after certain increase in compression ratio the efficiency of the model will decrease. This is due to the fact, excess compression ratio leads to over-expansion of the mixture in the expansion cylinder, causing the pressure to fall below the atmospheric pressure before the end of the expansion which results in work consumption by the model to displace the surroundings on the other side of the piston. The negative effect of the high compression ratio becomes more and more severe as the compression pressure is lowered.

Effects of compression temperature when oxygen is used as oxidant

In this case of study, a mixture of isooctane and oxygen is studied for a compression pressure of 10000 kPa, the compression temperature range is 500 K to 6000 K, the equivalence ratio is 1.0 and the compression ratio is 18.

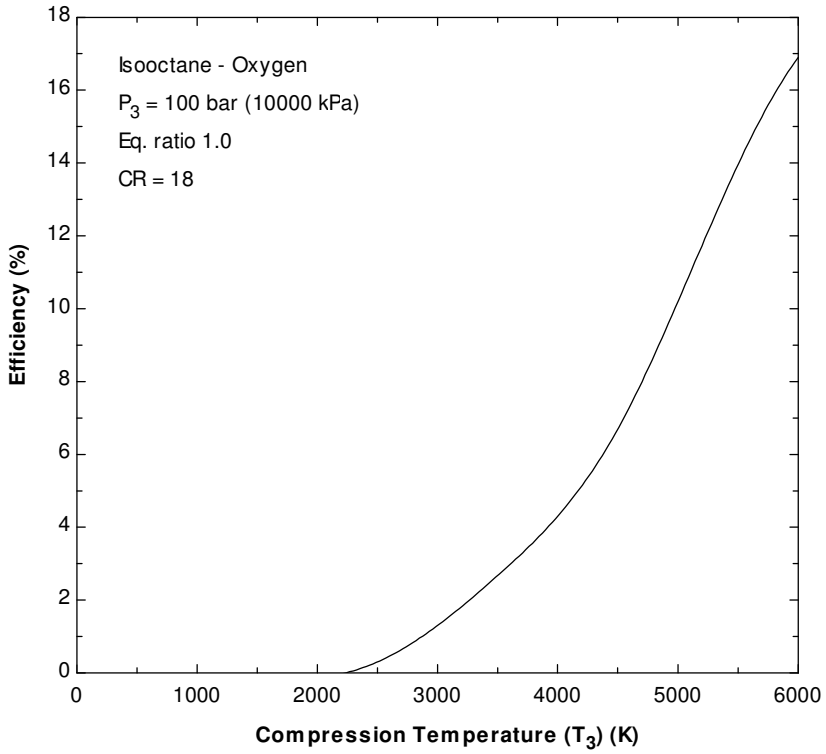

Fig. 38. Percentage efficiency as a function of compression temperature for isooctane-oxygen at 10000 kPa compression pressure, Φ = 1.0 and CR = 18.

Fig. 38 shows the efficiency as a function of compression temperatures. As seen earlier, for lower number of species due to dissociation at low temperature, the efficiency is zero. For temperatures higher than ~2300 K, the efficiency steadily increases, reaching ~16.9% at 6000 K. The efficiency when air was used as the oxidant was about 28% at 6000 K. The decrease in the efficiency when oxygen is used as an oxidant can be explained by comparing the work.

Fig. 39 shows the work as a function of compression temperatures ranging from 0 to 6000 K.

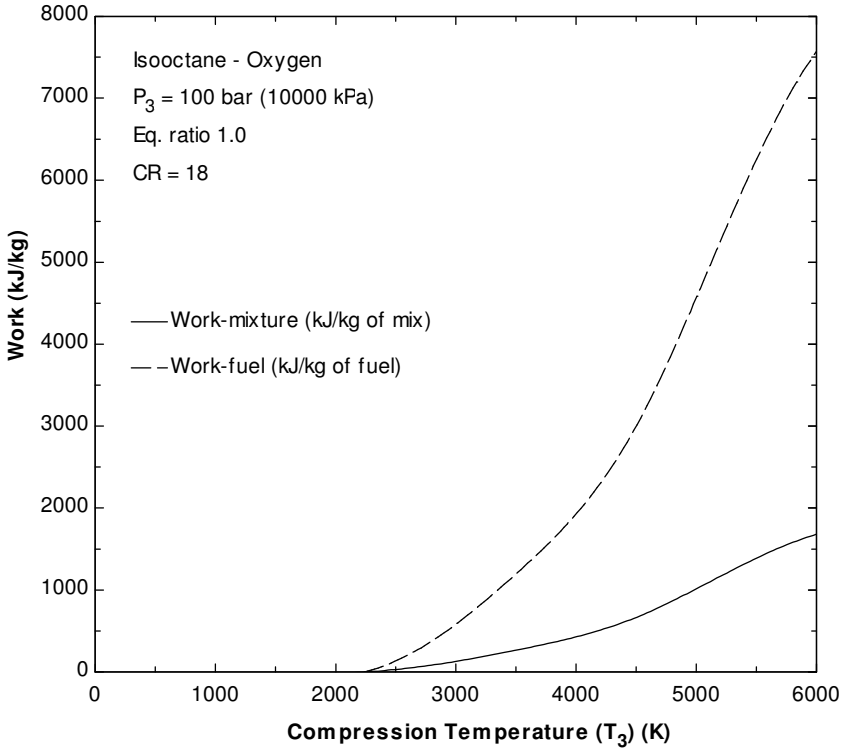

Fig. 39. Work as a function of compression temperature for isooctane-oxygen at 10000 kPa compression pressure, Φ = 1.0 and CR = 18.

As stated earlier, the efficiency is directly dependent upon the work. The work developed, when air was used as an oxidant, was about 12600 kJ/kg of fuel at 6000 K, which is only about 7500 kJ/kg of fuel when pure oxygen is used. This difference in numbers is because of the amount of oxidant in each case. For the same stoichiometric balance, the amount of air is

always greater (when air is used as the oxidant) than the amount of oxygen (when oxygen is used as the oxidant). As a result, when air was used, the mixture was comparatively lean. For lean mixtures, the fuel gets sufficient amount of oxidant that it needs to form products and hence the utilization of the fuel is better, resulting in more work.

However, for work per unit mixture mass, for rich mixture (when oxygen is used as an oxidant), the work produced is higher (1700 kJ/kg of mixture) as compared to when air was used (800 kJ/kg of mixture). This is because, even though there is incomplete utilization of fuel, when oxygen is used, the work per total mixture mass is still higher due to the higher chemical availability and less dilution.

Another reason for lower work developed per total mixture mass when air is used is because of the presence of nitrogen species. Nitrogen is comparatively more stable specie which requires very high temperature for its complete dissociation into nitrogen atoms. As a result of this resistance provided by nitrogen against dissociation, the number of species formed at the end of compression is less and so the work developed by the mixture is less, as compared to when pure oxygen is used as the oxidant.

The comparisons of the work and the efficiency, when air and oxygen are used as oxidants, can be found in the later part of this section.

Operation of model in a cycle

The current model is essentially made up of two main processes - the isentropic compression of species in the compression cylinders and the isentropic expansion of species in expansion cylinder. To extend this concept to a cycle, a process can be added at the end of the expansion process which can bring the species to the thermodynamic state at which state 1 exists. This can be done by using an appropriate heat transfer process 4-1.The resulting cycle would then be similar to that shown in fig. 40.

The process 0-1 will be the suction process where the species of the mixture will be taken inside the compression cylinders. The process 1-3 will be the isentropic compression of the species in the different compression cylinders. At point 3, instantaneous collection of species will take place in the collection chamber. The process 3-4 will be the expansion of the species, in equilibrium, in the expansion cylinder (the power stroke). The process 4-1 will be the heat transfer process, to bring the species back to the state 1. And finally, the process 1-0 will be the exhaust process during which the species of the mixture will be displaced out of the model.

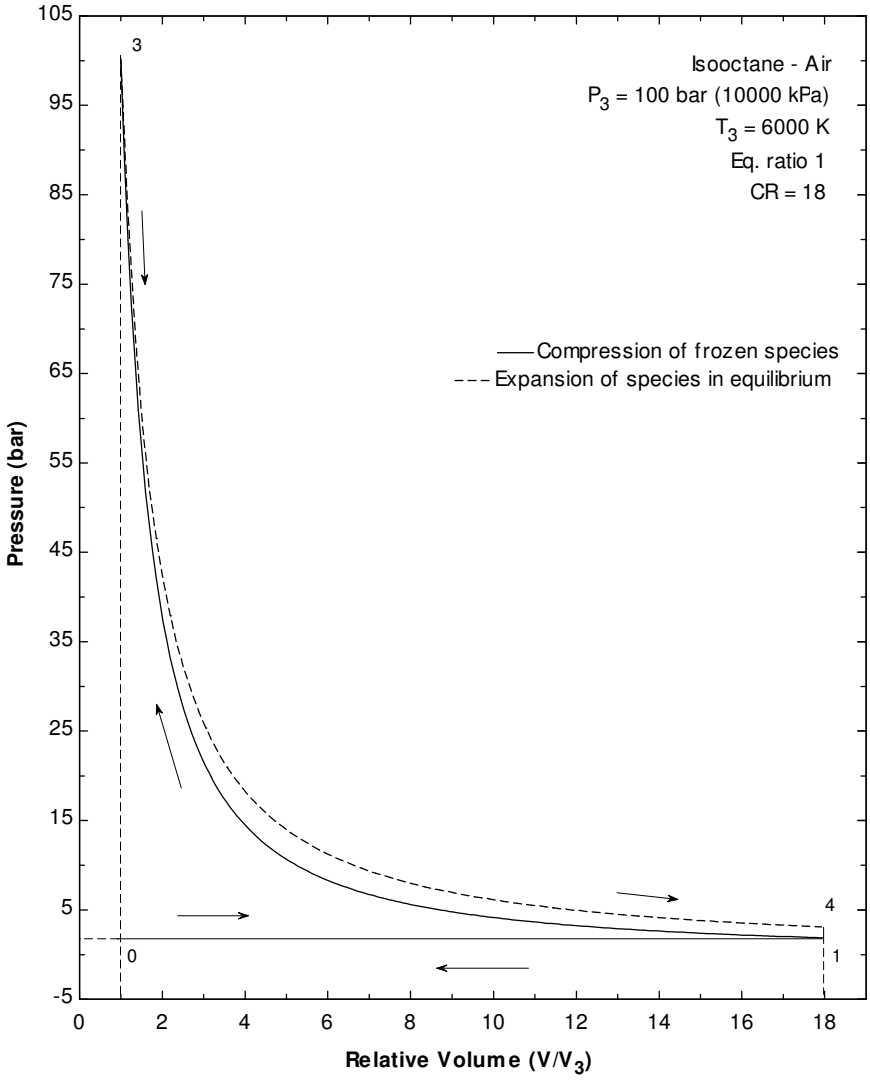

Fig. 40. Variation of pressure as a function of relative volume for model operating in a cycle using isooctane-air at 6000 K compression temperature, 10000 kPa compression pressure, Φ = 1.0 and CR = 18.

Parametric Study

The analyses completed so far were for the temperature range 500 K to 6000 K (for most of the cases), while the other parameters were held constant. To study the efficiency trend for the varying parameters with increasing temperatures, the parametric study was conducted. The parametric study provides basis for consistent comparison of the model for varying thermodynamic properties and allows the selection of the conditions which would provide the maximum efficiency.

Effects of compression pressure and compression temperature

This part of the section illustrates the results for a range of compression pressures (1000 kPa to 20000 kPa) and compression temperatures (500 K to 6000 K)

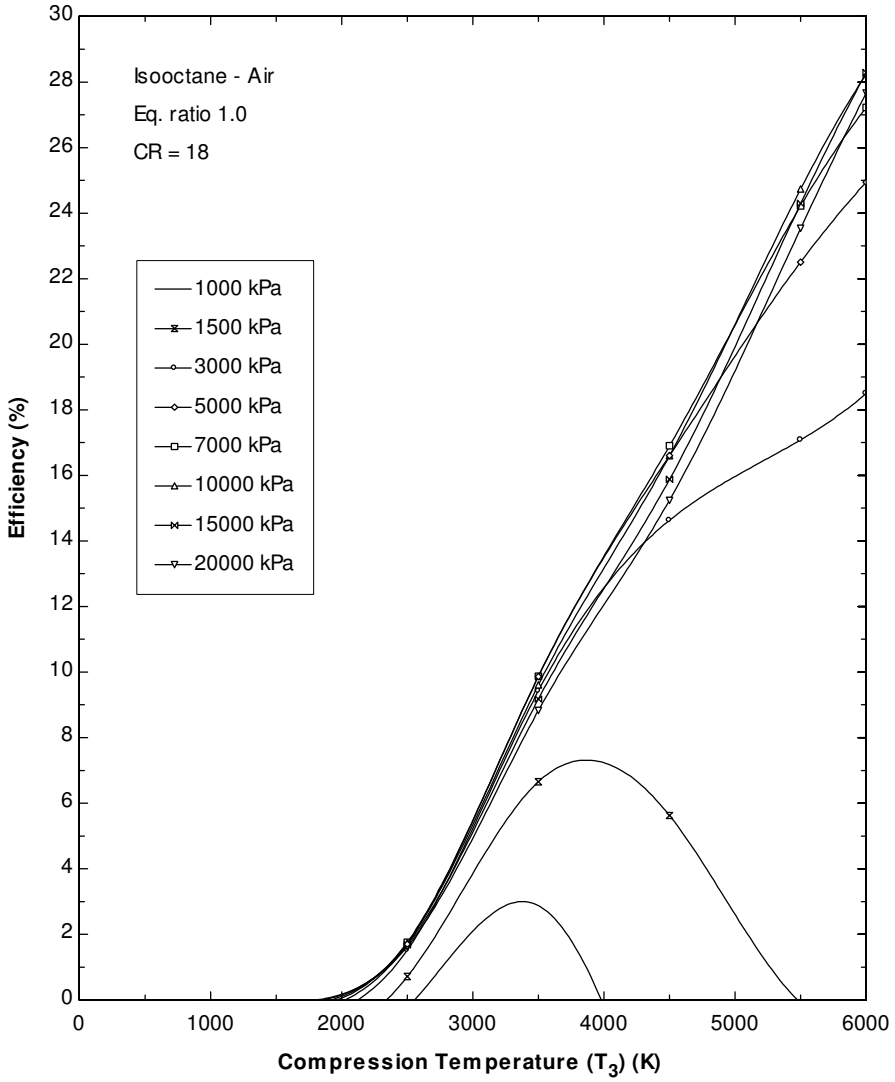

Fig. 41. Percentage efficiency as a function of compression temperature, for a range of compression pressures, for isooctane-air, Φ = 1.0 and CR = 18.

Fig. 41 shows efficiency as a function of temperature, for varying compression pressure, for an equivalence ratio of 1.0 and for a compression ratio of 18. For compression temperatures lower than 1900 K, the efficiency of the model for any compression pressure is zero.

For 1000 kPa compression pressure, until 2600 K the efficiency is zero. When the compression temperature is greater than 2600 K, the efficiency increases and continues to increase until the compression temperature is approximately 3400 K. Further increase in the compression temperature results in decrease in efficiency. The initial increase in efficiency with temperature is because as the compression temperature increases, the dissociation of the species at the end of compression increases, allowing more extraction of work when these species are expanded in equilibrium. However, after that when the temperature is greater than 3400 K, the dissociation is excessive for the 1000 kPa compression pressure, as a result of which partial pressures of each of the species reduces to such an extent that when they are expanded, the total pressure of the mixture falls below the atmospheric pressure, leading to the work loss in displacement of the surroundings. The maximum efficiency noted is ~3% for 1000 kPa compression pressure.

For 1500 kPa, the trend followed by the efficiency is similar to that seen for the earlier case. The initial increase in efficiency is the result of increase in dissociation of species while the later decrease in the efficiency curve is the result of the pressure of the mixture going below the atmospheric pressure causing loss of work. However, the distribution of this curve is spread for a larger range of temperatures.

The non-zero efficiency (in contrast to the earlier case when the compression pressure was 1000 kPa) for the compression temperature range of ~2350 K to 2600 K, is the result of the higher compression pressure (1500 kPa). Due to the higher pressure at the end of compression, there exists enough opportunity to extract work from the expansion process even for lower dissociation of species. This is because from the availability point of view, higher pressure increases the thermo-mechanical availability component of the availability allowing more opportunity to extract work. The decline of the efficiency curve after 4000 K compression temperature is also the result of higher compression pressure. When compression temperature is increased passed 3400 K, the dissociation of species is controlled by high pressure which suppresses dissociation. But however after 4000 K, due to excessive temperatures, the dissociation goes out of 1500 kPa reach, which causes loss of work due to expansion below the atmospheric pressure. Thus higher compression pressure allows higher efficiency, which is ~7.2% for 1500 kPa compression pressure.

Similarly, as the compression pressure is increased to 3000 kPa, 5000 kPa, 7000 kPa, 10000 kPa, 15000 kPa and 20000 kPa, the efficiency trends followed by the model are always

'dome' type. Until certain initial range of compression temperatures, the efficiency of the model increases and then it decreases for the further increases in temperature. However since the analysis was limited to 6000 K, the complete dome behavior at higher pressures was not trapped in the above figure.

Within a certain pressure range, as the pressure increases, the dome becomes bigger in width and height. At 6000 K, the efficiencies for 3000 kPa, 5000 kPa, 7000 kPa, 10000 kPa, 15000 kPa and 20000 kPa were approximately 12.8%, 18.5%, 24.9%, 28.2%, 28.2%, 27.8%, respectively. This shows that as the compression pressure increased the efficiency of the model increased, but after a certain limit, the efficiency again starts decreasing. This is because, at excessively high pressures, the dissociation of species is suppressed causing reduction in efficiency. Hence, the idea of using unrealistically high compression pressure to approach 100% efficiency is inappropriate.

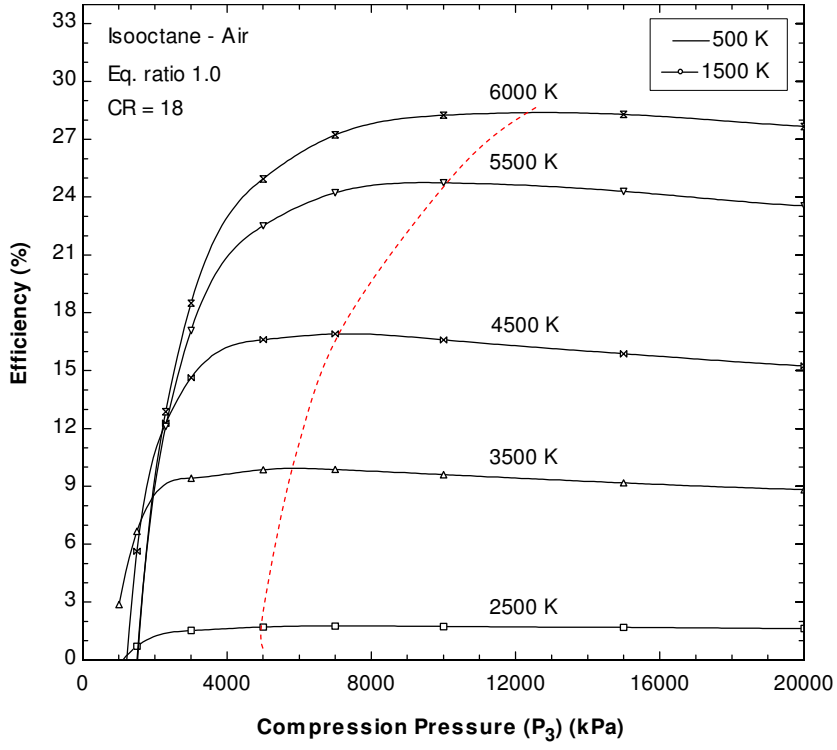

Fig. 42. Percentage efficiency as a function of compression pressure, for a range of compression temperatures, for isooctane-air, Φ = 1.0 and CR = 18.

As the maximum efficiency increases with pressure, the width of the “dome” type trend also increases. But this increase is restricted to about 1900 K for higher pressures on the left side of the temperature region. This is again due to suppression of species dissociation at lower temperatures.

Fig. 42 shows the efficiency as a function of compression pressure for several compression temperatures. At lower pressures and lower temperatures, the efficiency of the model is considerably low. Then as the temperature increases, the efficiency increases due to higher number of species available at the beginning of the expansion to generate work.

After 4000 kPa for lower temperatures and 8000 kPa for higher temperatures, for a particular compression temperature, the efficiency remains almost constant with a very gradual decrease at higher pressures (greater than 16000 kPa). This agrees with results in fig. 41 discussed earlier. The dotted line shown in the above figure represents the curve of maximum efficiency for each compression temperature. The maximum efficiency for the temperature and pressure range is ~28.2% for 6000 K compression temperature.

Effects of equivalence ratio and compression temperature

This part of the section investigates the effect of equivalence ratio on the efficiency for the compression temperature range of 500 K to 6000 K and for a constant compression pressure (10000 kPa) and a compression ratio (18).

Fig. 43 shows the variation of efficiency as a function of the compression temperature and the equivalence ratio. The equivalence ratio varies from 0.2 to 2.0. When the compression temperature increases, the development of work first occurs for the stoichiometric case, then for the lean case and later for the rich case (equivalence ratio 1.5 and 2.0). This is because, for rich mixture, due to higher number of isooctane molecules, the resistance to dissociation is high which leads to lower dissociation of species and so the work generation is delayed for increasing temperatures.

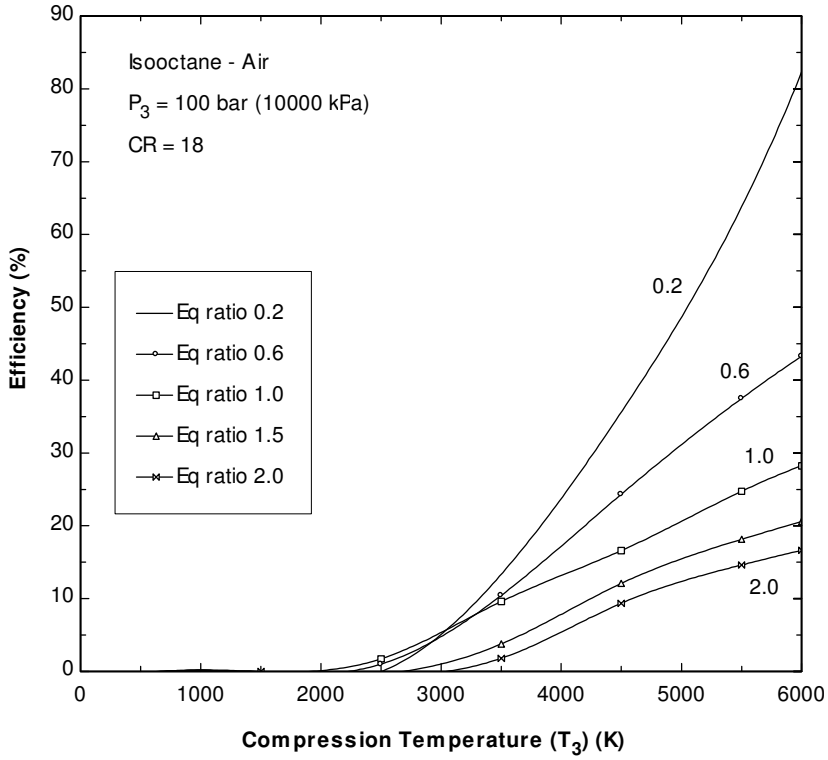

Fig. 43. Percentage efficiency as a function of compression temperature, for a range of equivalence ratios, for isooctane-air, 10000 kPa compression pressure and CR = 18.

For very lean mixtures, the efficiency is seen to be the highest. For an equivalence ratio of 0.2, the efficiency is ~82% at 6000 K. As the richness of the mixture increases, the efficiency decreases. For the stoichiometric case, the efficiency is about 28% and is about 16% for an equivalence ratio of 2.0, at 6000 K.

The decrease in efficiency with the increasing fuel richness is because for rich mixtures, the amount of air is less. Due to the lack of oxidant (air), some of the fuel gets less air than it needs, resulting in incomplete utilization of fuel.

Fig. 44 shows the efficiency for the same data of compression pressure and compression ratio, with equivalence ratio on the x-axis. This figure explains the efficiency trend for linear increase in equivalence ratio and for different compression temperatures.

The efficiency for lower temperatures (lesser than 2500 K) is almost zero for very lean and very rich mixture, the highest efficiency being for stoichiometric composition. As the temperature increases, the efficiency increases for rich, lean and stoichiometric cases. For any particular temperature variation greater than 3500 K, the efficiency is highest for the lean case

and it gradually decreases as the equivalence ratio increases. This consistent to that observed in fig. 43. For the compression temperatures lower than 2000 K, the percentage efficiency is almost zero.

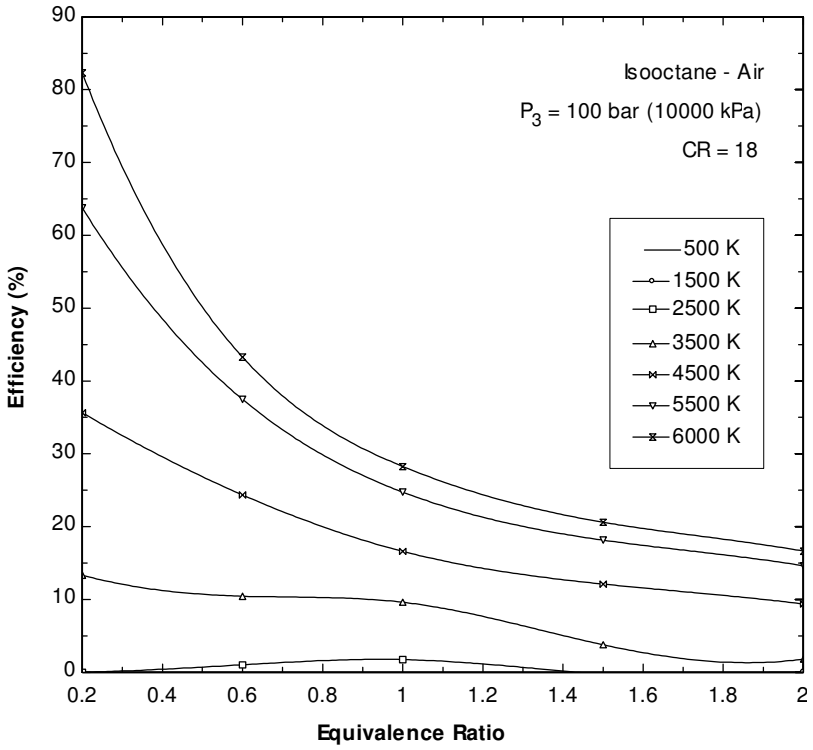

Fig. 44. Percentage efficiency as a function of equivalence ratio, for a range of compression temperatures, for isooctane-air, 10000 kPa compression pressure and CR = 18.

Effects of compression ratio and compression temperature

To analyze the combined effect of compression temperature and compression ratio, the following study was completed. Fig. 45 shows the effects of compression ratio on the efficiency of the model for a range of temperatures.

The model was examined for different compression ratios ranging from 4 to 24 to see the trends of the efficiency for a 10000 kPa compression pressure and an equivalence ratio of 1.0. For compression temperatures above ~2000 K (that were not high enough to produce significant work), further increase in temperature leads to efficiencies greater than zero. For all

the compression ratio variations, as the compression temperature increases, work generation from the system also increases due to the increase in species dissociation.

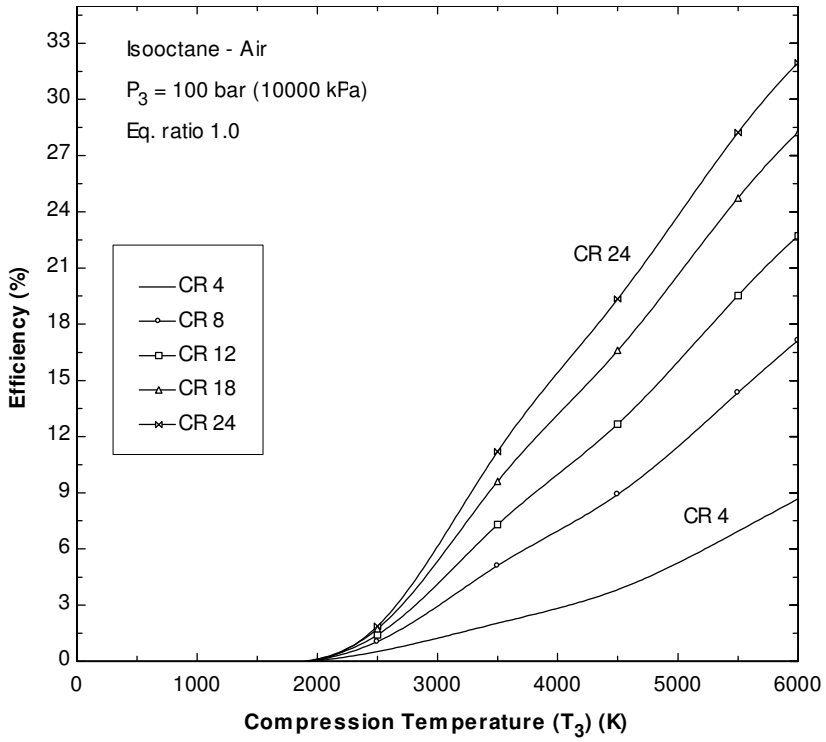

Fig. 45. Percentage efficiency as a function of compression temperature, for a range of compression ratios, for isooctane-air, 10000 kPa compression pressure and Φ = 1.0.

The efficiency for the lowest compression ratio (4) is ~8.7%, while for the highest compression ratio (24), it is about 32% (for the selected temperature range of study). The higher efficiency for the high compression ratio is due to the fact that, for higher compression ratios, there exists more opportunity to extract work due to longer stroke length.

It should be well understood that these trends are for 10000 kPa compression pressure and for the range of compression ratios of 4-24 only. The idea of achieving higher efficiency, by merely increasing compression ratio may be inappropriate as discussed earlier in this section.

Fig. 46 shows the efficiency as a function of compression ratio for various compression temperatures. The compression pressure and equivalence ratio are again kept the same, i.e. 10000 kPa and 1.0, respectively.

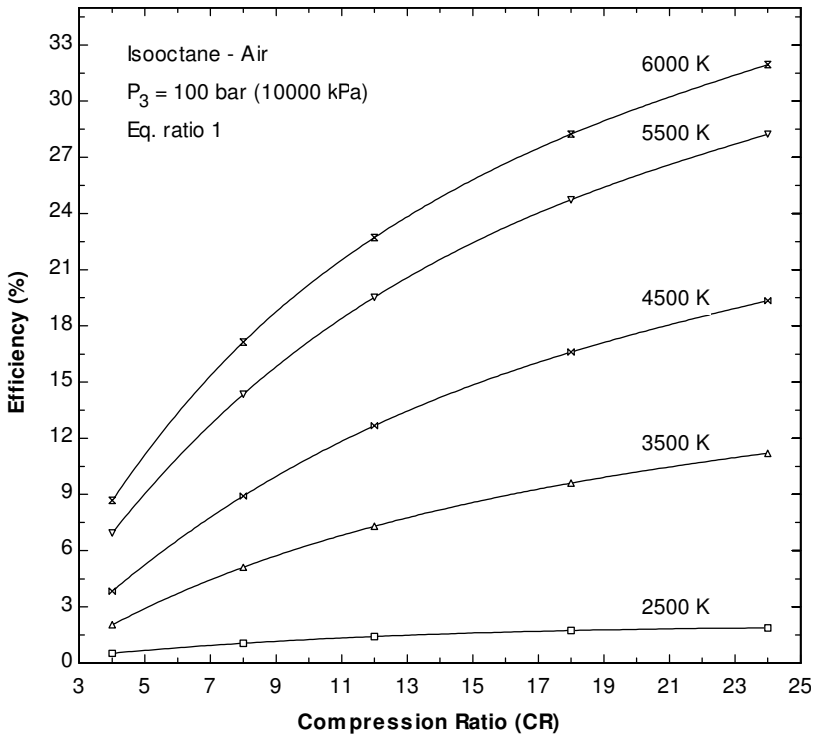

Fig. 46. Percentage efficiency as a function of compression ratio, for a range of compression temperatures, for isooctane-air, 10000 kPa compression pressure and Φ = 1.0.

As shown in fig. 45 and in agreement with the earlier discussion, as the compression temperature (and the dissociation of the species) increases, the efficiency also increases. Also, as the compression ratio increases, for any particular compression temperature, the efficiency monotonically increases. However, the efficiency increase is seen to be more rapid at higher temperatures as compared to that at lower temperatures. This is due to the presence of more species available for expansion at the higher temperatures. At a compression ratio of 24, the efficiency for 2500 K compression temperature is ~1.6% and for 6000 K compression temperature, it is ~32%.

Effects of fuels at different compression temperatures

The earlier analyses used isooctane as the fuel. The analysis was also conducted using other fuels. In all, eight fuels were included in the study. This part of the study allows comparison among the different fuels. The study is for 10000 kPa compression pressure, 1.0 equivalence ratio and 18 compression ratio. The detailed analysis for the other conditions can however be conducted similar to that conducted for isooctane. Some important results for different fuels can also be found in the appendix V.

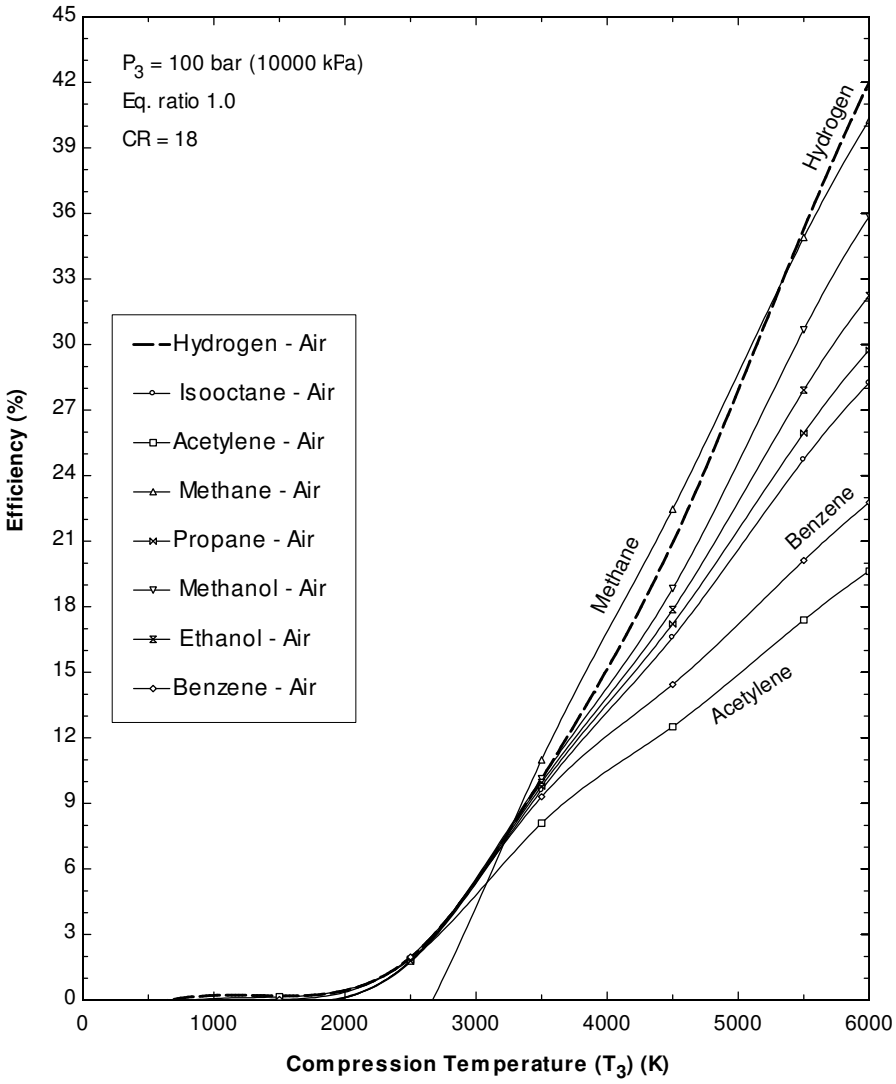

Fig. 47. Percentage efficiency as a function of compression temperature, for a range of fuels, for 10000 kPa compression pressure, Φ = 1.0 and CR = 18.

Fig. 47 shows the efficiency variation in case of various fuels as a function of compression temperature. As per the repetitive discussion done so far, the dissociation of the species at the end of compression (which is the beginning of expansion) plays a critical role in the work developed by the model. Lower the dissociation, lower are the number of species available for work generation and so lower is the efficiency. As discussed, the dissociation is directly dependent upon temperature and pressure. The higher temperature supports dissociation while the higher pressure suppresses dissociation.

For the conditions considered in the present case, the dissociation is less at low temperature and so the efficiency of the model is very low until approximately 2000 K. The efficiency for different fuels for temperatures lower than 2000 K may not be clearly visible due to the selected scale of the plot. However, the calculations show that, the efficiency is close to zero for most of the fuels including isooctane until 2000 K mark while for other fuels like benzene and hydrogen, the efficiency is ~0.3%.

At lower temperatures, the behavior of methane is seen to be different than the rest. The efficiency of the model, when methane is used, is zero until about 2700 K. This is because out of the eight fuels, methane is the most stable fuel. In order to dissociate it, higher temperatures are needed as compared to the other fuels. For methane significant dissociation is only observed for temperatures greater than 2700 K for 10000 kPa compression pressure. Hence, non-zero efficiency is only seen after 2700 K.

When the compression temperatures are further increased, the efficiency of the model of hypothetical processes increases for all the fuels. The efficiency increase for methane is seen to be quite linear as compared to the other fuels while for acetylene, the efficiency increase is most gradual.

For better understanding of the efficiency trends, the above fig. 47 is divided into three figures 48, 49 and 50. Each figure represents the efficiency for different fuels at a particular temperature.

Fig. 48 shows the efficiency of the different fuels at 2500 K compression temperature. The efficiency for most of the fuels lies in the range of 1.5-2.0% except for methane. The efficiency of the model is close to zero for methane at 2500 K.

Apart from the efficiency variations, this figure also allows to compare the amount of dissociation of each fuel for temperature and pressure considered in this case. Higher the efficiency for a particular fuel, lower is its resistance to the dissociation.

The efficiency is highest for benzene (~2%) which is higher only by a marginal difference than the other fuels excluding methane.

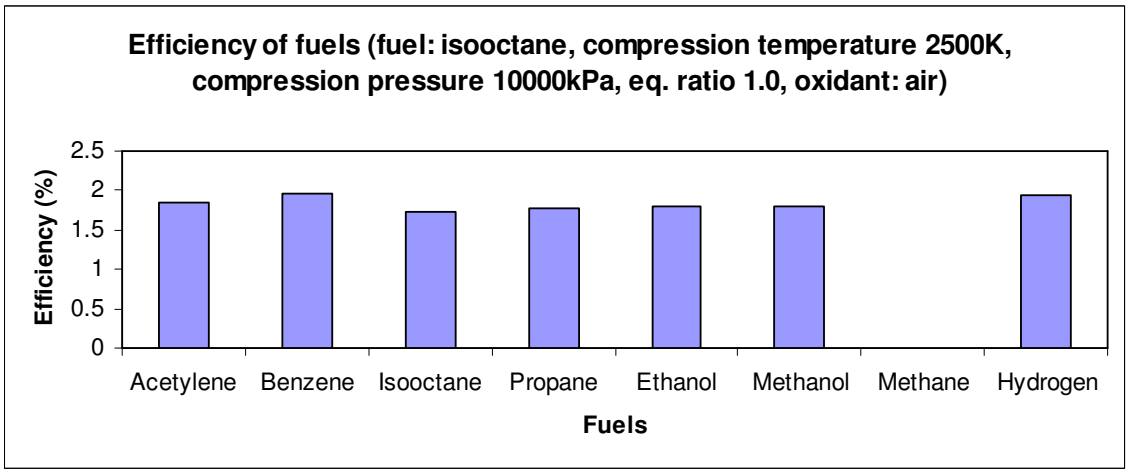

Fig. 48. Comparison of efficiency for a range of fuels, for 10000 kPa compression pressure, 2500 K compression temperature, Φ = 1.0 and CR = 18.

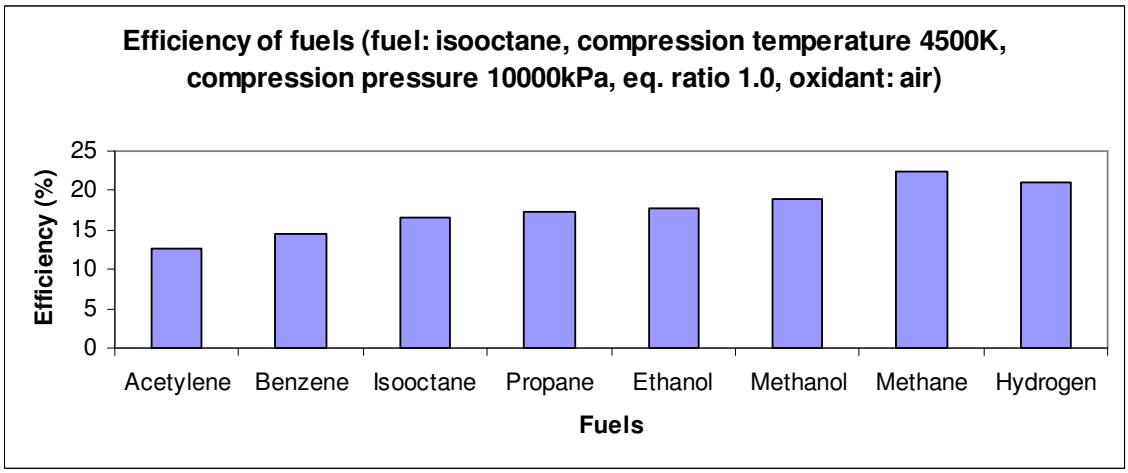

Fig. 49. Comparison of efficiency for a range of fuels, for 10000 kPa compression pressure, 4500 K compression temperature, Φ = 1.0 and CR = 18.

Fig. 49 shows the efficiency of different fuels at 4500 K compression temperature. For higher compression temperature of 4500 K, the efficiency of all the fuels increases by a significant number. In contrast to the case of 2500 K, for this case the efficiency is highest for methane and is about 22.5%. This is due to the rapid increase of dissociation rate for methane at

higher temperatures. The second highest efficiency is that of hydrogen (~21%) and the least efficiency is when acetylene is used as fuel (~12.5%).

Fig. 50 shows the efficiency of different fuels at 6000 K compression temperature. At this temperature, efficiency of the model is higher when hydrogen is used as a fuel as compared to when methane is used. This is again in contrast to what was seen in the earlier case (4500 K). This reversal is due to the difference in behavior between two fuels. Methane tends to be more stable than hydrogen. Even at high temperatures (greater than 4000 K), the dissociation of methane species is fairly controlled and so the efficiency variation is almost linear. For hydrogen fuel, for higher temperatures, the dissociation rates are comparatively higher and so the efficiency varies exponentially. Due to faster dissociation, the efficiency is slightly higher in case of hydrogen.

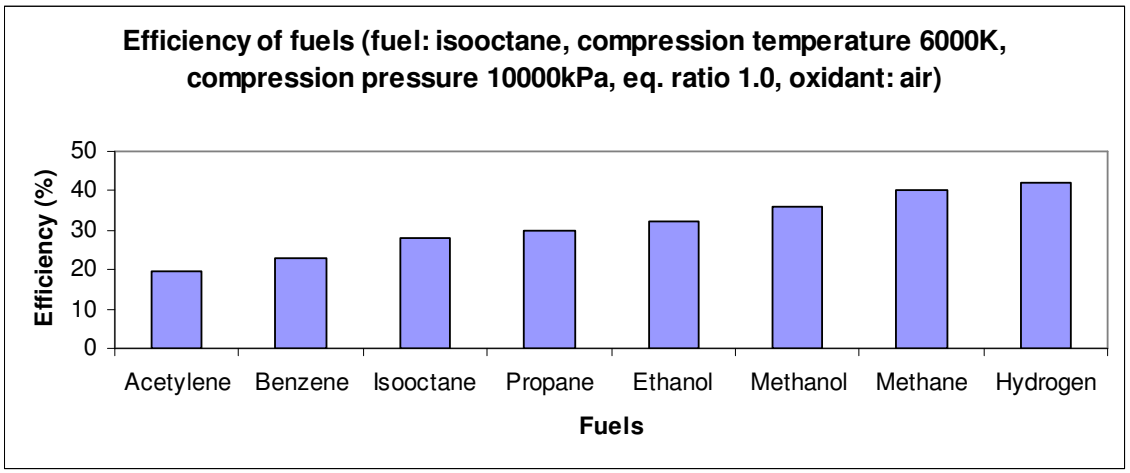

Fig. 50. Comparison of efficiency for a range of fuels, for 10000 kPa compression pressure, 6000 K compression temperature, Φ = 1.0 and CR = 18.

In fig. 50, the fuels are arranged in the increasing order of their efficiencies. The efficiency of the model is highest for hydrogen (~42%). For methane the efficiency is slightly lower (~40%) and for acetylene, again, the efficiency is lowest (~19.6%).

Effects of fuel-oxidant combinations at different compression temperatures

The earlier part of this section deals with the effects on the efficiency of the model for different fuels. This subsection discusses the effects on the efficiency of the model for two different fuels when they are used in combination with different oxidants.

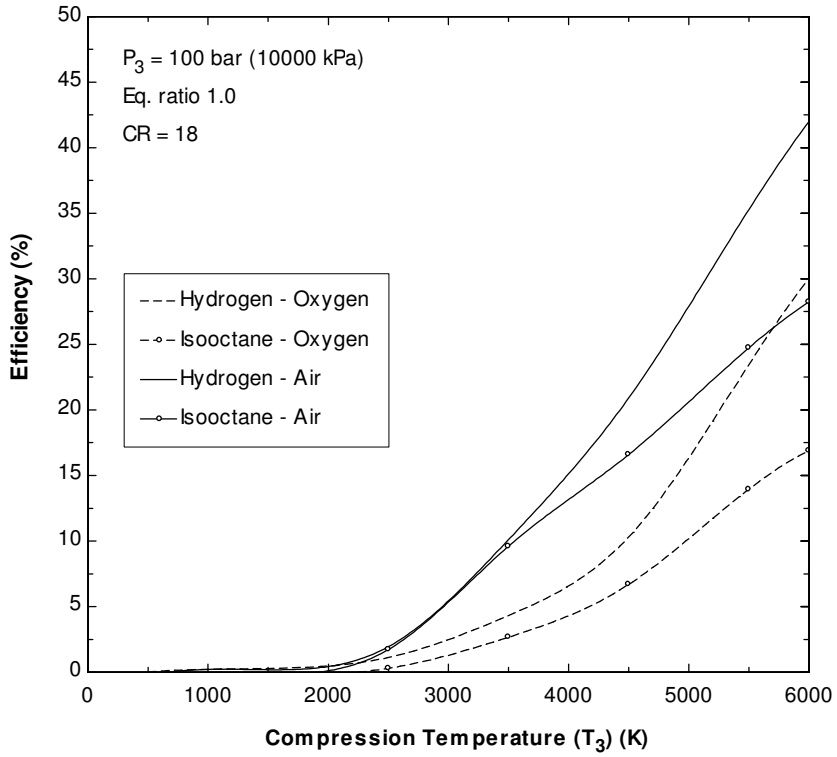

Fig. 51. Percentage efficiency as a function of compression temperature, for hydrogen and isooctane used with air and oxygen, for 10000 kPa compression pressure, Φ = 1.0 and CR = 18.

Fig. 51 shows the efficiency for hydrogen and isooctane fuel when used in combination with air and oxygen as the oxidants for a compression pressure of 10000 kPa, a compression temperature of 0-6000 K, an equivalence ratio of 1.0 and a compression ratio of 18. The efficiency is zero until about 2000 K compression temperature for isooctane, while it is slightly higher (~0.35%) for hydrogen, when used with air or oxygen. For temperatures greater than 2000 K, the efficiency for all four combinations– hydrogen-air, hydrogen-oxygen, isooctane-air and isooctane-oxygen, increases with increase in temperature. For both, air and oxygen, the

efficiency, when hydrogen is used as the fuel, is greater than when isooctane is used. Moreover, the trends followed by hydrogen-air and hydrogen-oxygen are similar, and also that followed by isooctane-air and isooctane-oxygen are nearly the same in nature. For both the fuels, the efficiency is higher when air is used as oxidant. The percentage efficiency is highest for hydrogen-air combination (~42%) and is least for isooctane-oxygen combination which is about 17% at 6000 K. The percentage efficiency for isooctane-air and hydrogen-oxygen are quite close in the range of 25-30%.

Similar few other cases of study, as illustrated in this section of Results and Discussion, can be found in the appendix V. In current section, the behavior of the model of the hypothetical processes is analyzed when it is operated at different thermodynamic conditions. The base case study includes some specific cases that give a brief overview of the work and the efficiency trends for a particular operating condition, while the parametric study includes the illustration of the efficiency trends for varying range of properties which helps selection of the most favorable condition for efficient working of the model.

For a compression pressure of 10000 kPa, the thermodynamic conditions that would provide highest efficiency will be when a compression temperature of 6000 K, an equivalence ratio of 0.2 and a compression ratio of 24 is used.

VII. SUMMARY AND CONCLUSION

Conventional combustion processes are highly irreversible. The potential to obtain useful work (availability or exergy) from the fuel always degrades during the combustion process. In the case of reciprocating internal combustion engines, about one-fourth of the availability from the fuel is destroyed due to combustion. To understand these losses, several studies based on the second law have been conducted in the past [1, 4, 8, 10-17]. The concept of a reversible combustion process was first proposed by Keenan [10]. The purpose of the current work was to develop a quantitative model of this concept, and to use the model in a series of computations to examine the effects of temperature, pressure, and other parameters on the work production capability of the concept.

In the current work, a theoretical model was designed in accordance to the concept stated by Keenan. In this model, the individual species of the reactant mixture were compressed individually and isentropically in different cylinders, to increase their temperature and pressure and bring them to a state at which work extraction was possible from them. The type, the amount and the thermodynamic properties of the individual species, introduced in the different compression cylinders at the beginning of the compression process, were “preselected” such that when the species were collected at the end of the compression, they did not react and stayed stable in complete equilibrium. The species, in equilibrium, were then expanded slowly and isentropically in an expansion cylinder. Due to this, the temperature of the mixture reduced, and so the species tried to constantly adjust to attain equilibrium. As a result, more product species were formed which allowed net work production, due to release of chemical energy, during the expansion process. For this concept, therefore, “combustion” was avoided and the conversion of reactants to products was reversible.

The main results of the current work are -

- The temperature and pressure at the end of compression (compression temperature and compression pressure) played a significant role in the value of the thermal efficiency. This was because the compression temperature and compression pressure controlled the amount of dissociation which was the key to the possible net work production. The higher compression temperatures supported dissociation while the higher compression pressures suppressed dissociation. The more the dissociation of the species, the more were the number of products formed during every step of the equilibrium expansion process and so higher work generation was possible.
- For sufficiently high compression temperatures and pressures, the concept resulted in net work produced without destroying any fuel availability. A base case set of conditions

were identified for a set of computations. These base conditions included isooctane and air, an equivalence ratio of 1.0, and a compression ratio of 18. For the base case set of conditions, for example, for a pressure and temperature at the end of compression of 10 MPa and 2500 K, respectively, a small amount of net work was produced. By using higher temperatures and pressures, even more work could be produced. For example, for a pressure and temperature of 10 MPa and 6000 K, the thermal efficiency was ~28.2%. Although these high temperatures and pressures are well beyond practical values for today's materials and designs, the concept was demonstrated. In general, for appropriate pressures, the efficiency increased with increasing compression temperatures.

- For a particular compression pressure and temperature, the equivalence ratio had a significant effect on the thermal efficiency. In general, the efficiency increased as the equivalence ratio decreased from stoichiometric. This was because for rich mixtures, due to lack of oxidant, some of the fuel did not get enough oxidant and hence the fuel was not utilized fully resulting lower efficiencies. For the similar initial conditions (a compression pressure of 10 MPa and a compression ratio of 18), with equivalence ratio of 0.2, the thermal efficiency was highest ~82%, at 6000 K.
- The thermal efficiencies also depended on the selection of compression ratio. For high compression temperatures and pressures, the work obtained during expansion was observed to be always greater than the work consumed due to compression. Hence, for a particular higher pressure, the higher compression ratio resulted in higher thermal efficiency. At a compression pressure of 10 MPa, a compression ratio of 24, the thermal efficiency was ~32% at a compression temperature of 6000 K. However, for a low compression pressures, high compression ratio may result in lower may result in a lower efficiency.
- Among the eight (8) different fuels, for similar initial conditions, the efficiency was highest for hydrogen and methane. For these two fuels, the thermal efficiency was about 40%, for a 6000 K compression temperature, a 10 MPa compression pressure, an equivalence ratio of 1.0 and a compression ratio of 18. Other fuels such as isooctane, propane, methanol, ethanol, acetylene and benzene, resulted in lower thermal efficiencies for the same conditions. It was noted that, for higher compression temperatures (greater than 4000 K), the efficiency of the model decreased with the increasing complexity of the structure of the fuel molecule which indicate the use of hydrogen for higher efficiency. However, most of the time, in actual practice, the selection of the fuel is governed by other issues.

- Finally, the concept was also examined for pure oxygen as the oxidant instead of air. For both, hydrogen and isooctane fuel, the efficiency was higher when air was used as the oxidant as against when oxygen was used. At a compression temperature of 6000 K, a compression pressure of 10 MPa, a compression ratio of 18, for stoichiometric conditions, the efficiency was seen to be highest for hydrogen-air combination, which was about 42%.

The key feature of this concept (and the reason that the combustion irreversibility is avoided) is the “preselection” of the reactants. Since the preselected reactants represent the equilibrium composition at the end of compression, no “combustion” occurs. This composition, at high temperatures, will be largely dissociated molecules. During the expansion process, the molecules recombine and chemical energy is released, and therefore, the work during expansion exceeds the work of compression. Although not part of the current study, the processes needed to produce the preselected reactants would be an additional concern. The current work has quantified the overall concept, and has determined the effects of temperatures, pressures, equivalence ratio, and compression ratio on the work production and thermal efficiency.

In summary, a concept based on special processes was explored which eliminated the destruction of availability due to combustion. Although the processes must be completed at high temperatures and pressures, the general result is that conditions can be identified to eliminate the combustion irreversibility. For lower pressures and temperatures, the concept may not result in any net useful work. For moderate pressures and temperatures, a modest amount of net work is produced and the availability of the working fluid is high at the end of the expansion stroke. For the highest pressures and temperatures, the concept does indicate high work outputs with high thermal efficiencies. Unfortunately, these highest pressures and temperatures are much too high for current materials and designs.

REFERENCES

[1] Dunbar WR, Lior N. Sources of Combustion Irreversibility. Combustion Science and Technology; 103, 41-61, 1994.

[2] Nag PK. Engineering Thermodynamics. Second edition. Tata McGraw-Hill, New Delhi, 2001.

[3] Annamalai K, Puri IK. Advanced Thermodynamics Engineering. CRC Press: New York, 2002.

[4] Caton JA. On the Destruction of Availability (Exergy) Due to Combustion Processes – with Specific Application to Internal Combustion Engines. Energy; 25: 1097-1117, 2002.

[5] Wark K. Advanced Thermodynamics for Engineers. McGraw-Hill Series in Mechanical Engineering, McGraw-Hill, Inc: New York, 1995.

[6] Heywood JB. Internal Combustion Engine Fundamentals. McGraw–Hill, Inc: New York, 1988.

[7] Moran MJ, Shapiro HN. Fundamentals of Engineering Thermodynamics. Fourth edition. John Wiley and Sons Inc: New York, 2004.

[8] Chavannavar PS. Parametric Examination of the Destruction of Availability Due to Combustion for a Range of Conditions and Fuels. M.S. thesis, Department of Mechanical Engineering, Texas A&M University, College Station, TX, 2005.

[9] Gordon S, McBride BJ. Computer Program for Calculation of Complex Chemical Equilibrium Compositions and Applications. National Aeronautics and Space Administration, Lewis Research Center, Reference Publication 1311, October 1994.

[10] Keenan JH. Thermodynamics. John Wiley & Sons, Inc: New York, 1941.

[11] Obert EF, Gaggioli RA. Thermodynamics. Second edition. McGraw-Hill, Inc: New York, 1963.

[12] Obert EF. Internal Combustion Engine Analysis and Practice. Second edition. The Haddon Craftsmen, Inc: Scranton, PA, 1950.

[13] Caton JA. A Review of Investigations Using the Second Law of Thermodynamics to Study Internal Combustion Engines. SAE Technical Paper Series, Society of Automotive Engineers, 2000.

[14] Lutz AE, Larson RS, Keller JO. Thermodynamic Comparison of Fuel Cells to the Carnot Cycle. International Journal of Hydrogen Energy; 27: 1103-1111. 2002.

[15] Daw S, Chakravarthy K, Conklin J, Graves R. Refining Understanding of Combustion Irreversibility. In: Proceedings of the 2004 Technical Meeting of the Central States Section of the Combustion Institute, 2004, March 21 – 23, Austin, TX.

[16] Richter HJ, Knoche KF. Reversibility of Combustion Processes. In: Efficiency and Costing: Second Law Analysis of Processes, ACS Symposium series 235, 1983: 71-85.

[17] Hassanzadeh H, Mansouri SH. Efficiency of Ideal Fuel Cell and Carnot Cycle from a Fundamental Prospective. Proc. IMechE Vol.219 Part A: J. Power and Energy, 245-254, 2005

[18] Chemical Equilibrium with Applications, Thermodynamic Properties. http://cea.grc.nasa.gov (accessed February 2005).

[19] Zehe MJ, Gordon S, McBride BJ. CAP: A Computer Code for Generating Tabular Thermodynamic Functions from NASA Lewis Coefficients. National Aeronautics and Space Administration, Glenn Research Center, NASA/TP – 2001 – 210959/REV1. 2001.

APPENDIX I

Standard Wet Atmosphere

Table I.1. Environment used to calculate the Chemical availability analysis [4, 8]

T_0 = 298.15 K

P_0 = 1.01325 bar

Substance in Gas Phase	Mole Fraction
N_2	0.7565
O_2	0.2029
H_2O	0.0313
CO_2	0.0003
Ar	0.0090

APPENDIX II

Lower heating values of fuels

Table II.1. Values for molecular weight and lower heating values for various fuels [6]

T_0 = 298.15 K

P_0 = 1.01325 bar

Fuels in gaseous form	**Chemical Formula**	**Molecular weight**	**LHV (kJ/kg)**
Hydrogen	H_2	2.016	119940
Acetylene	C_2H_2	26.04	48210
Methane	CH_4	16.04	50010
Propane	C_3H_8	44.09	46350
Iso-octane	C_8H_{18}	114.14	44800
Methyl alcohol	CH_3OH	32.04	21100
Ethyl alcohol	C_2H_5OH	46.07	27720
Benzene	C_6H_6	78.11	40570

APPENDIX III

NASA Lewis Polynomial Coefficients

Table III.1. Coefficients for use with the NASA Lewis polynomials [8, 18]

Fuel	Formula	Range	a1	a2	a3	a4	a5	a6	a7	b1	b2	hf
Methane	CH4	200 - 1000	-1.766851E+05	2.786181E+03	-1.202578E+01	3.917619E-02	-3.619054E-05	2.026853E-08	-4.976705E-12	-2.331314E+04	8.904323E+01	-74600
		1000 - 6000	3.730043E+06	-1.383501E+04	2.049107E+01	-1.961975E-03	4.727313E-07	-3.728815E-11	1.623737E-15	7.532067E+04	-1.219125E+02	
Acetylene	C2H2	200 - 1000	1.598112E+05	-2.216644E+03	1.265708E+01	-7.979651E-03	8.054993E-06	-2.433308E-09	-7.529233E-14	3.712619E+04	-5.244339E+01	228200
		1000 - 6000	1.713847E+06	-5.929107E+03	1.236128E+01	1.314187E-04	-1.362764E-07	2.712656E-11	-1.302066E-15	6.266579E+04	-5.818961E+01	
Ethylene	C2H4	200 - 1000	-1.163606E+05	2.554852E+03	-1.609746E+01	6.625779E-02	-7.885082E-05	5.125225E-08	-1.370340E-11	-6.176191E+03	1.093338E+02	52500
		1000 - 6000	3.408764E+06	-1.374848E+04	2.365898E+01	-2.423804E-03	4.431396E-07	-4.352683E-11	1.775411E-15	8.820429E+04	-1.371278E+02	
Ethane	C2H6	200 - 1000	-1.862044E+05	3.406192E+03	-1.951705E+01	7.565836E-02	-8.204173E-05	5.061136E-08	-1.319282E-11	-2.702933E+04	1.298140E+02	-83851
		1000 - 6000	5.025782E+06	-2.033022E+04	3.322553E+01	-3.836703E-03	7.238406E-07	-7.319183E-11	3.065469E-15	1.115964E+05	-2.039411E+02	
Propylene	C3H6	200 - 1000	-1.912462E+05	3.542074E+03	-2.114879E+01	8.901485E-02	-1.001429E-04	6.267959E-08	-1.637871E-11	-1.529962E+04	1.407641E+02	20000
		1000 - 6000	5.017620E+06	-2.086084E+04	3.644156E+01	-3.881191E-03	7.278677E-07	-7.321205E-11	3.052176E-15	1.261245E+05	-2.195716E+02	
Propane	C3H8	200 - 1000	-2.433144E+05	4.656271E+03	-2.939466E+01	1.188953E-01	-1.376308E-04	8.814824E-08	-2.342988E-11	-3.540335E+04	1.841749E+02	-104680
		1000 - 6000	6.420732E+06	-2.659791E+04	4.534357E+01	-5.020664E-03	9.471217E-07	-9.575405E-11	4.009673E-15	1.455582E+05	-2.818375E+02	
n-Butane	C4H10	200 - 1000	-3.175873E+05	6.176332E+03	-3.891562E+01	1.584654E-01	-1.860050E-04	1.199676E-07	-3.201671E-11	-4.540363E+04	2.379489E+02	-125790
		1000 - 6000	7.682322E+06	-3.256052E+04	5.736733E+01	-6.197917E-03	1.180186E-06	-1.221894E-10	5.250635E-15	1.774527E+05	-3.587919E+02	
n-Pentane	C5H12	200 - 1000	-2.768895E+05	5.834283E+03	-3.617541E+01	1.533340E-01	-1.528396E-04	8.191092E-08	-1.792328E-11	-4.665375E+04	2.265544E+02	-146760
		1000 - 6000	-2.530779E+06	-8.972593E+03	4.536223E+01	-2.626990E-03	3.135136E-06	-5.318729E-10	2.886897E-14	1.484617E+04	-2.516550E+02	
Benzene	C6H6	200 - 1000	-1.677341E+05	4.404500E+03	-3.717378E+01	1.640510E-01	-2.020812E-04	1.307915E-07	-3.444284E-11	-1.035455E+04	2.169853E+02	82880
		1000 - 6000	4.538576E+06	-2.260503E+04	4.694007E+01	-4.206677E-03	7.907994E-07	-7.968302E-11	3.328212E-15	1.391465E+05	-2.868751E+02	
n-Hexane	C6H14	200 - 1000	-5.815927E+05	1.079098E+04	-6.633947E+01	2.523715E-01	-2.904345E-04	1.802202E-07	-4.617224E-11	-7.271545E+04	3.938284E+02	-166920
		1000 - 6000	-3.106626E+06	-7.346088E+03	4.694132E+01	1.693964E-03	2.068997E-06	-4.212142E-10	2.452346E-14	5.237503E+02	-2.549968E+02	

Table III.1. Continued [8, 18]

Fuel	Formula	Range	a1	a2	a3	a4	a5	a6	a7	b1	b2	hf
n-Heptane	C7H16	200 - 1000	-6.127433E+05	1.184085E+04	-7.487189E+01	2.918466E-01	-3.416795E-04	2.159285E-07	-5.655853E-11	-8.013409E+04	4.407213E+02	-187780
		1000 - 6000	9.135632E+06	-3.923320E+04	7.889781E+01	-4.654252E-03	2.071774E-06	-3.442539E-10	1.976835E-14	2.050708E+05	-4.851104E+02	
n-Octane	C8H18	200 - 1000	-6.986647E+05	1.338501E+04	-8.415166E+01	3.271937E-01	-3.777210E-04	2.339837E-07	-6.010893E-11	-9.026223E+04	4.939222E+02	-208750
		1000 - 6000	6.365407E+06	-3.105365E+04	6.969162E+01	1.048060E-02	-4.129622E-06	5.543226E-10	-2.651436E-14	1.500969E+05	-4.169896E+02	
Iso-Octane (I	C8H18	165.79 - 380	1.419158E+05	-2.937251E+03	4.168835E+01	-8.436942E-02	2.894148E-04	-2.200564E-07	7.234226E-11	-2.479399E+04	-1.930220E+02	-259160
Iso-Octane	C8H18	200 - 1000	-1.688759E+05	3.126903E+03	-2.123503E+01	1.489152E-01	-1.151180E-04	4.473216E-08	-5.554882E-12	-4.468061E+04	1.417456E+02	-224010
		1000 - 6000	1.352765E+07	-4.663370E+04	7.795313E+01	1.423730E-02	-5.073594E-06	7.248233E-10	-3.819190E-14	2.541178E+05	-4.933887E+02	
Methanol	CH3OH	200 - 1000	-2.416643E+05	4.032147E+03	-2.046415E+01	6.903698E-02	-7.598933E-05	4.598208E-08	-1.158707E-11	-4.433261E+04	1.400142E+02	-200940
		1000 - 6000	3.411571E+06	-1.345500E+04	2.261408E+01	-2.141029E-03	3.730051E-07	-3.498846E-11	1.366073E-15	5.636082E+04	-1.277814E+02	
Ethanol	C2H5OH	200 - 1000	-2.342791E+05	4.479181E+03	-2.744817E+01	1.088679E-01	-1.305309E-04	8.437346E-08	-2.234559E-11	-5.022229E+04	1.764829E+02	-234950
		1000 - 6000	4.694818E+06	-1.929798E+04	3.447584E+01	-3.236166E-03	5.784948E-07	-5.564600E-11	2.226226E-15	8.601623E+04	-2.034802E+02	
Carbon	C	200 - 1000	6.495031E+02	-9.649011E-01	2.504675E+00	-1.281448E-05	1.980134E-08	-1.606144E-11	5.314483E-15	8.545763E+04	4.747924E+00	716680
		1000 - 6000	-1.289136E+05	1.719529E+02	2.646044E+00	-3.353069E-04	1.742093E-07	-2.902818E-11	1.642182E-15	8.410598E+04	4.130047E+00	
		6000 - 2000	4.432528E+08	-2.886018E+05	7.737108E+01	-9.715282E-03	6.649595E-07	-2.230079E-11	2.899389E-16	2.355273E+06	-6.405123E+02	
Hydrogen	H2	200 - 1000	4.078323E+04	-8.009186E+02	8.214702E+00	-1.269714E-02	1.753605E-05	-1.202860E-08	3.368093E-12	2.682485E+03	-3.043789E+01	0
		1000 - 6000	5.608128E+05	-8.371505E+02	2.975365E+00	1.252249E-03	-3.740716E-07	5.936625E-11	-3.606994E-15	5.339824E+03	-2.202775E+00	
		6000 - 2000	4.966884E+08	-3.147547E+05	7.984122E+01	-8.414789E-03	4.753248E-07	-1.371873E-11	1.605462E-16	2.488434E+06	-6.695728E+02	
Carbon	CO	200 - 1000	1.489045E+04	-2.922286E+02	5.724527E+00	-8.176235E-03	1.456903E-05	-1.087746E-08	3.027942E-12	-1.303132E+04	-7.859241E+00	-110535
Monoxide		1000 - 6000	4.619197E+05	-1.944705E+03	5.916714E+00	-5.664283E-04	1.398815E-07	-1.787680E-11	9.620936E-16	-2.466261E+03	-1.387413E+01	
		6000 - 2000	8.868663E+08	-7.500378E+05	2.495475E+02	-3.956351E-02	3.297772E-06	-1.318410E-10	1.998938E-15	5.701421E+06	-2.060705E+03	

APPENDIX IV

Change in Gibbs Energy for oxidation of fuels

Table IV.1. Change in Gibbs energy (ΔG) for various fuels

FUEL	ΔG (kJ/kg)*
Oxygen atom, O	14480
Nitrogen atom, N	32520
Hydrogen atom, H	315055
Hydrogen, H_2	115372
Hydroxyl radical, OH	8765
Carbon monoxide, CO	9187
Methane, CH_4	49914
Acetylene, C_2H_2	47108
Propane, C_3H_8	47036
Benzene, C_6H_6	40707
Iso-octane (g), C_8H_{18}	45748
Methanol, CH_3OH	21511
Ethanol, C_2H_5OH	28409
Carbon (g), C	88808
Carbon (solid), C(gr)	32836

Table IV.1. Continued

FUEL	ΔG **(kJ/kg)***
C_2	65125
C_3	54344
CH	82773
Nitrogen oxide	2896

* Values based on data from [3, 6, 7, 8].

APPENDIX V

Results for some other similar cases considered in the analysis

This section shows the results for some other similar cases that were not considered in the Results and Discussion section, but were considered in the analysis of the model. The first sub-section illustrates the results for the model of hypothetical processes when isooctane is used as the fuel and air is used as the oxidant. The second sub-section deals with the results when hydrogen is used as the fuel. The last sub-section includes the results for six other fuels for the base case conditions only.

The results illustrated in this section follow the trends similar to that observed for some peculiar cases considered in section VI and hence to avoid repetition, the description of the results is skipped.

For Isooctane (remaining results only)

Effects of compression temperature for compression pressures - 5000 kPa, 15000 kPa and 20000 kPa

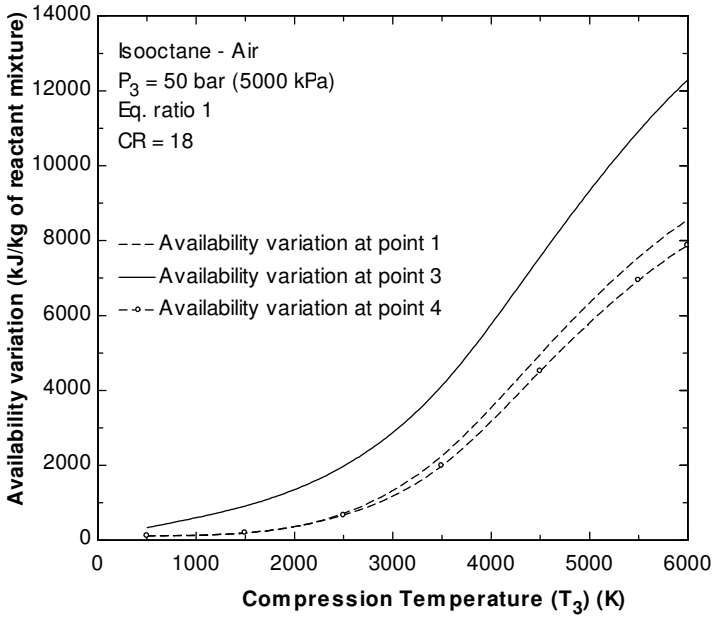

Fig. 52. Availabilities as a function of compression temperature for isooctane-air at 5000 kPa compression pressure, Φ = 1.0 and CR = 18.

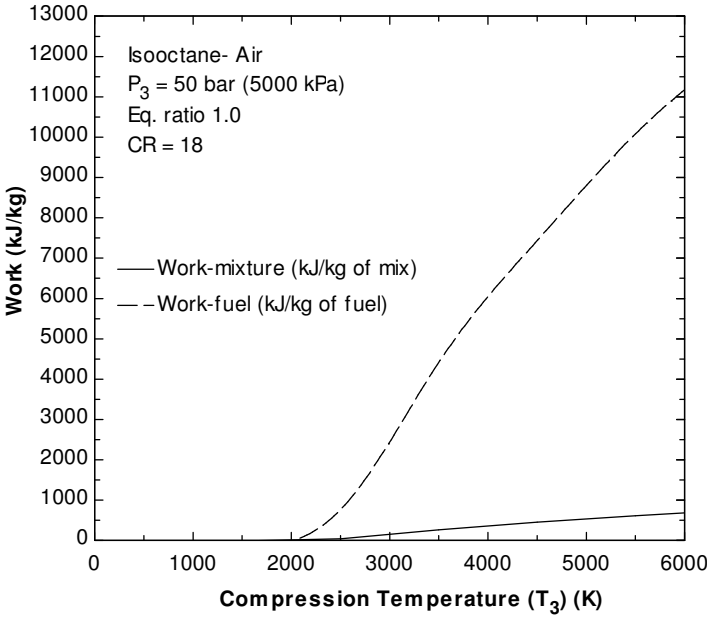

Fig. 53. Work as a function of compression temperature for isooctane-air at 5000 kPa compression pressure, Φ = 1.0 and CR = 18.

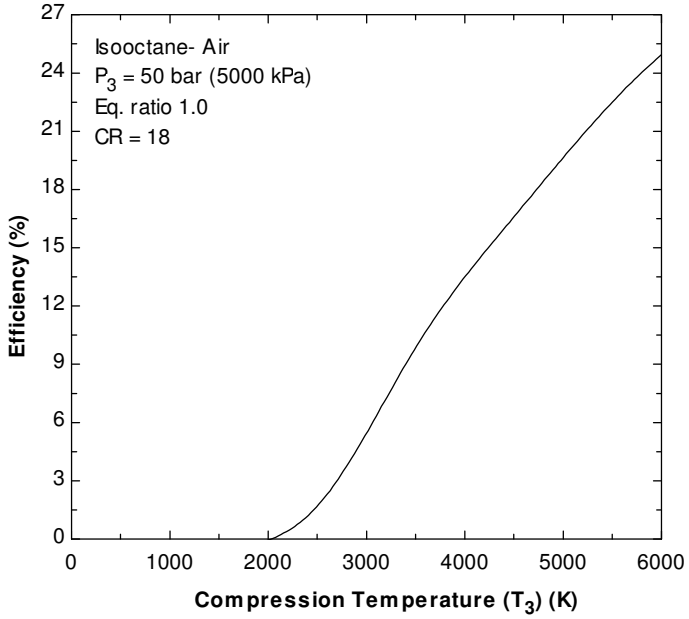

Fig. 54. Percentage efficiency as a function of compression temperature for isooctane-air at 5000 kPa compression pressure, Φ = 1.0 and CR = 18.

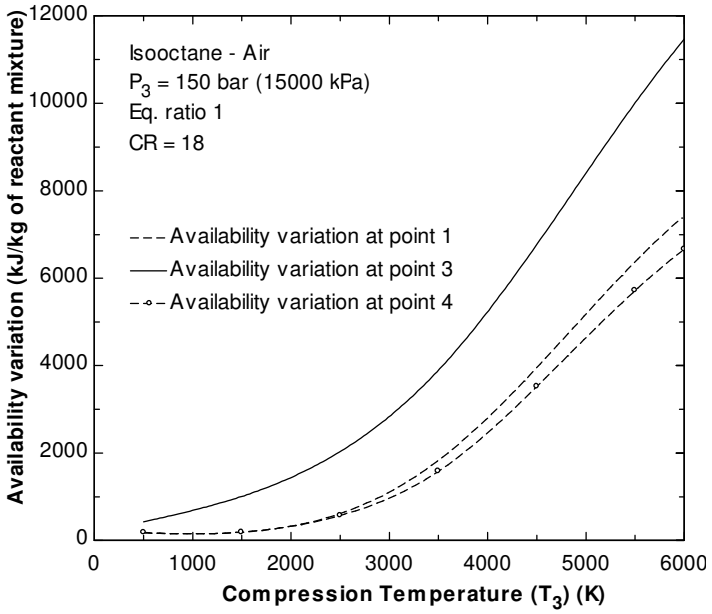

Fig. 55. Availabilities as a function of compression temperature for isooctane-air at 15000 kPa compression pressure, Φ = 1.0 and CR = 18.

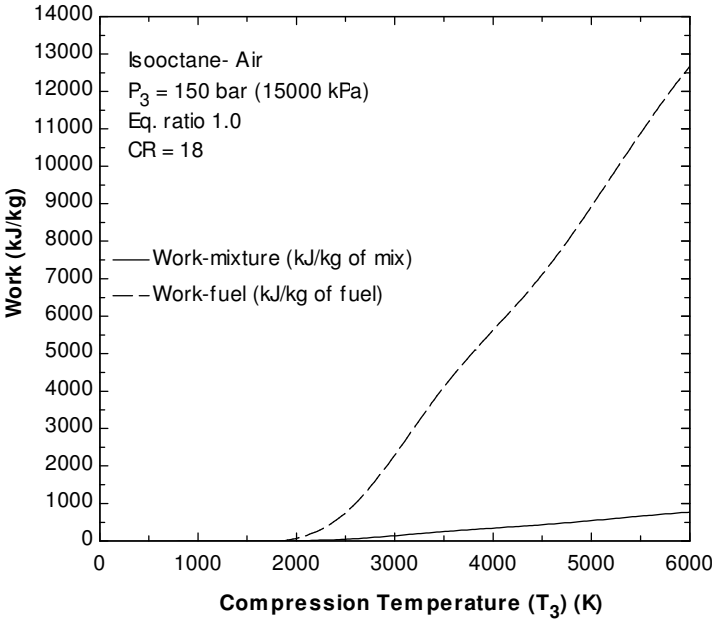

Fig. 56. Work as a function of compression temperature for isooctane-air at 15000 kPa compression pressure, Φ = 1.0 and CR = 18.

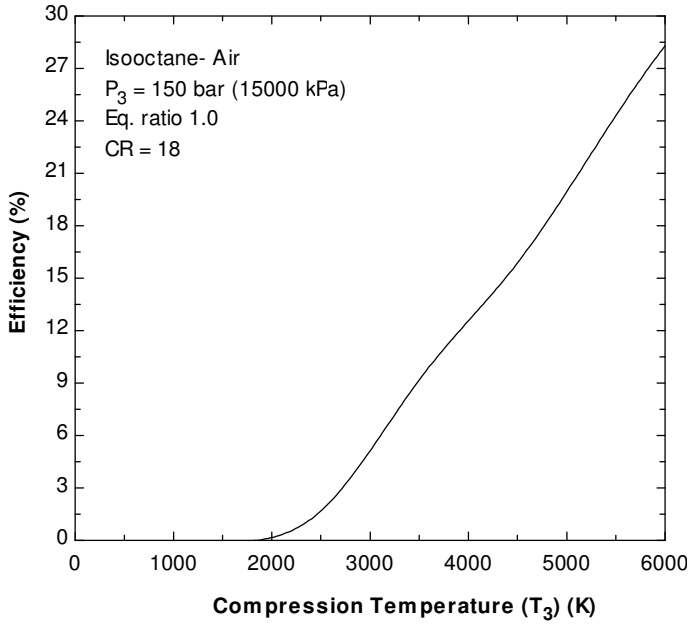

Fig. 57. Percentage efficiency as a function of compression temperature for isooctane-air at 15000 kPa compression pressure, Φ = 1.0 and CR = 18.

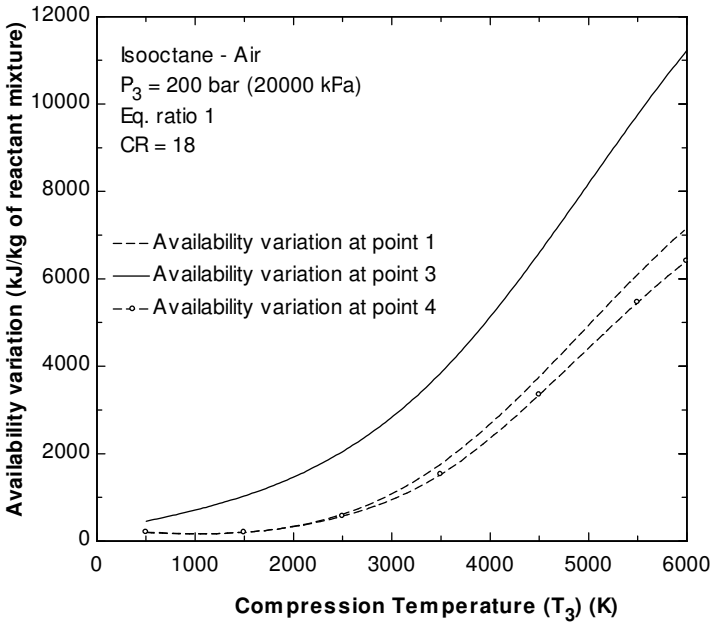

Fig. 58. Availabilities as a function of compression temperature for isooctane-air at 20000 kPa compression pressure, Φ = 1.0 and CR = 18.

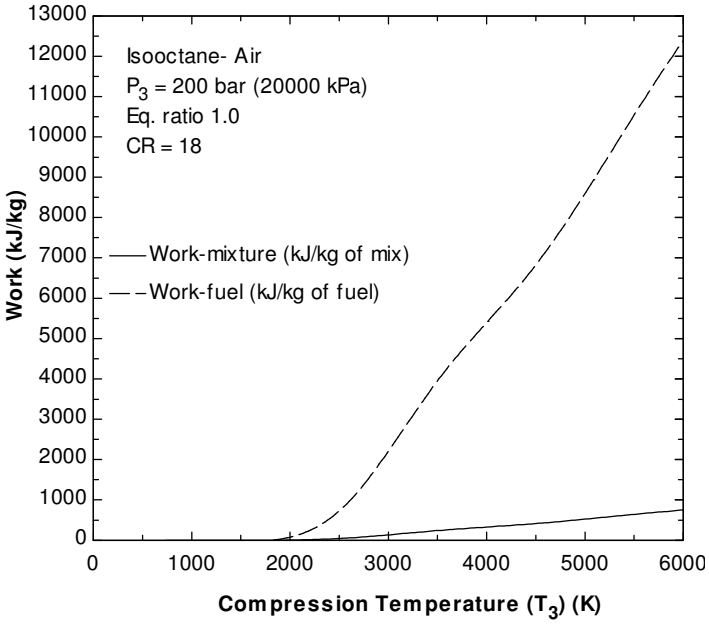

Fig. 59. Work as a function of compression temperature for isooctane-air at 20000 kPa compression pressure, Φ = 1.0 and CR = 18.

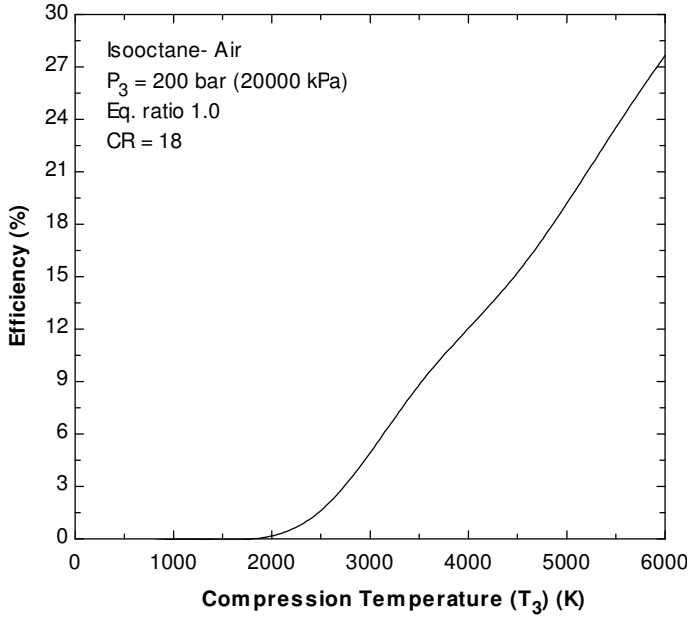

Fig. 60. Percentage efficiency as a function of compression temperature for isooctane-air at 20000 kPa compression pressure, Φ = 1.0 and CR = 18.

Effects of compression temperature for equivalence ratios – 0.6 and 1.5

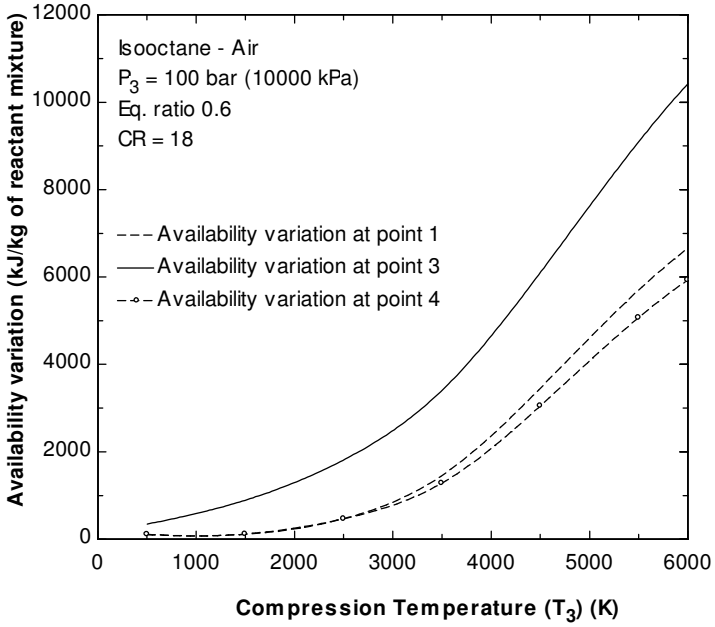

Fig. 61. Availabilities as a function of compression temperature for isooctane-air at 10000 kPa compression pressure, Φ = 0.6 and CR = 18.

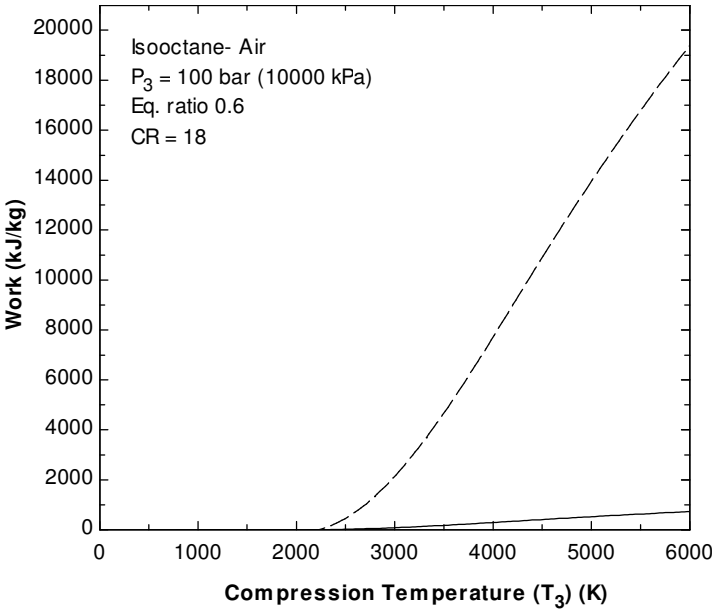

Fig. 62. Work as a function of compression temperature for isooctane-air at 10000 kPa compression pressure, Φ = 0.6 and CR = 18.

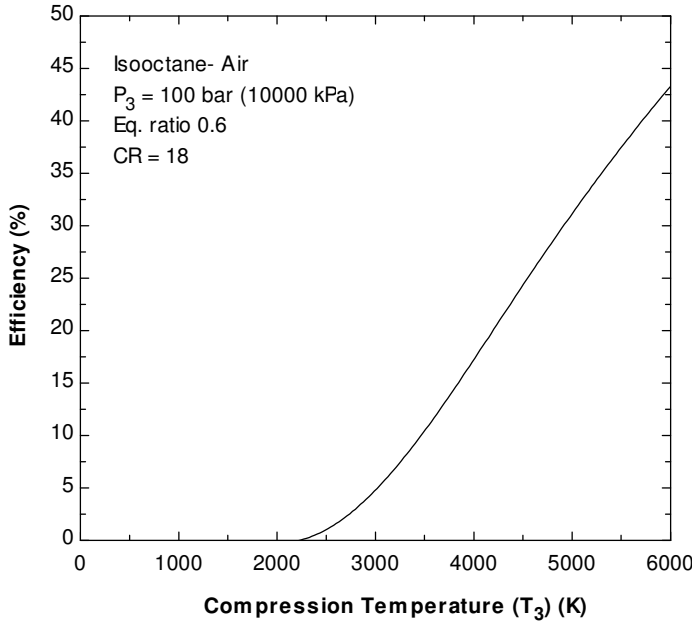

Fig. 63. Percentage efficiency as a function of compression temperature for isooctane-air at 10000 kPa compression pressure, Φ = 0.6 and CR = 18.

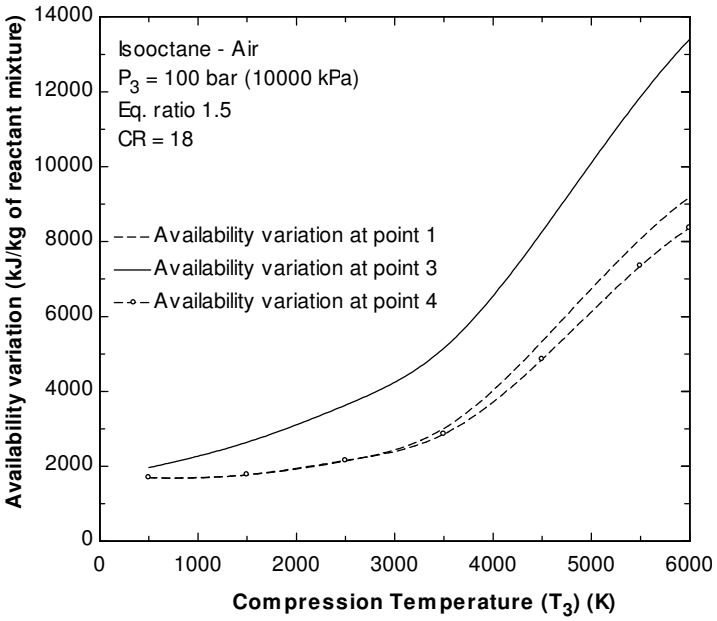

Fig. 64. Availabilities as a function of compression temperature for isooctane-air at 10000 kPa compression pressure, Φ = 1.5 and CR = 18.

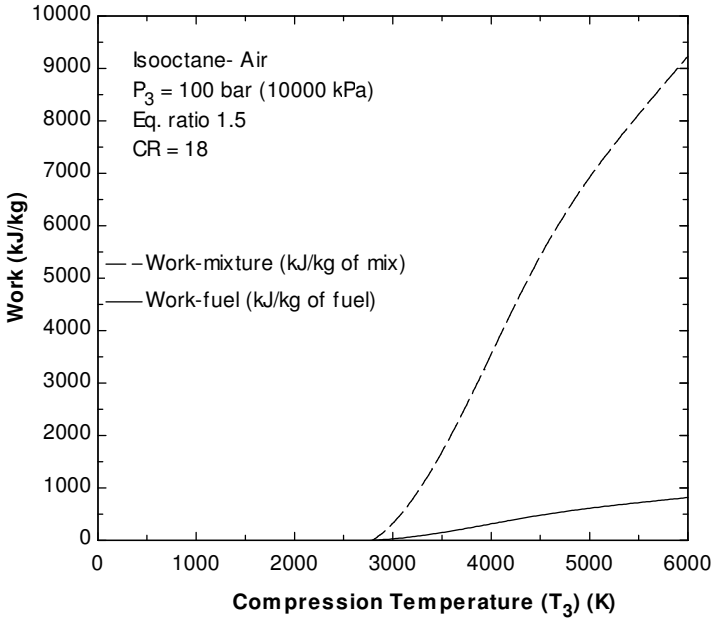

Fig. 65. Work as a function of compression temperature for isooctane-air at 10000 kPa compression pressure, Φ = 1.5 and CR = 18.

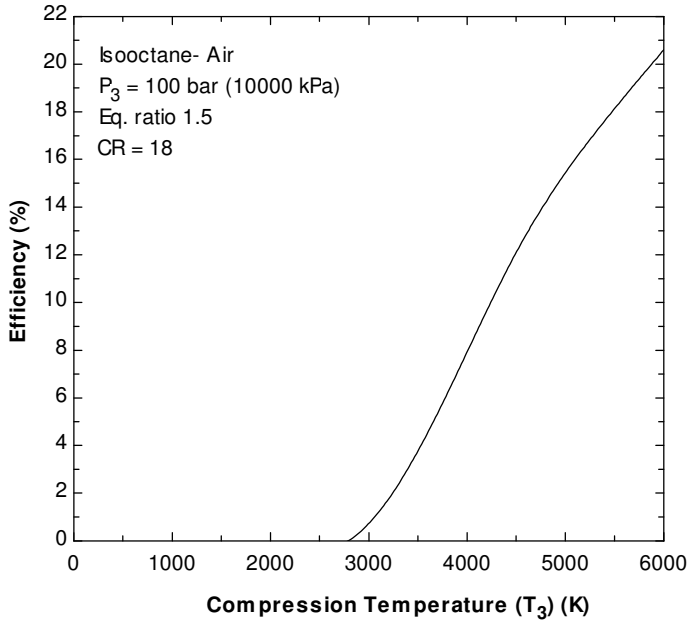

Fig. 66. Percentage efficiency as a function of compression temperature for isooctane-air at 10000 kPa compression pressure, Φ = 1.5 and CR = 18.

Effects of compression temperature for compression ratios – 4, 8, 12 and 24

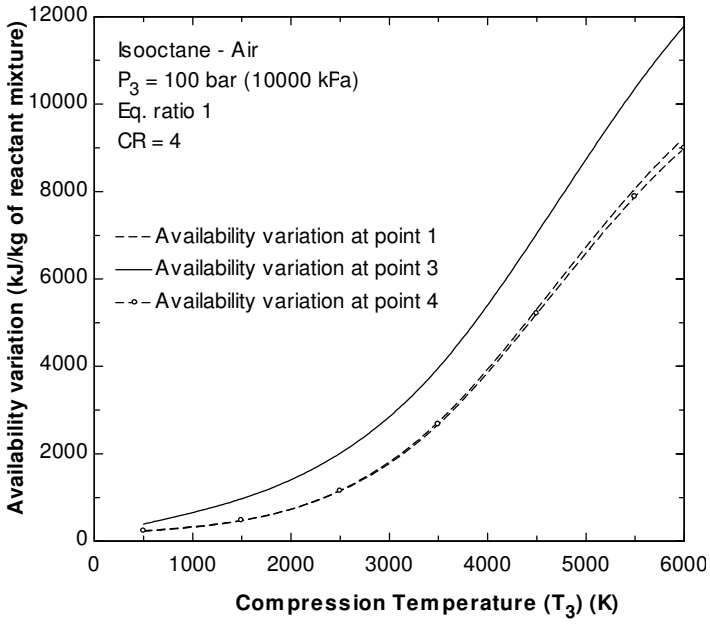

Fig. 67. Availabilities as a function of compression temperature for isooctane-air at 10000 kPa compression pressure, Φ = 1.0 and CR = 4.

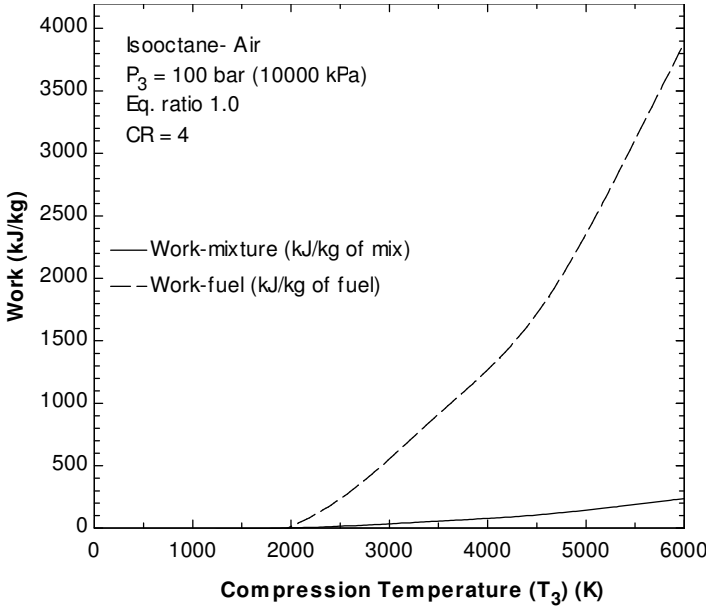

Fig. 68. Work as a function of compression temperature for isooctane-air at 10000 kPa compression pressure, Φ = 1.0 and CR = 4.

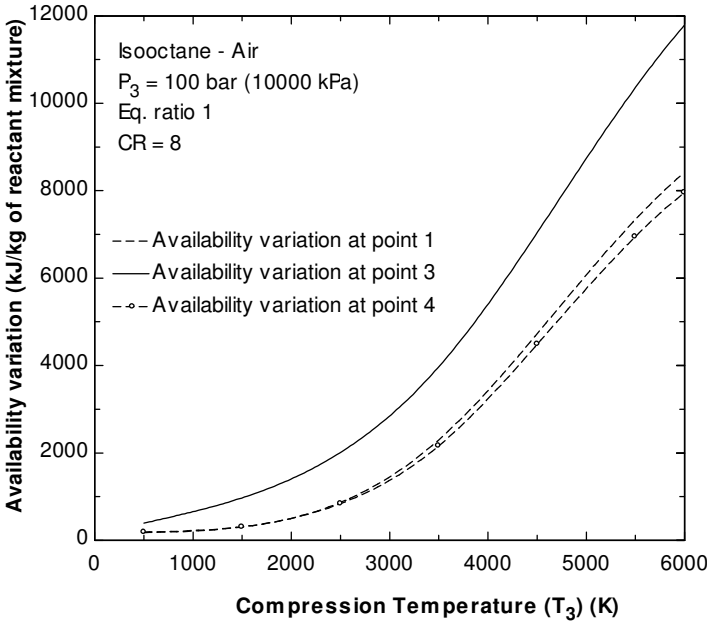

Fig. 69. Availabilities as a function of compression temperature for isooctane-air at 10000 kPa compression pressure, Φ = 1.0 and CR = 8.

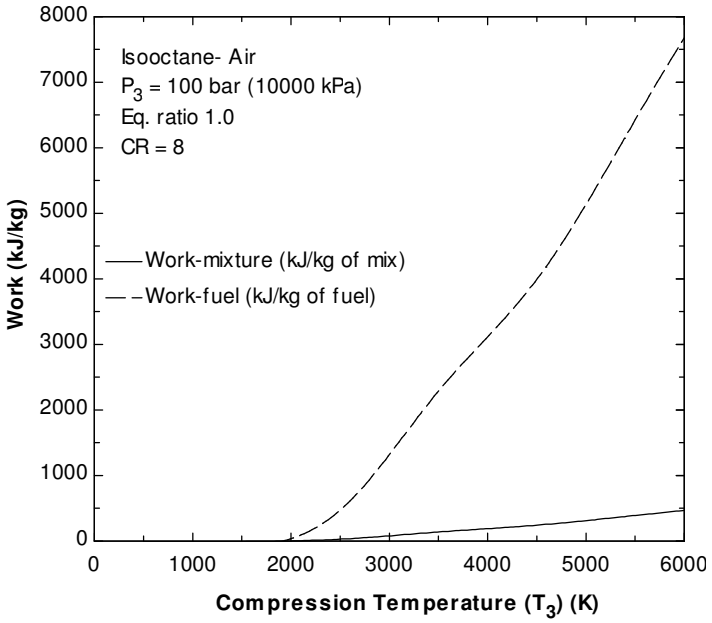

Fig. 70. Work as a function of compression temperature for isooctane-air at 10000 kPa compression pressure, Φ = 1.0 and CR = 8.

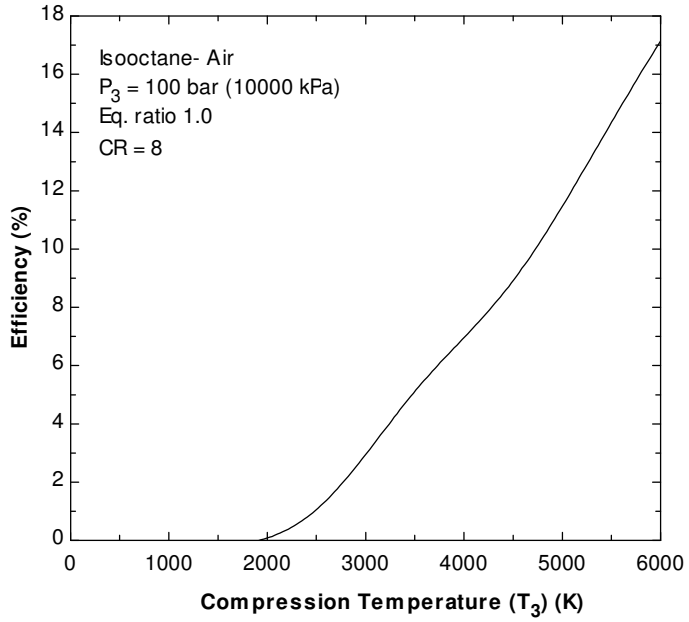

Fig. 71. Percentage efficiency as a function of compression temperature for isooctane-air at 10000 kPa compression pressure, Φ = 1.0 and CR = 8.

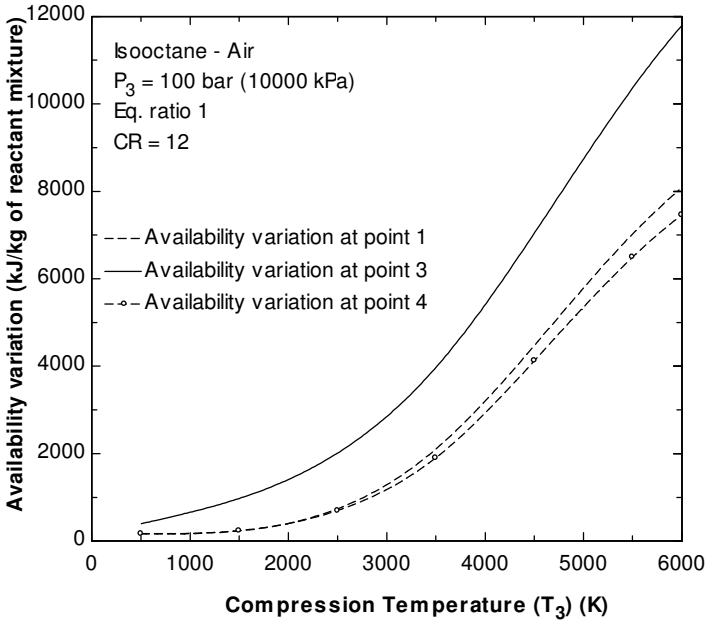

Fig. 72. Availabilities as a function of compression temperature for isooctane-air at 10000 kPa compression pressure, Φ = 1.0 and CR = 12.

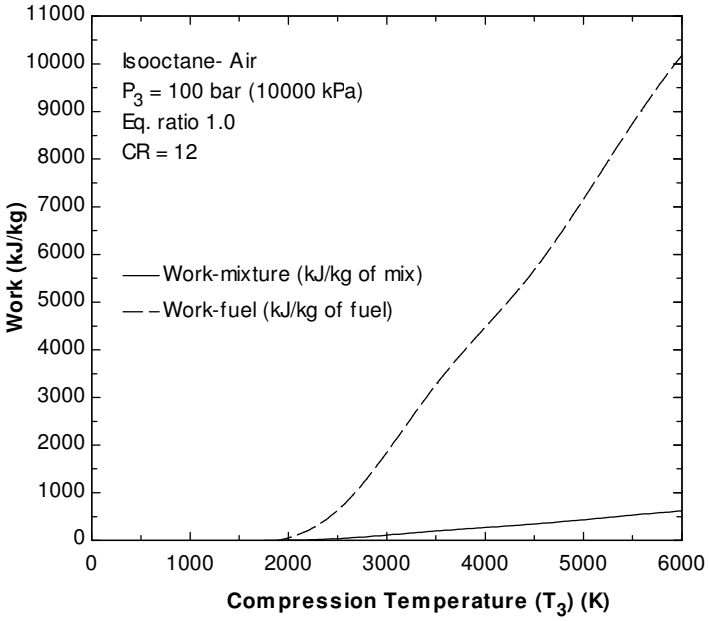

Fig. 73. Work as a function of compression temperature for isooctane-air at 10000 kPa compression pressure, Φ = 1.0 and CR = 12.

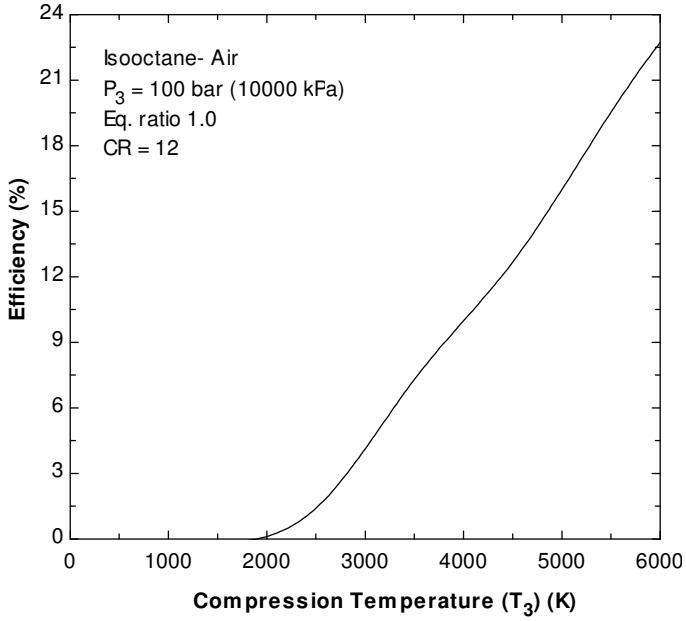

Fig. 74. Percentage efficiency as a function of compression temperature for isooctane-air at 10000 kPa compression pressure, Φ = 1.0 and CR = 12.

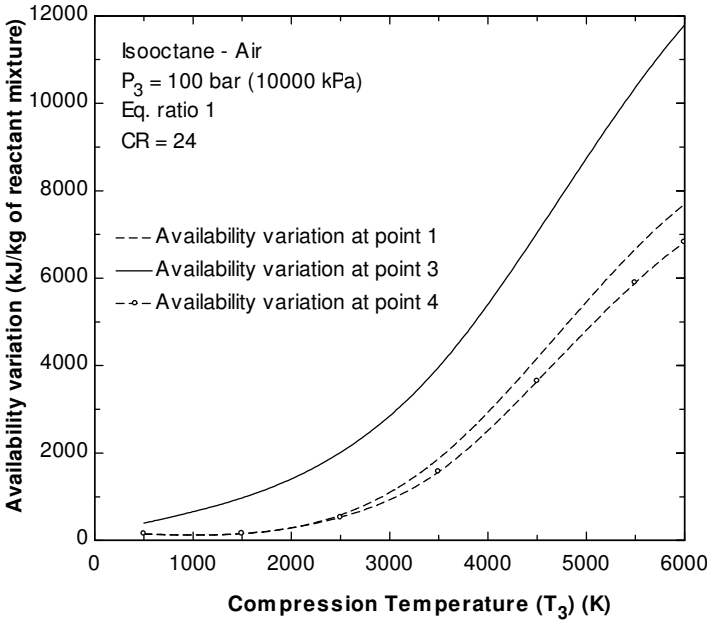

Fig. 75. Availabilities as a function of compression temperature for isooctane-air at 10000 kPa compression pressure, Φ = 1.0 and CR = 24.

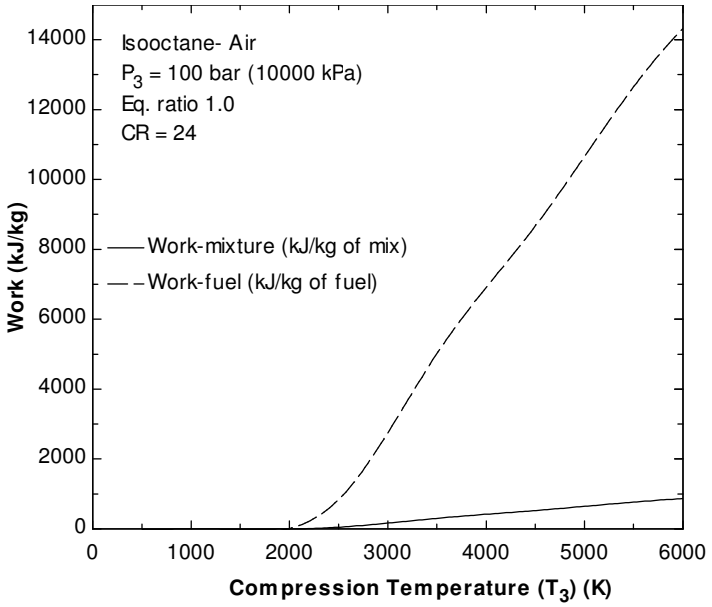

Fig. 76. Work as a function of compression temperature for isooctane-air at 10000 kPa compression pressure, Φ = 1.0 and CR = 24.

For Hydrogen (complete set of results)

Effects of compression temperature for compression pressures – 1000 kPa, 5000 kPa, 10000 kPa, 15000 kPa and 20000 kPa

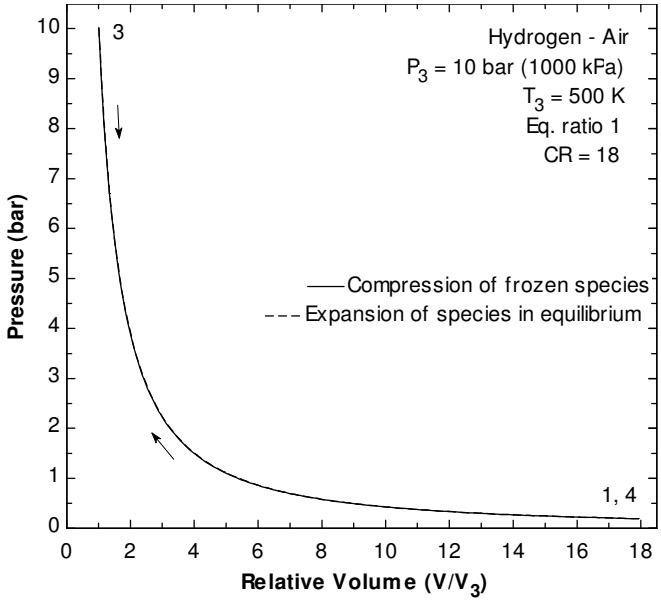

Fig. 77. Variation of pressure as a function of relative volume for hydrogen-air at 500 K compression temperature, 1000 kPa compression pressure, Φ = 1.0 and CR = 18.

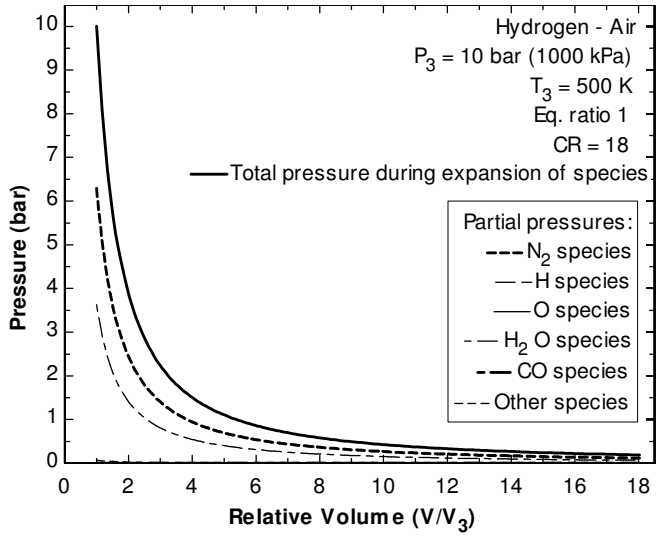

Fig. 78. Partial pressures of the species and the total pressure of the mixture, during isentropic expansion, as a function of relative volume for hydrogen-air at 500 K compression temperature, 1000 kPa compression pressure, Φ = 1.0 and CR = 18.

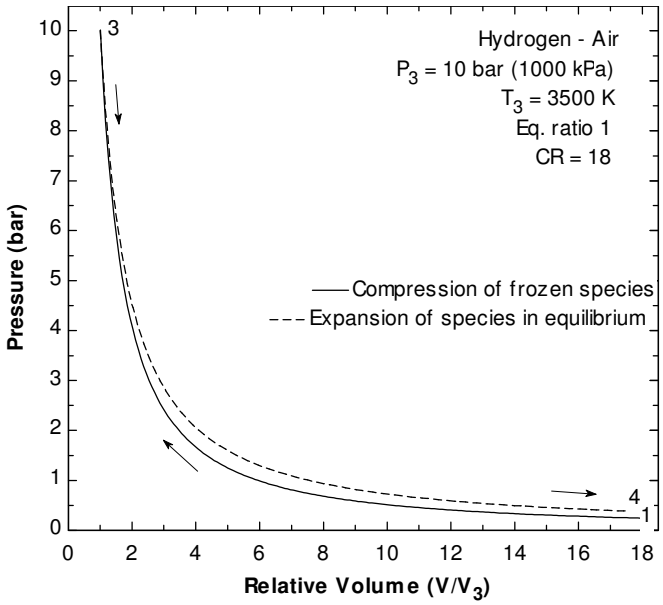

Fig. 79. Variation of pressure as a function of relative volume for hydrogen-air at 3500 K compression temperature, 1000 kPa compression pressure, Φ = 1.0 and CR = 18.

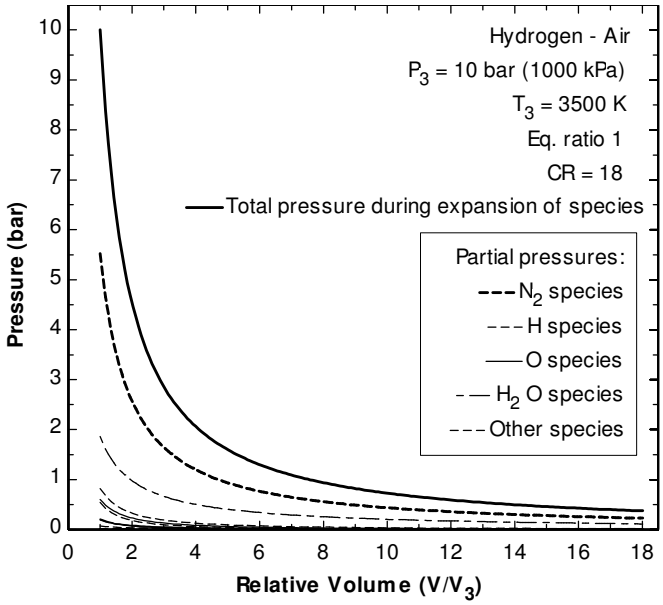

Fig. 80. Partial pressures of the species and the total pressure of the mixture, during isentropic expansion, as a function of relative volume for hydrogen-air at 3500 K compression temperature, 1000 kPa compression pressure, Φ = 1.0 and CR = 18.

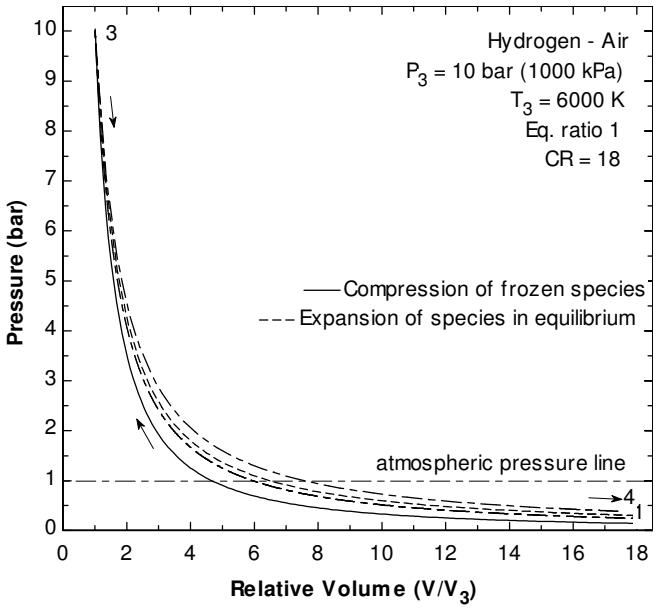

Fig. 81. Variation of pressure as a function of relative volume for hydrogen-air at 3500 K and 6000 K compression temperatures, 1000 kPa compression pressure, Φ = 1.0 and CR = 18.

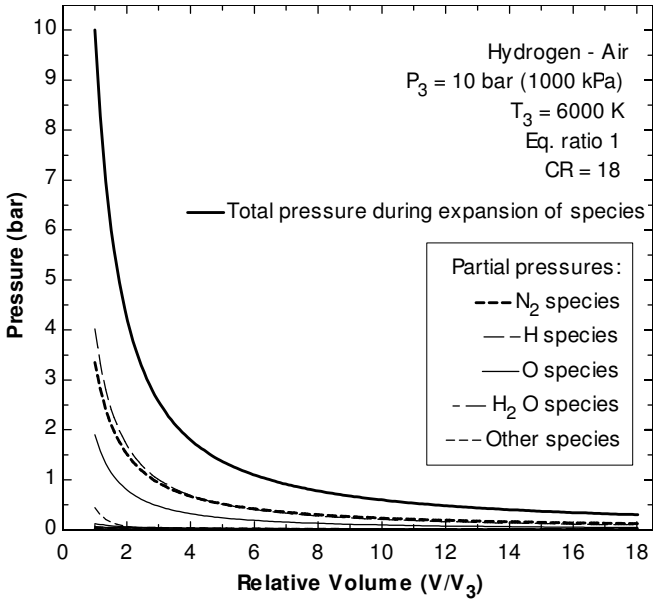

Fig. 82. Partial pressures of the species and the total pressure of the mixture, during isentropic expansion, as a function of relative volume for hydrogen-air at 6000 K compression temperature, 1000 kPa compression pressure, Φ = 1.0 and CR = 18.

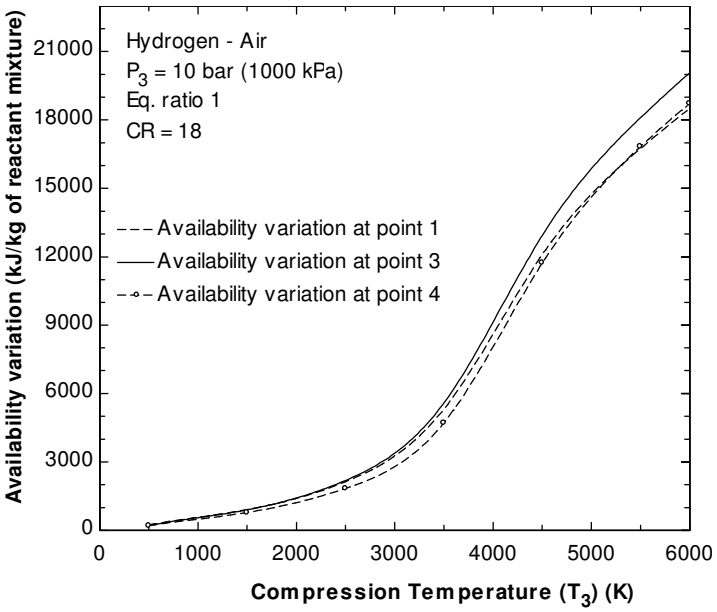

Fig. 83. Availabilities as a function of compression temperature for hydrogen-air at 1000 kPa compression pressure, Φ = 1.0 and CR = 18.

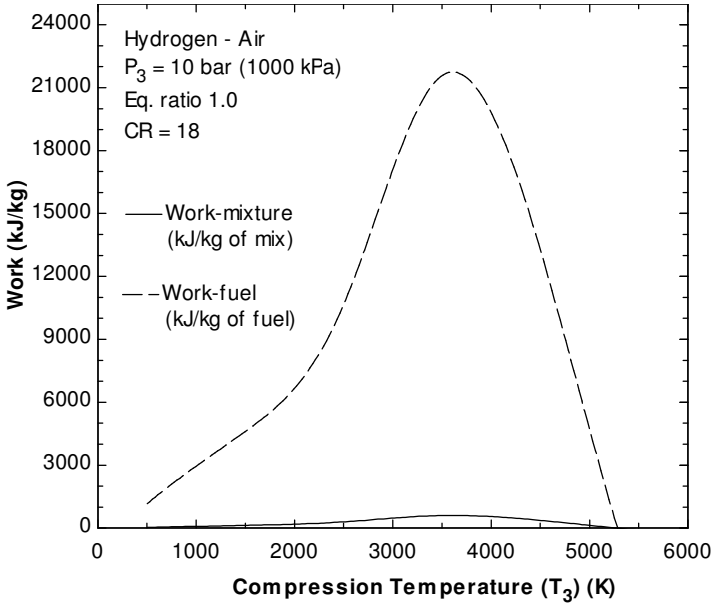

Fig. 84. Work as a function of compression temperature for hydrogen-air at 1000 kPa compression pressure, Φ = 1.0 and CR = 18.

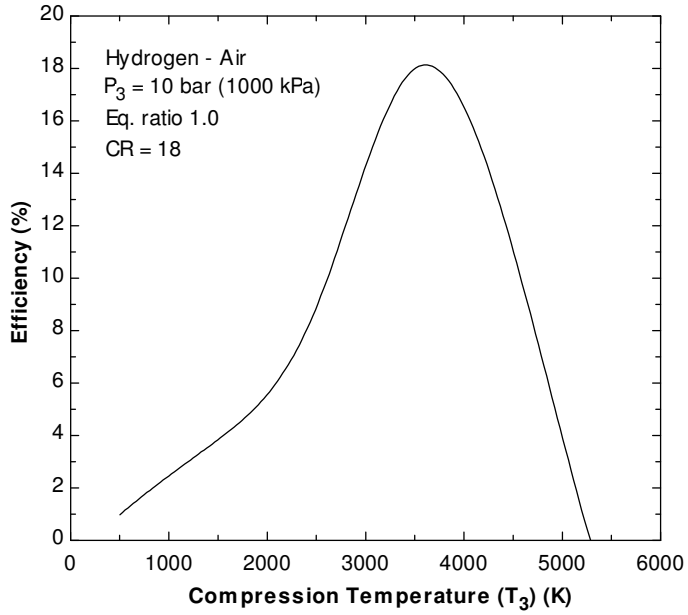

Fig. 85. Percentage efficiency as a function of compression temperature for hydrogen-air at 1000 kPa compression pressure, Φ = 1.0 and CR = 18.

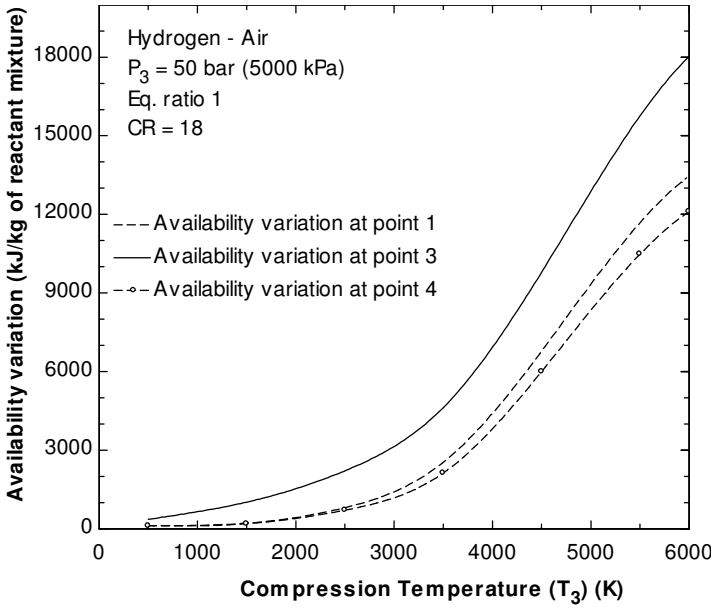

Fig. 86. Availabilities as a function of compression temperature for hydrogen-air at 5000 kPa compression pressure, Φ = 1.0 and CR = 18.

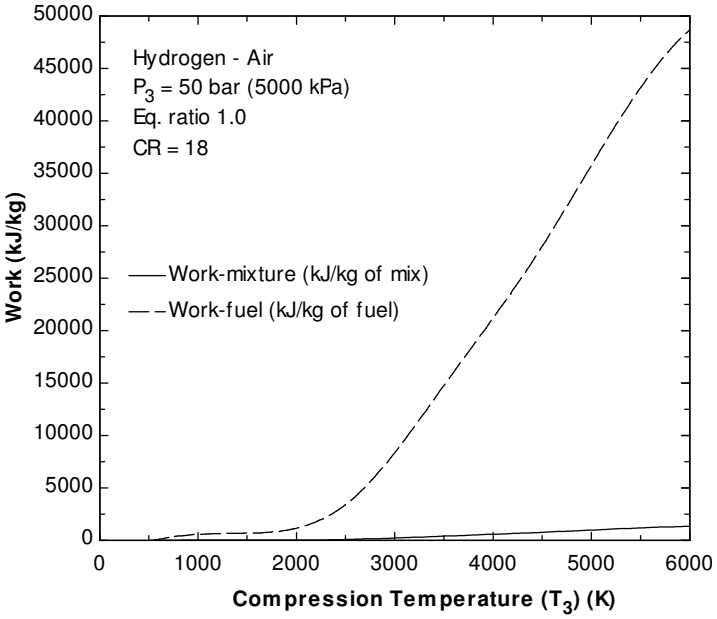

Fig. 87. Work as a function of compression temperature for hydrogen-air at 5000 kPa compression pressure, Φ = 1.0 and CR = 18.

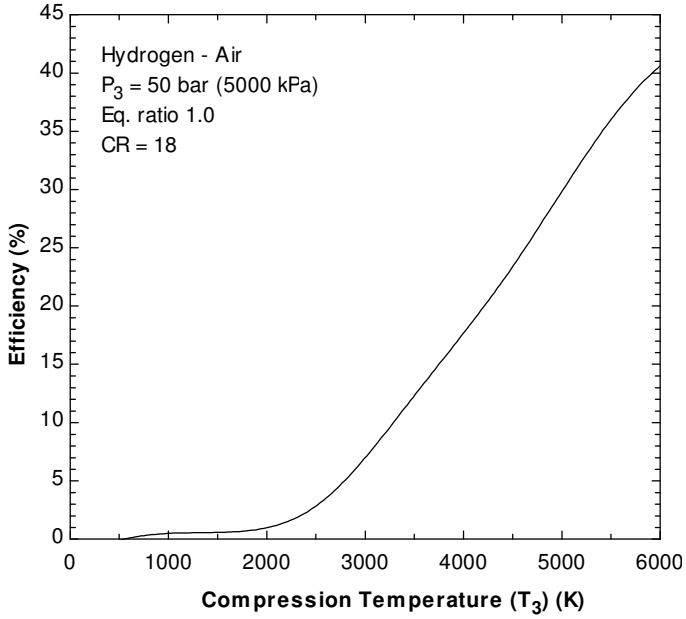

Fig. 88. Percentage efficiency as a function of compression temperature for hydrogen-air at 5000 kPa compression pressure, Φ = 1.0 and CR = 18.

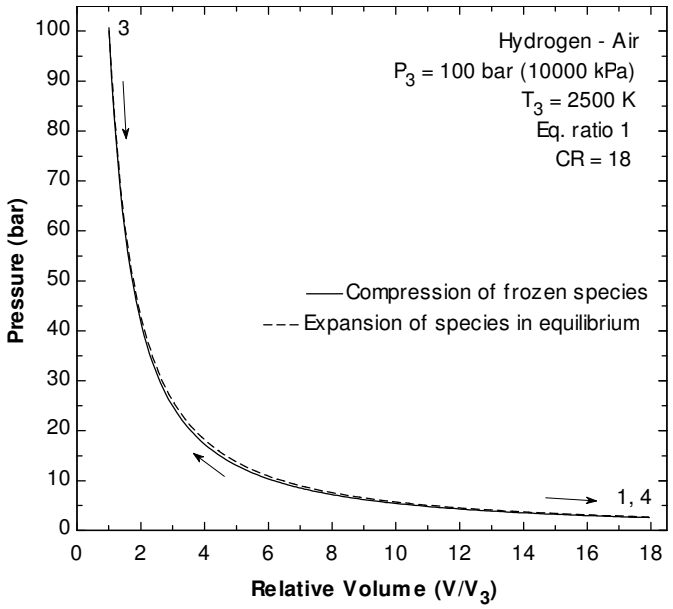

Fig. 89. Variation of pressure as a function of relative volume for hydrogen-air at 2500 K compression temperature, 10000 kPa compression pressure, Φ = 1.0 and CR = 18.

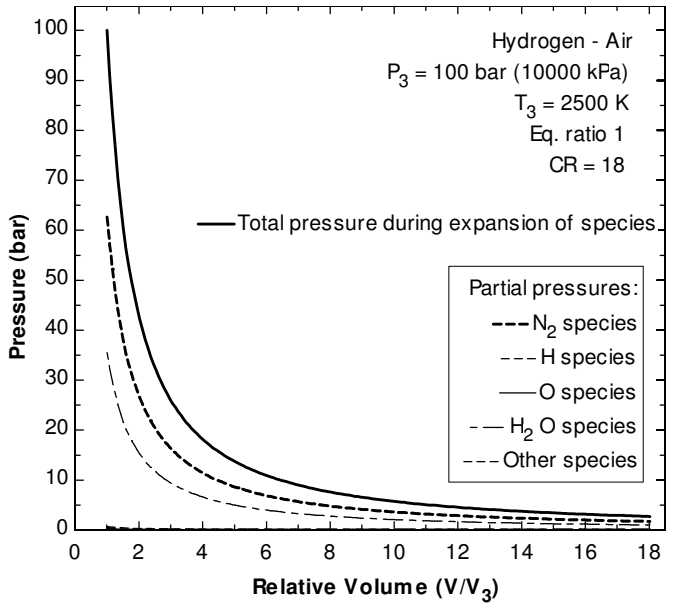

Fig. 90. Partial pressures of the species and the total pressure of the mixture, during isentropic expansion, as a function of relative volume for hydrogen-air at 2500 K compression temperature, 10000 kPa compression pressure, Φ = 1.0 and CR = 18.

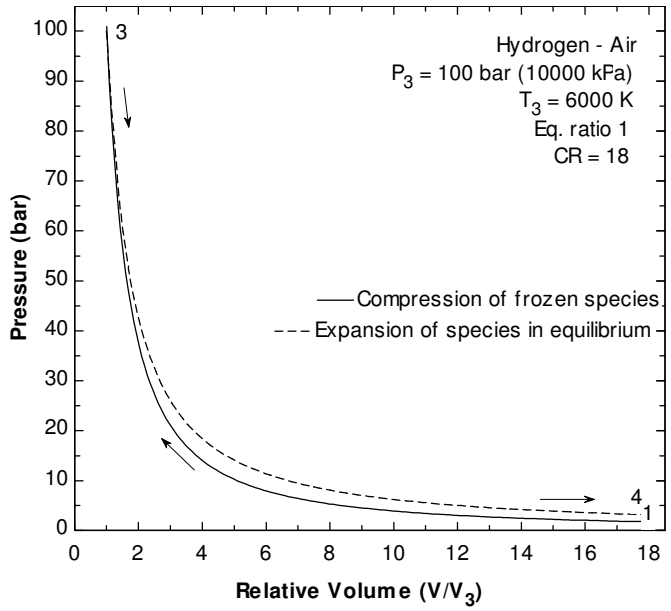

Fig. 91. Variation of pressure as a function of relative volume for hydrogen-air at 6000 K compression temperature, 10000 kPa compression pressure, Φ = 1.0 and CR = 18.

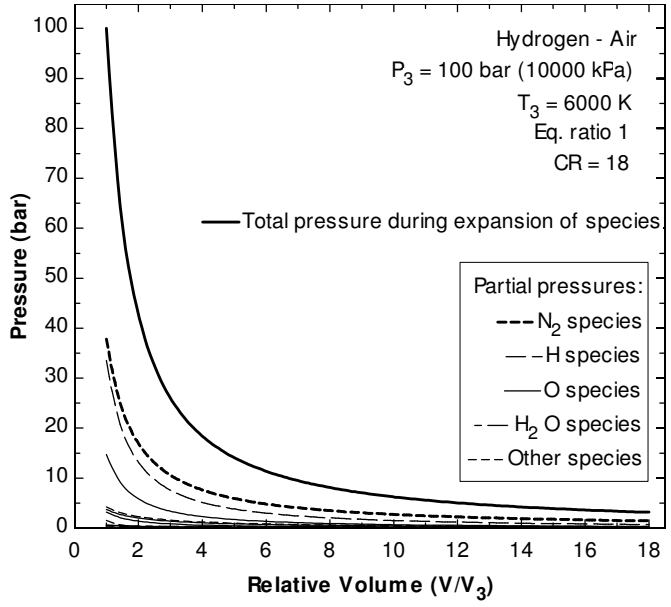

Fig. 92. Partial pressures of the species and the total pressure of the mixture, during isentropic expansion, as a function of relative volume for hydrogen-air at 6000 K compression temperature, 10000 kPa compression pressure, Φ = 1.0 and CR = 18.

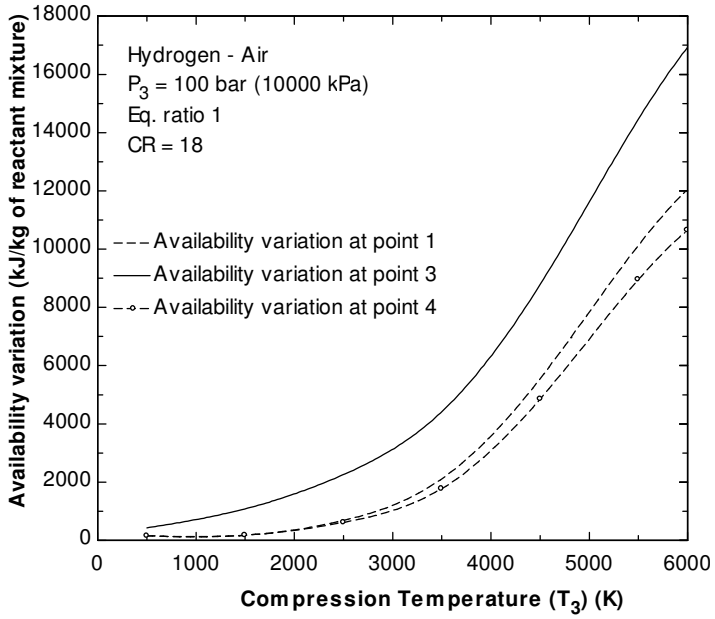

Fig. 93. Availabilities as a function of compression temperature for hydrogen-air at 10000 kPa compression pressure, Φ = 1.0 and CR = 18.

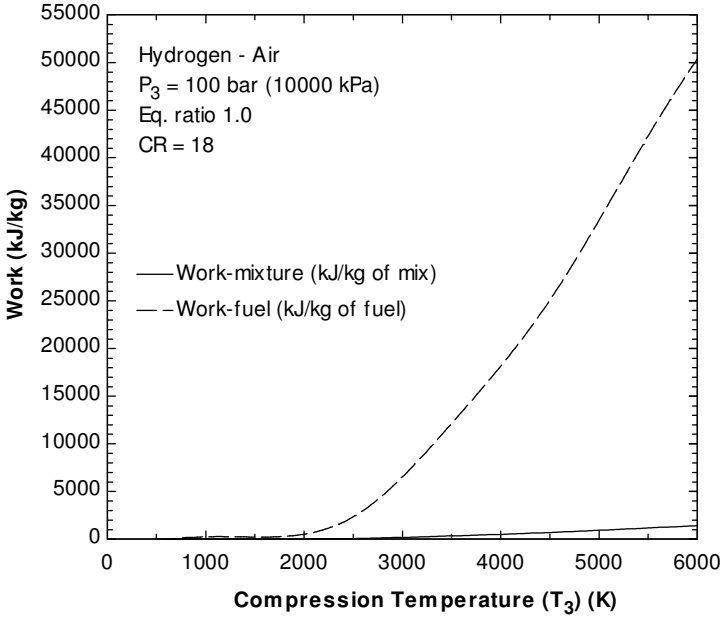

Fig. 94. Work as a function of compression temperature for hydrogen-air at 10000 kPa compression pressure, Φ = 1.0 and CR = 18.

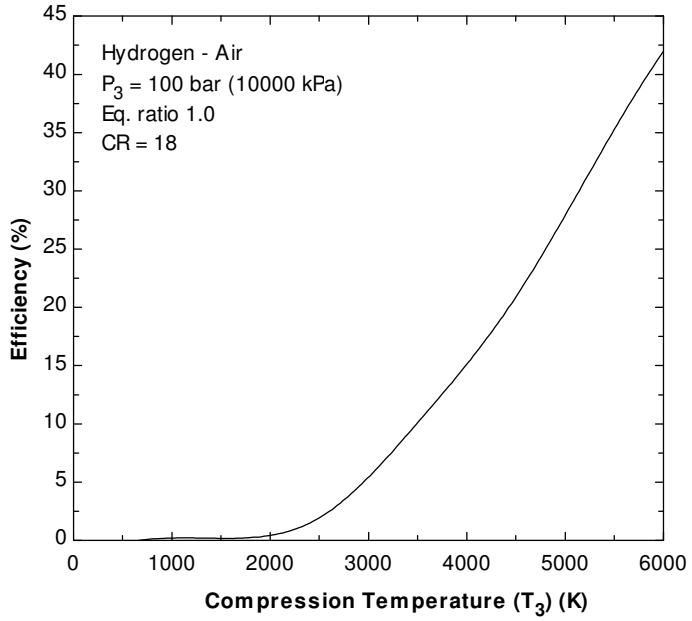

Fig. 95. Percentage efficiency as a function of compression temperature for hydrogen-air at 10000 kPa compression pressure, Φ = 1.0 and CR = 18.

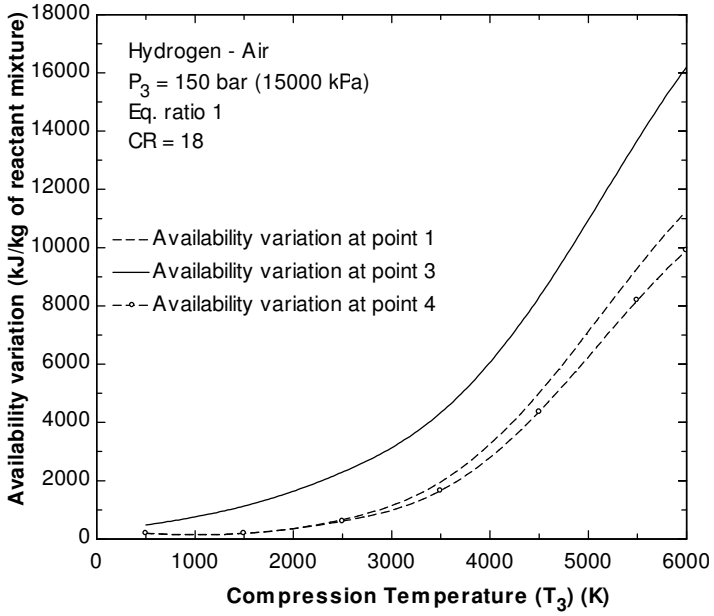

Fig. 96. Availabilities as a function of compression temperature for hydrogen-air at 150000 kPa compression pressure, Φ = 1.0 and CR = 18.

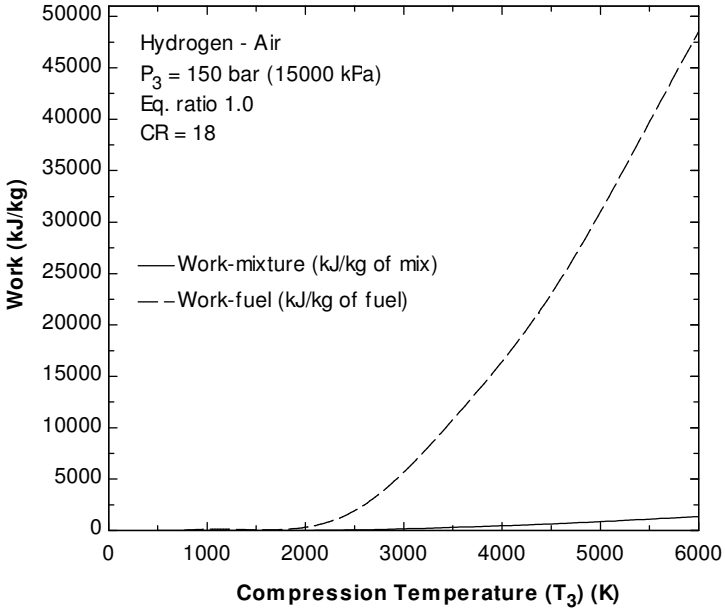

Fig. 97. Work as a function of compression temperature for hydrogen-air at 15000 kPa compression pressure, Φ = 1.0 and CR = 18.

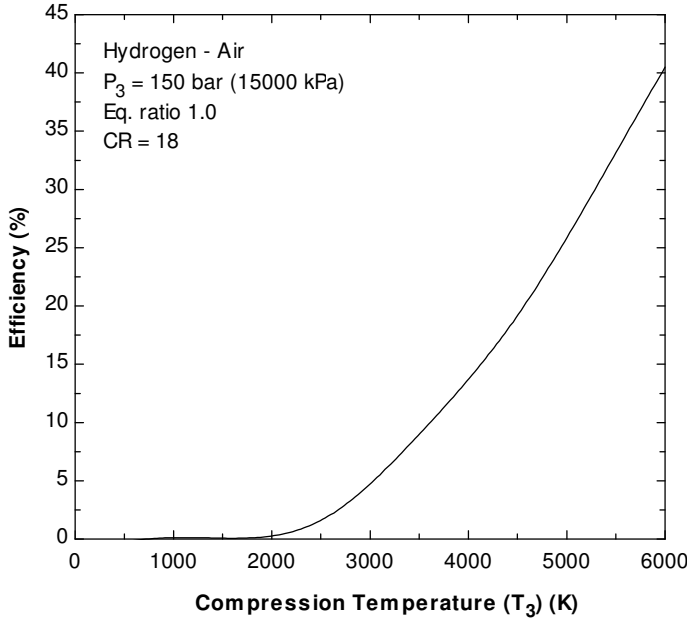

Fig. 98. Percentage efficiency as a function of compression temperature for hydrogen-air at 15000 kPa compression pressure, Φ = 1.0 and CR = 18.

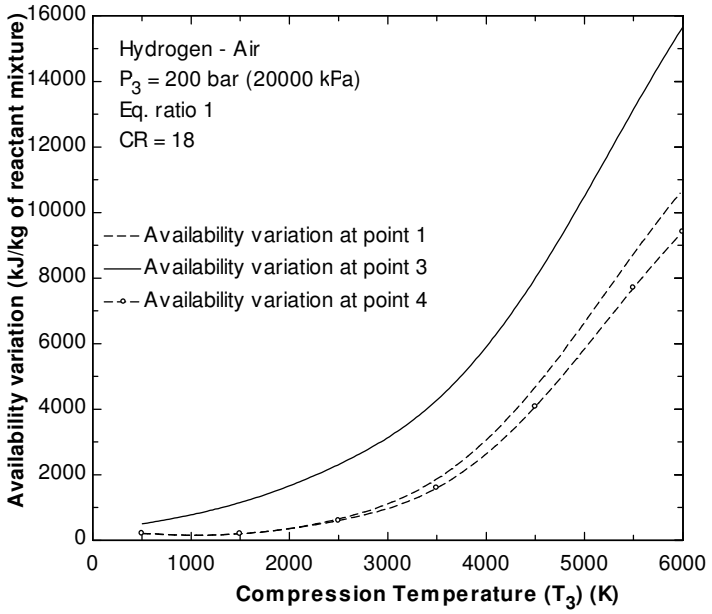

Fig. 99. Availabilities as a function of compression temperature for hydrogen-air at 20000 kPa compression pressure, Φ = 1.0 and CR = 18.

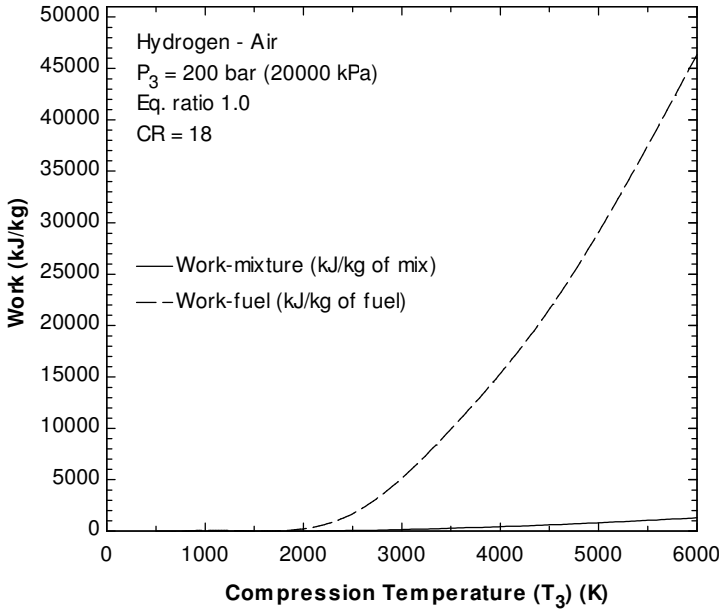

Fig. 100. Work as a function of compression temperature for hydrogen-air at 20000 kPa compression pressure, Φ = 1.0 and CR = 18.

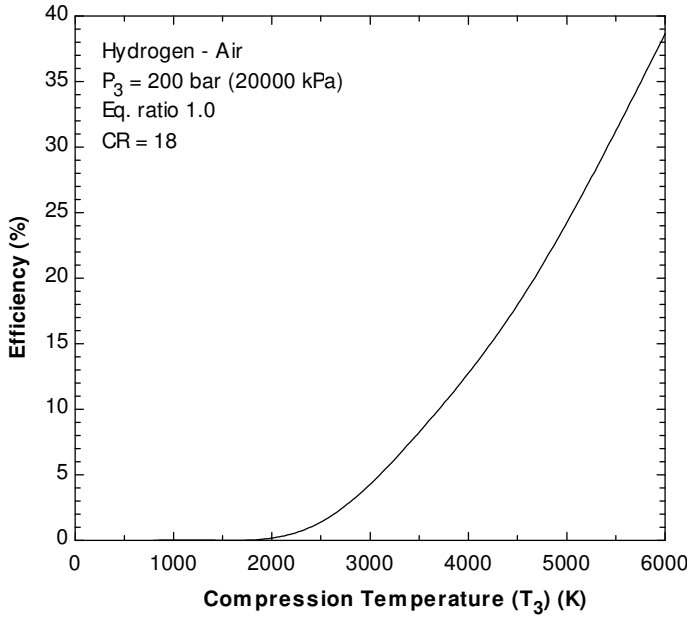

Fig. 101. Percentage efficiency as a function of compression temperature for hydrogen-air at 20000 kPa compression pressure, Φ = 1.0 and CR = 18.

Effects of compression temperature for equivalence ratios –0.2, 0.6, 1.0 and 1.5, 2.0

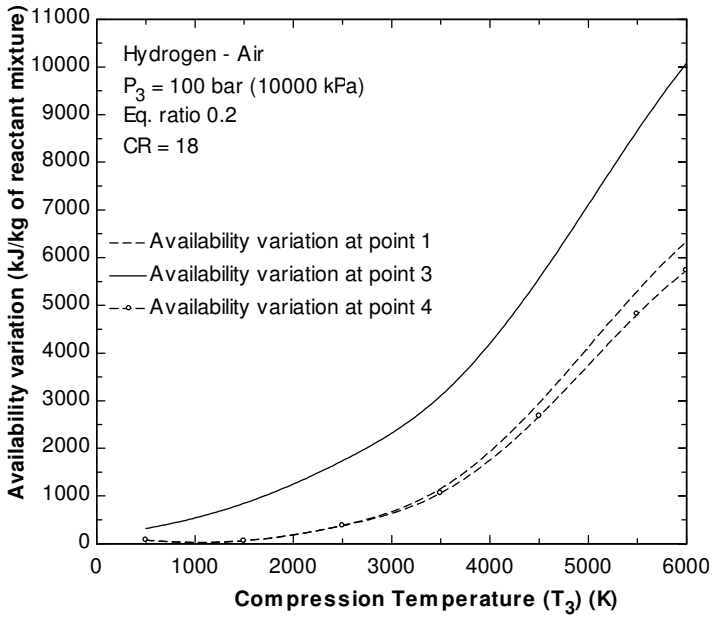

Fig. 102. Availabilities as a function of compression temperature for hydrogen-air at 10000 kPa compression pressure, Φ = 0.2 and CR = 18.

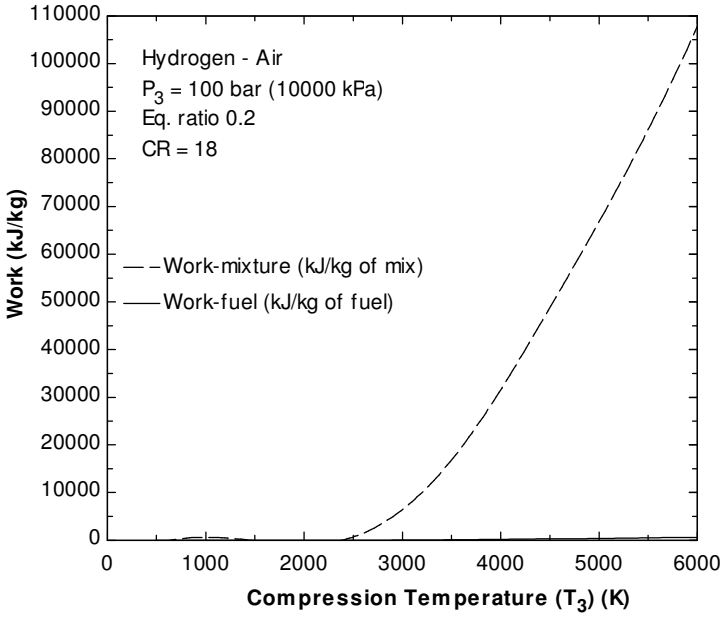

Fig. 103. Work as a function of compression temperature for hydrogen-air at 10000 kPa compression pressure, Φ = 0.2 and CR = 18.

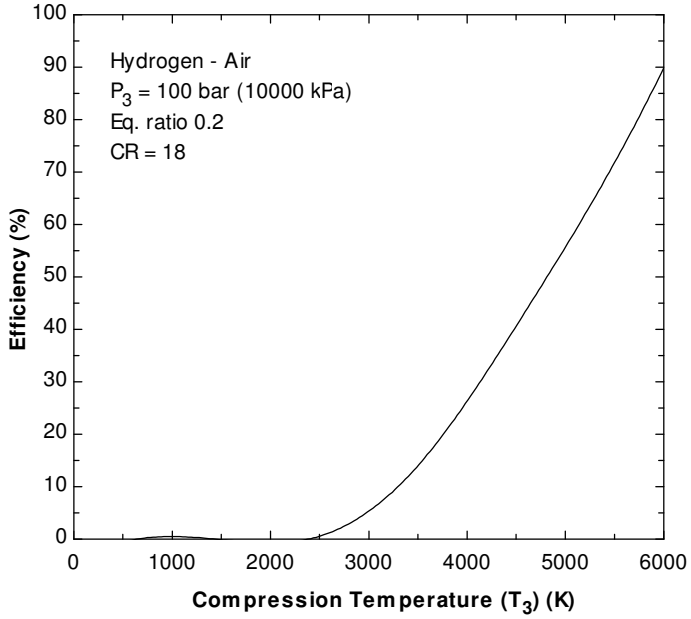

Fig. 104. Percentage efficiency as a function of compression temperature for hydrogen-air at 10000 kPa compression pressure, Φ = 0.2 and CR = 18.

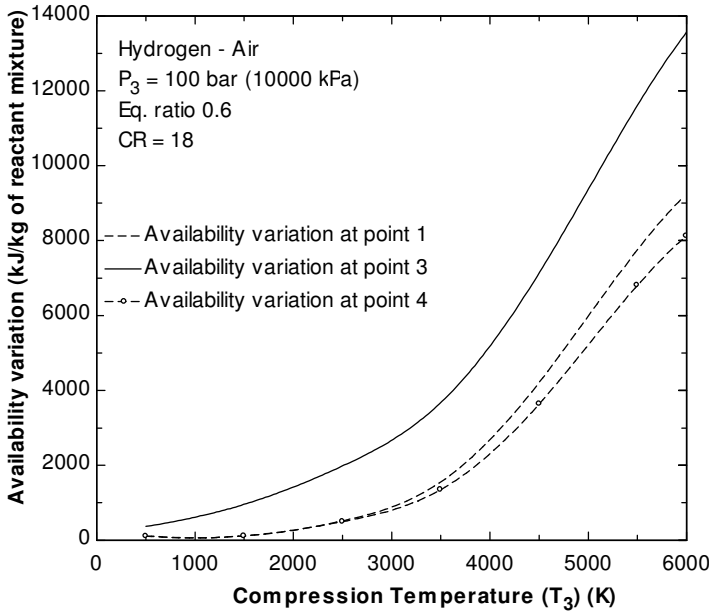

Fig. 105. Availabilities as a function of compression temperature for hydrogen-air at 10000 kPa compression pressure, Φ = 0.6 and CR = 18.

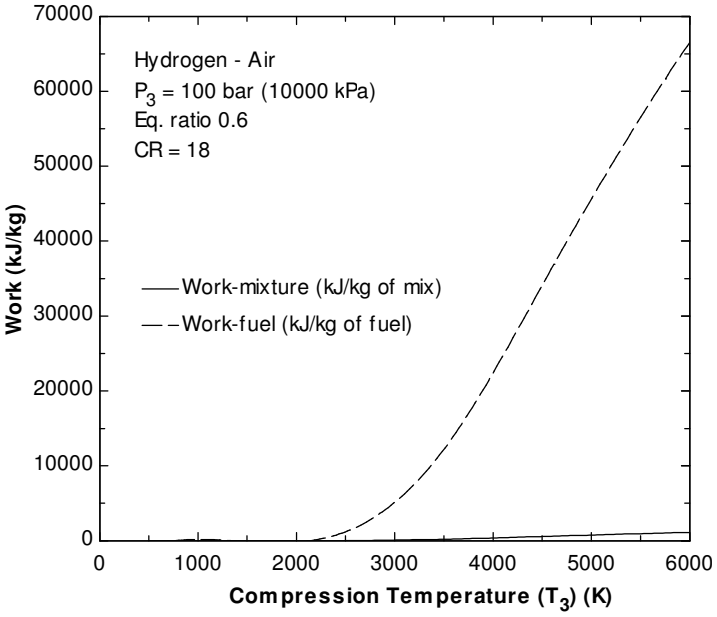

Fig. 106. Work as a function of compression temperature for hydrogen-air at 10000 kPa compression pressure, Φ = 0.6 and CR = 18.

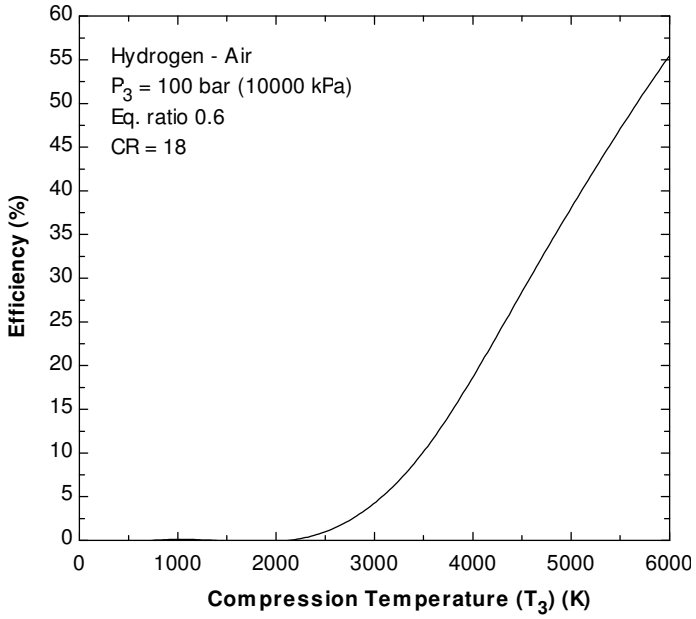

Fig. 107. Percentage efficiency as a function of compression temperature for hydrogen-air at 10000 kPa compression pressure, Φ = 0.6 and CR = 18.

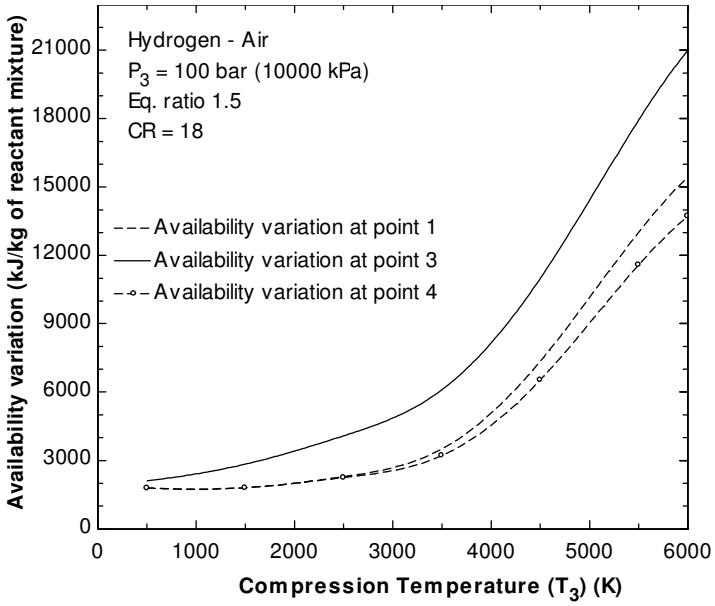

Fig. 108. Availabilities as a function of compression temperature for hydrogen-air at 10000 kPa compression pressure, Φ = 1.5 and CR = 18.

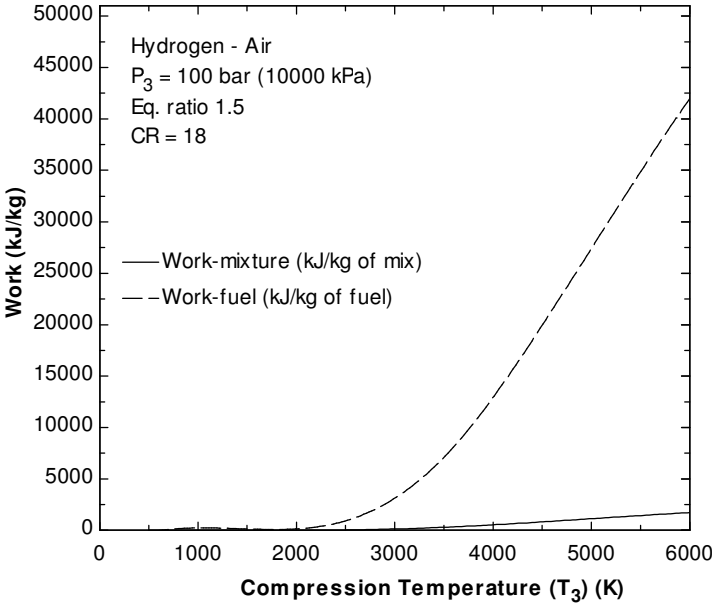

Fig. 109. Work as a function of compression temperature for hydrogen-air at 10000 kPa compression pressure, Φ = 1.5 and CR = 18.

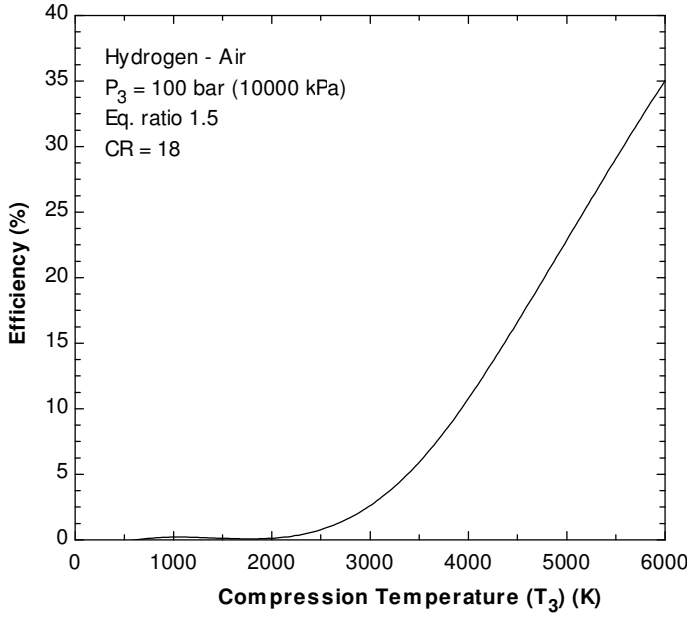

Fig. 110. Percentage efficiency as a function of compression temperature for hydrogen-air at 10000 kPa compression pressure, Φ = 1.5 and CR = 18.

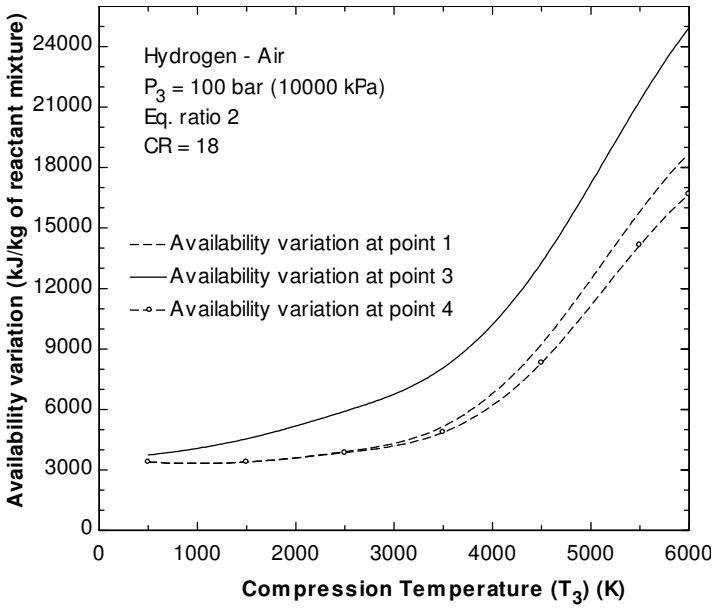

Fig. 111. Availabilities as a function of compression temperature for hydrogen-air at 10000 kPa compression pressure, Φ = 2.0 and CR = 18.

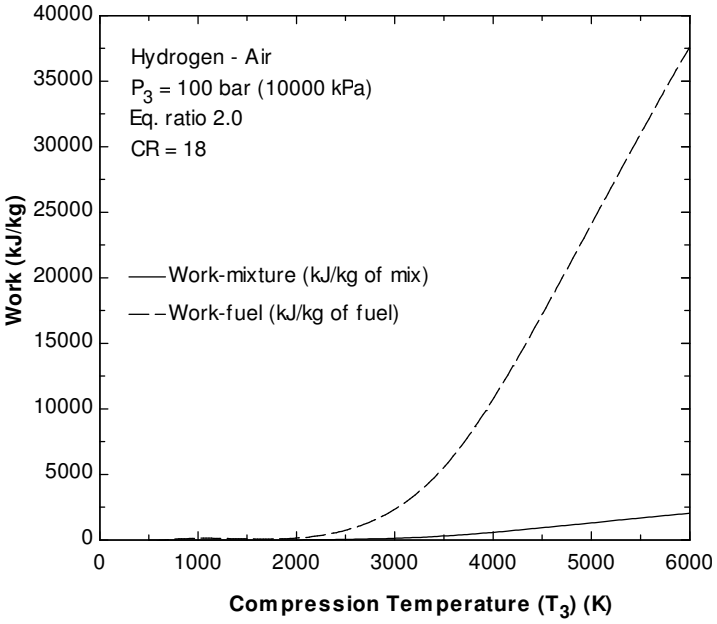

Fig. 112. Work as a function of compression temperature for hydrogen-air at 10000 kPa compression pressure, Φ = 2.0 and CR = 18.

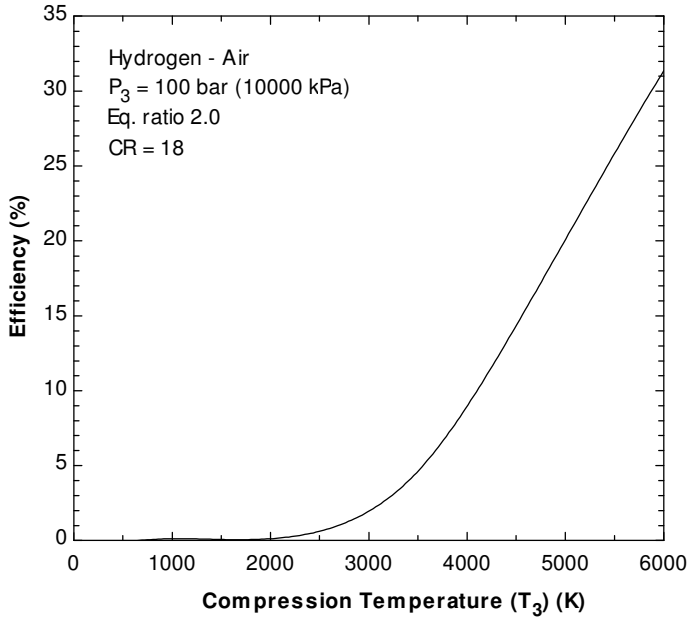

Fig. 113. Percentage efficiency as a function of compression temperature for hydrogen-air at 10000 kPa compression pressure, Φ = 2.0 and CR = 18.

Effects of compression temperature for compression pressures –4, 8, 12, 18 and 24

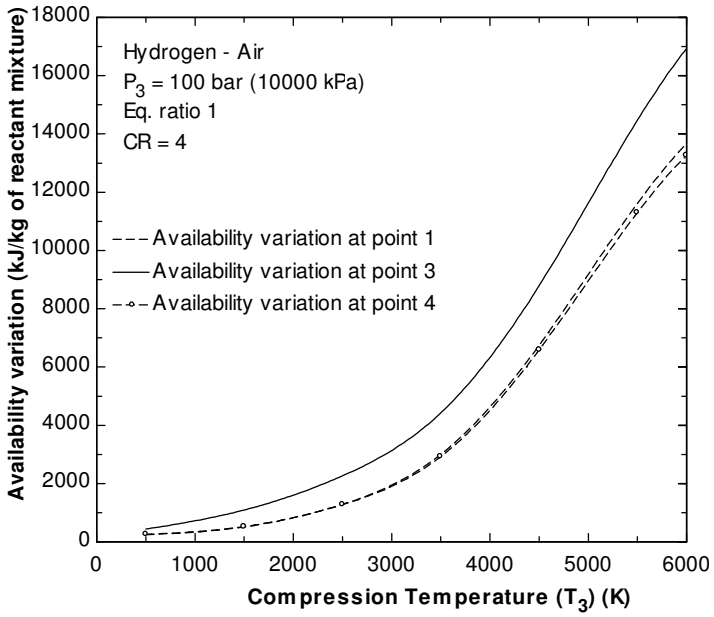

Fig. 114. Availabilities as a function of compression temperature for hydrogen-air at 10000 kPa compression pressure, Φ = 1.0 and CR = 4.

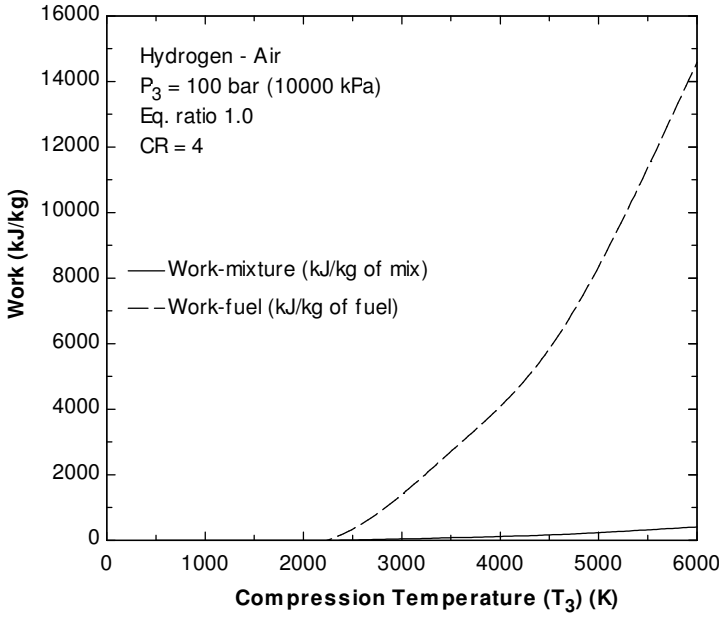

Fig. 115. Work as a function of compression temperature for hydrogen-air at 10000 kPa compression pressure, Φ = 1.0 and CR = 4.

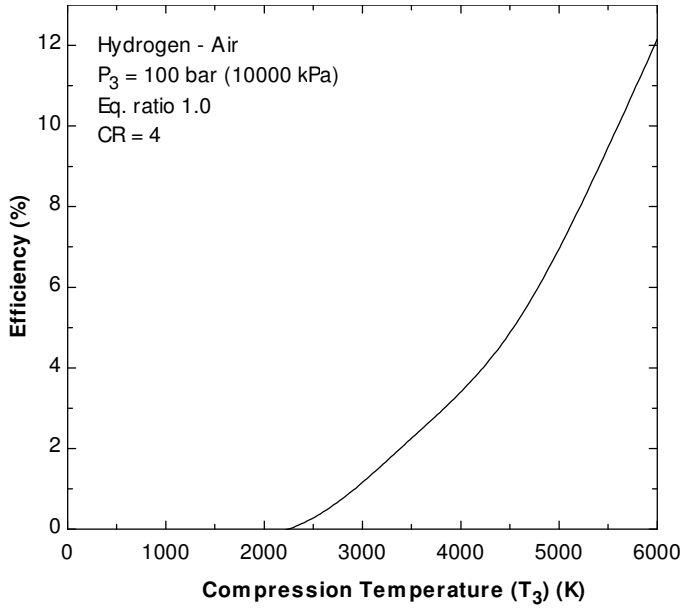

Fig. 116. Percentage efficiency as a function of compression temperature for hydrogen-air at 10000 kPa compression pressure, Φ = 1.0 and CR = 4.

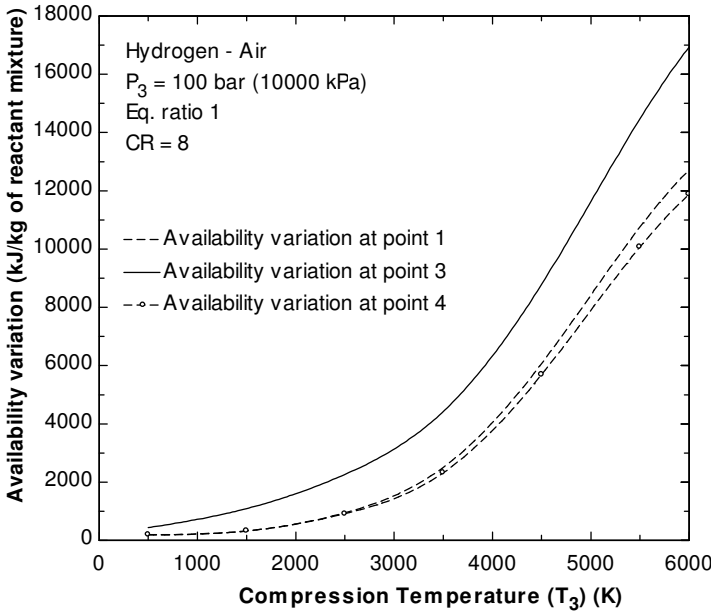

Fig. 117. Availabilities as a function of compression temperature for hydrogen-air at 10000 kPa compression pressure, Φ = 1.0 and CR = 8.

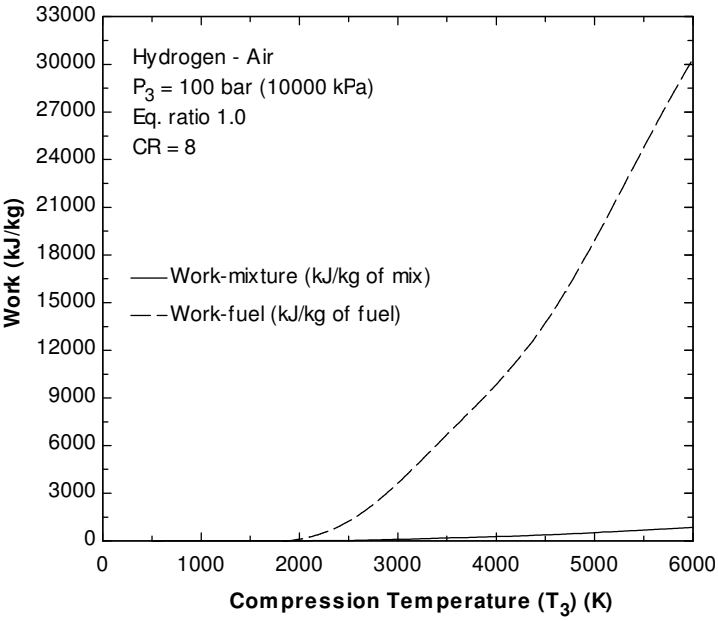

Fig. 118. Work as a function of compression temperature for hydrogen-air at 10000 kPa compression pressure, Φ = 1.0 and CR = 8.

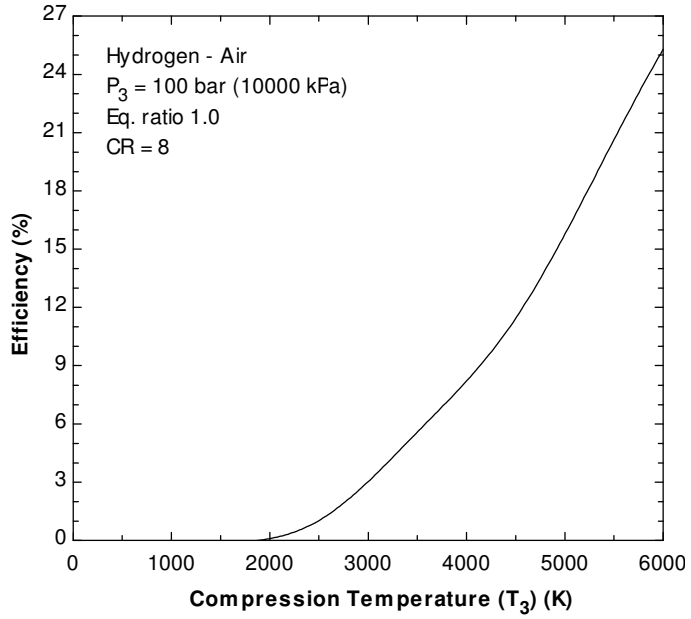

Fig. 119. Percentage efficiency as a function of compression temperature for hydrogen-air at 10000 kPa compression pressure, Φ = 1.0 and CR = 8.

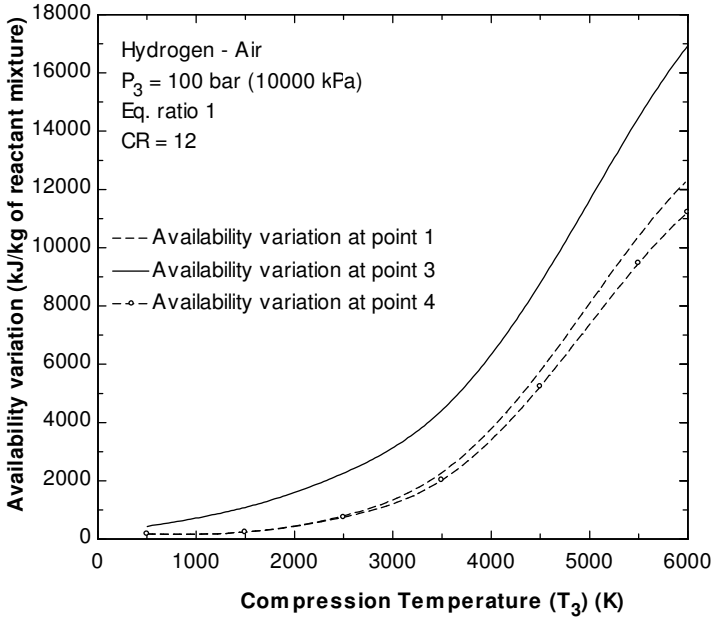

Fig. 120. Availabilities as a function of compression temperature for hydrogen-air at 10000 kPa compression pressure, Φ = 1.0 and CR = 12.

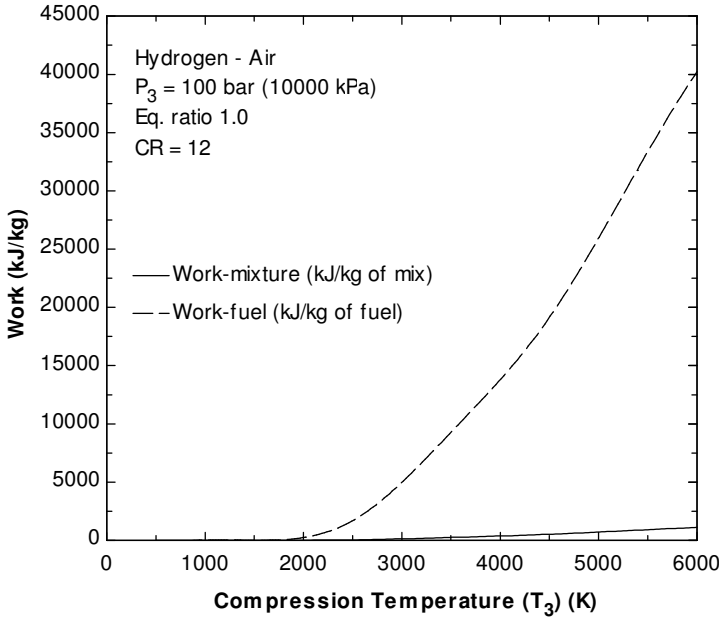

Fig. 121. Work as a function of compression temperature for hydrogen-air at 10000 kPa compression pressure, Φ = 1.0 and CR = 12.

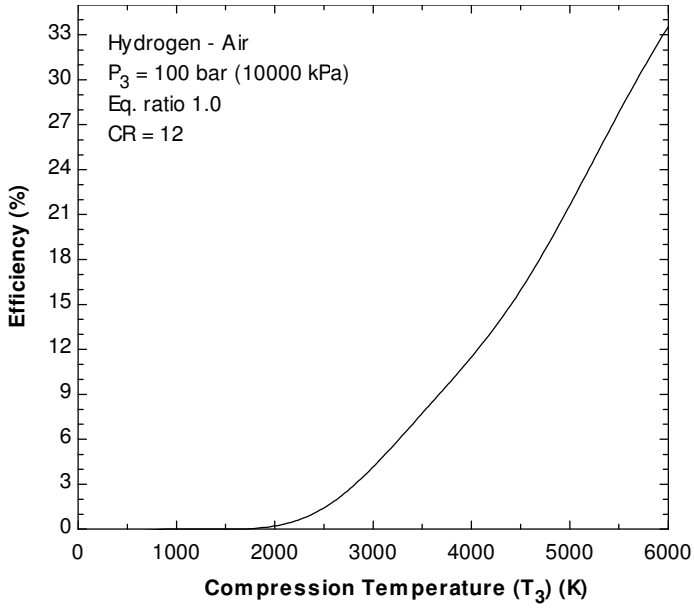

Fig. 122. Percentage efficiency as a function of compression temperature for hydrogen-air at 10000 kPa compression pressure, Φ = 1.0 and CR = 12.

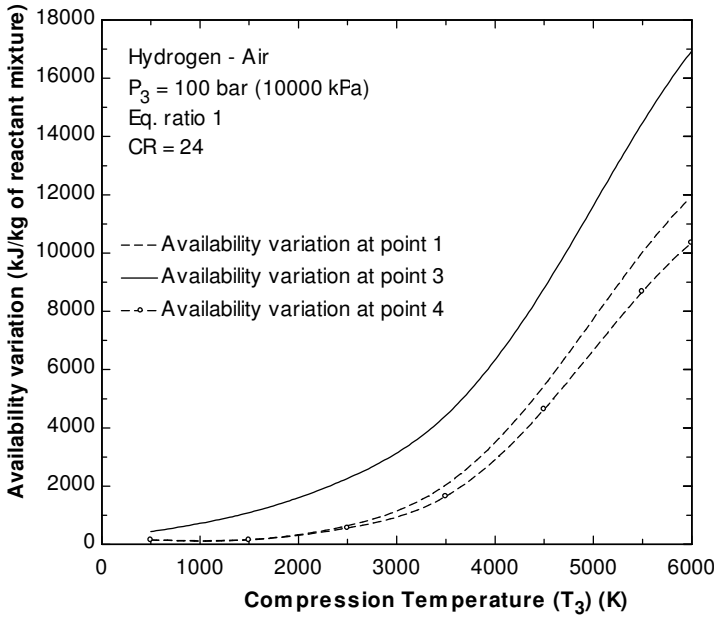

Fig. 123. Availabilities as a function of compression temperature for hydrogen-air at 10000 kPa compression pressure, Φ = 1.0 and CR = 24.

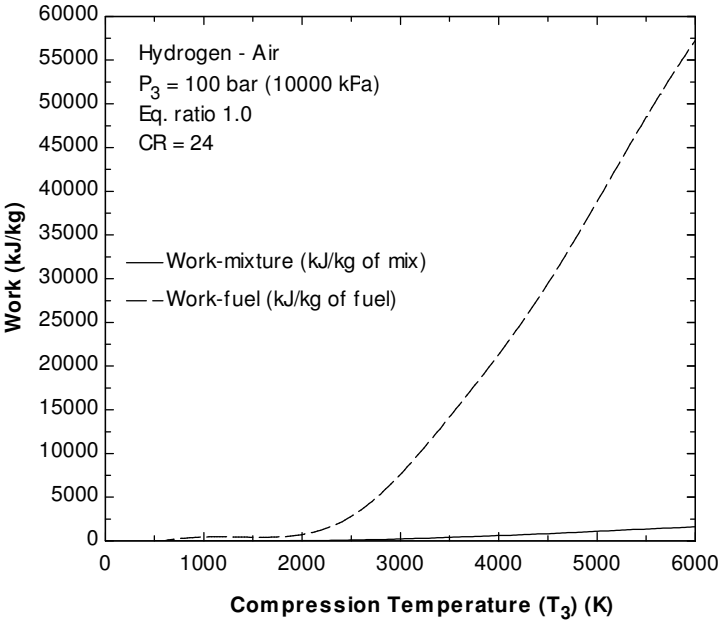

Fig. 124. Work as a function of compression temperature for hydrogen-air at 10000 kPa compression pressure, Φ = 1.0 and CR = 24.

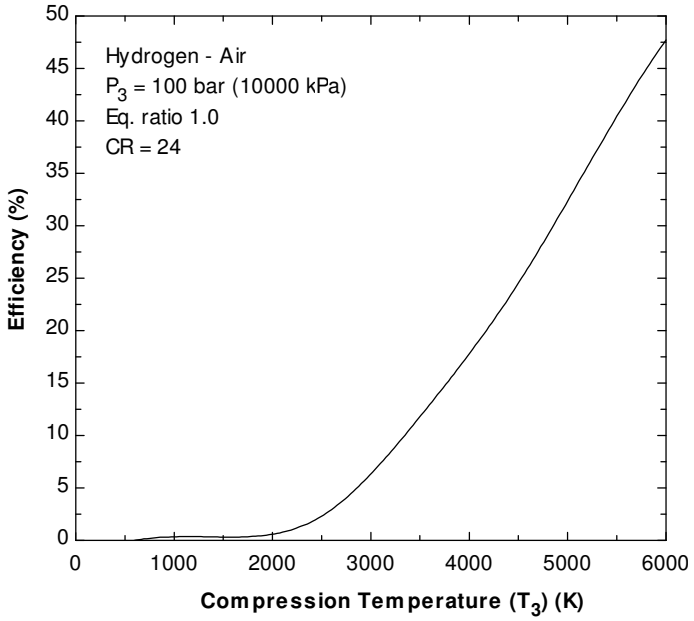

Fig. 125. Percentage efficiency as a function of compression temperature for hydrogen-air at 10000 kPa compression pressure, Φ = 1.0 and CR = 24.

Effects of compression temperature when oxygen is used as oxidant

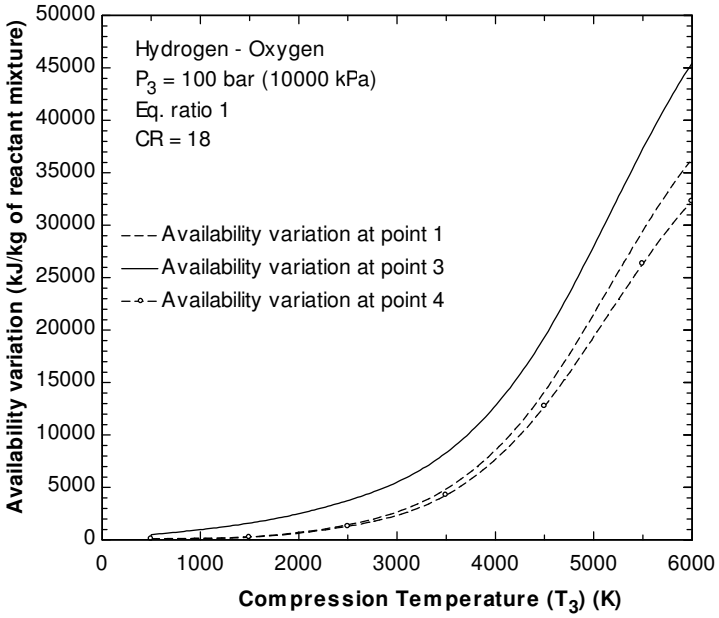

Fig. 126. Availabilities as a function of compression temperature for hydrogen-oxygen at 10000 kPa compression pressure, Φ = 1.0 and CR = 18.

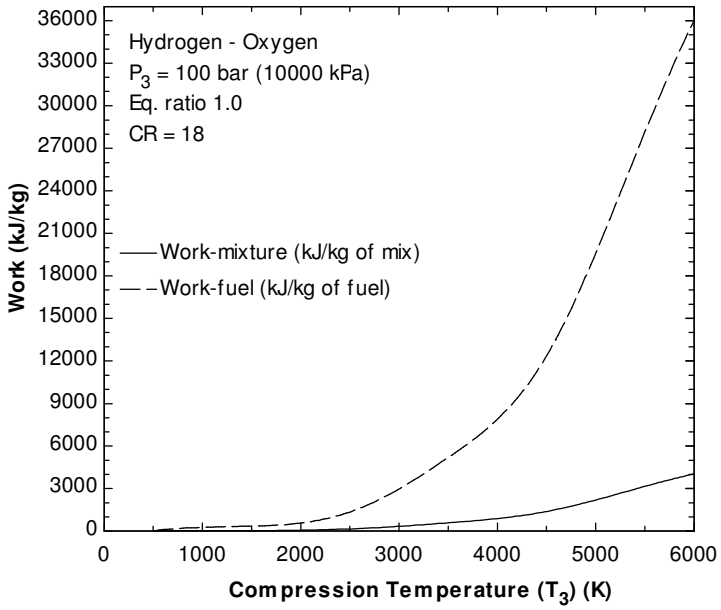

Fig. 127. Work as a function of compression temperature for hydrogen-oxygen at 10000 kPa compression pressure, Φ = 1.0 and CR = 18.

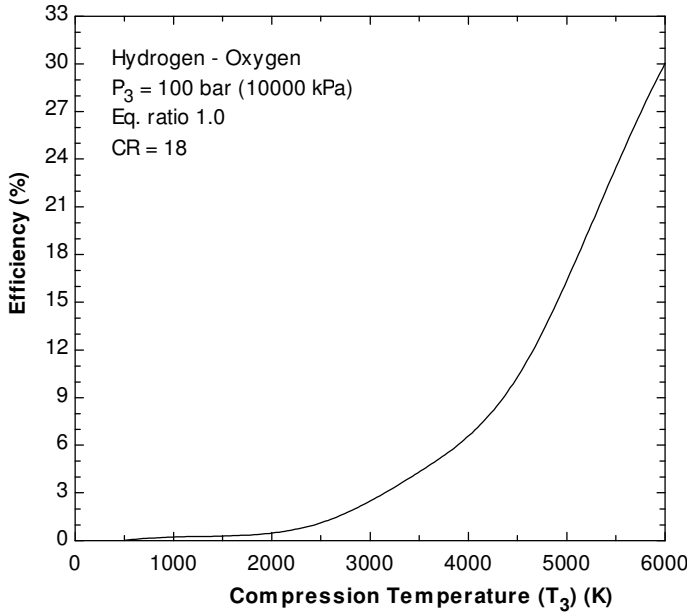

Fig. 128. Percentage efficiency as a function of compression temperature for hydrogen-oxygen at 10000 kPa compression pressure, Φ = 1.0 and CR = 18.

Effects of compression pressure and compression temperature

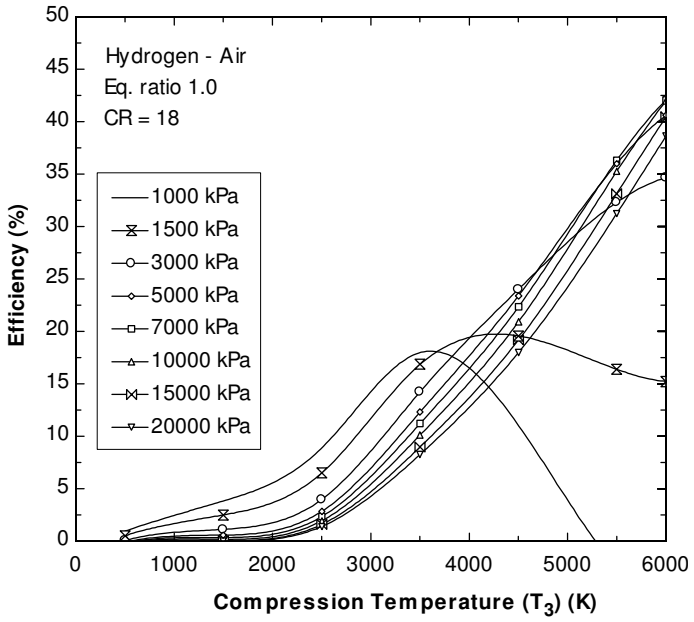

Fig. 129. Percentage efficiency as a function of compression temperature, for a range of compression pressures, for hydrogen-air, Φ = 1.0 and CR = 18.

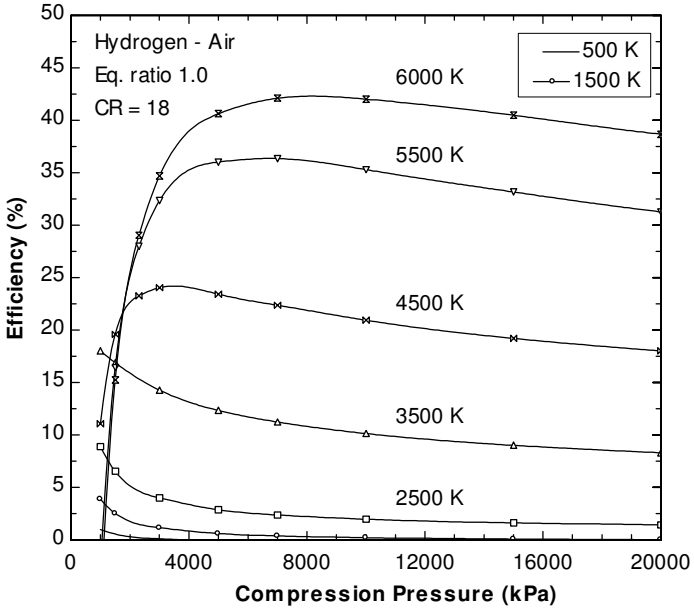

Fig. 130. Percentage efficiency as a function of compression pressure, for a range of compression temperatures, for hydrogen-air, Φ = 1.0 and CR = 18.

Effects of equivalence ratio and compression temperature

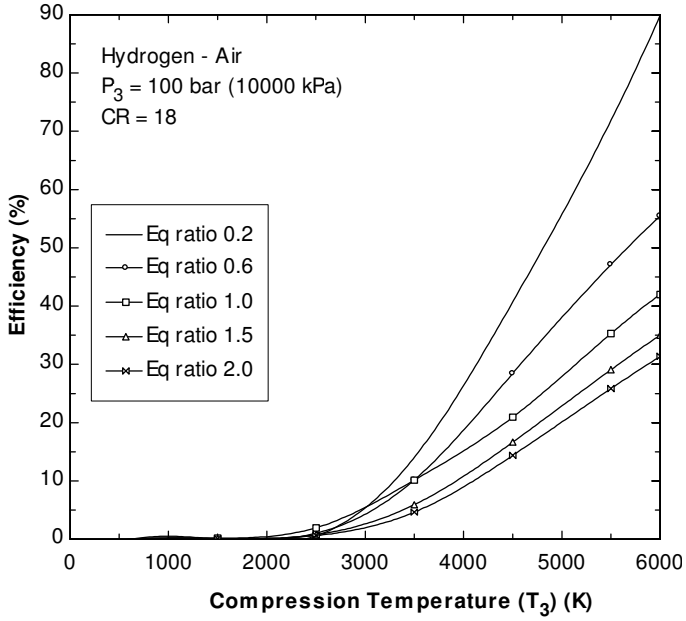

Fig. 131. Percentage efficiency as a function of compression temperature, for a range of equivalence ratios, for hydrogen-air, 10000 kPa compression pressure and CR = 18.

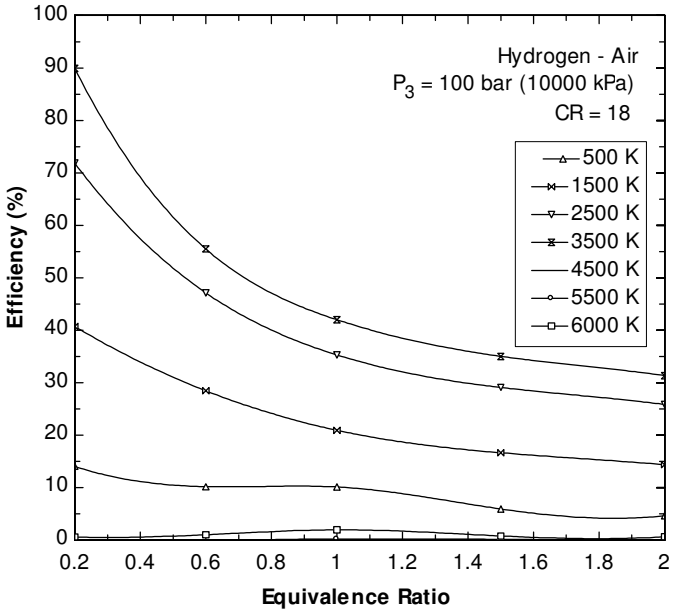

Fig. 132. Percentage efficiency as a function of equivalence ratio, for a range of compression temperatures, for hydrogen-air, 10000 kPa compression pressure and CR = 18.

Effects of compression ratio and compression temperature

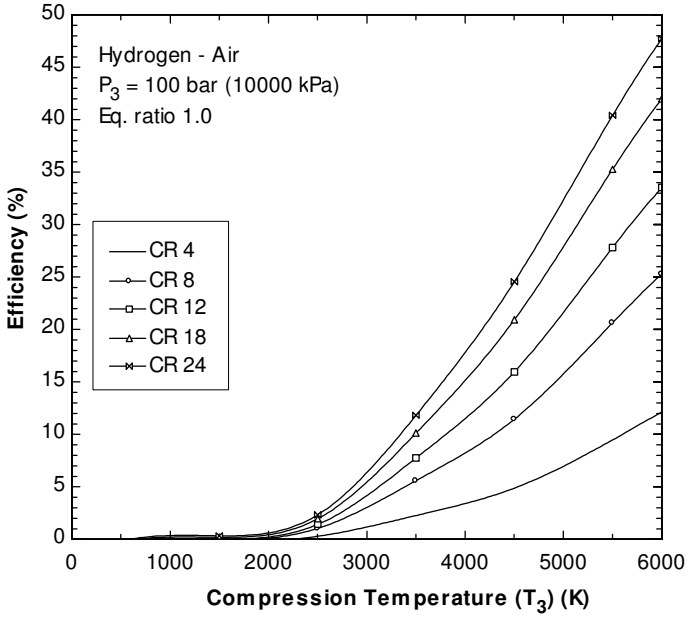

Fig. 133. Percentage efficiency as a function of compression temperature, for a range of compression ratios, for hydrogen-air, 10000 kPa compression pressure and Φ = 1.0.

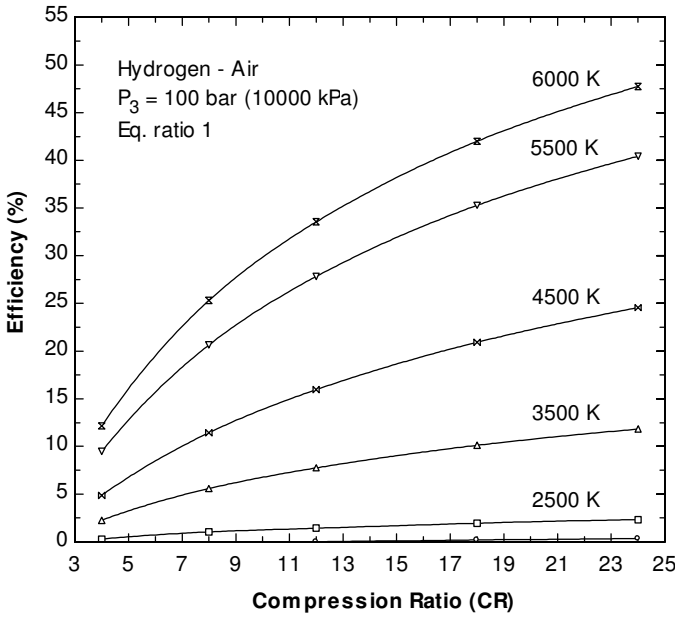

Fig. 134. Percentage efficiency as a function of compression ratio, for a range of compression temperatures, for hydrogen-air, 10000 kPa compression pressure and Φ = 1.0.

For Acetylene

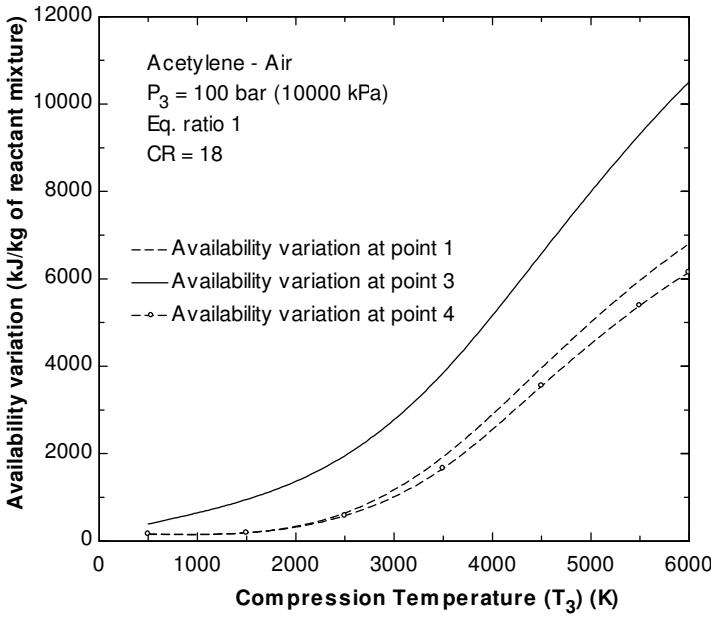

Fig. 135. Availabilities as a function of compression temperature for acetylene-air at 10000 kPa compression pressure, Φ = 1.0 and CR = 18.

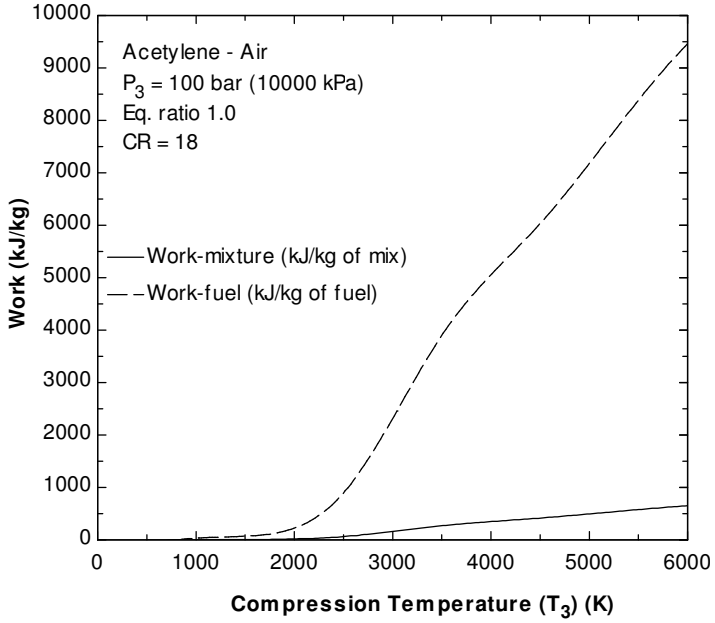

Fig. 136. Work as a function of compression temperature for acetylene-air at 10000 kPa compression pressure, Φ = 1.0 and CR = 18.

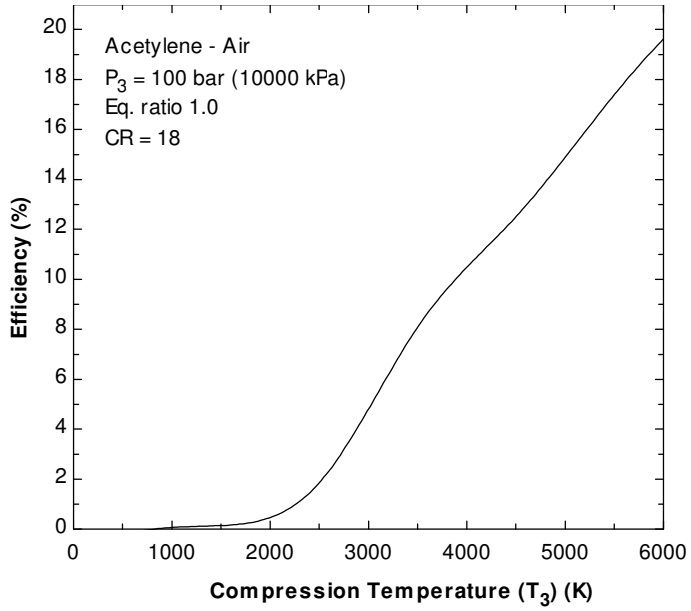

Fig. 137. Percentage efficiency as a function of compression temperature for acetylene-air at 10000 kPa compression pressure, Φ = 1.0 and CR = 18.

For Methane

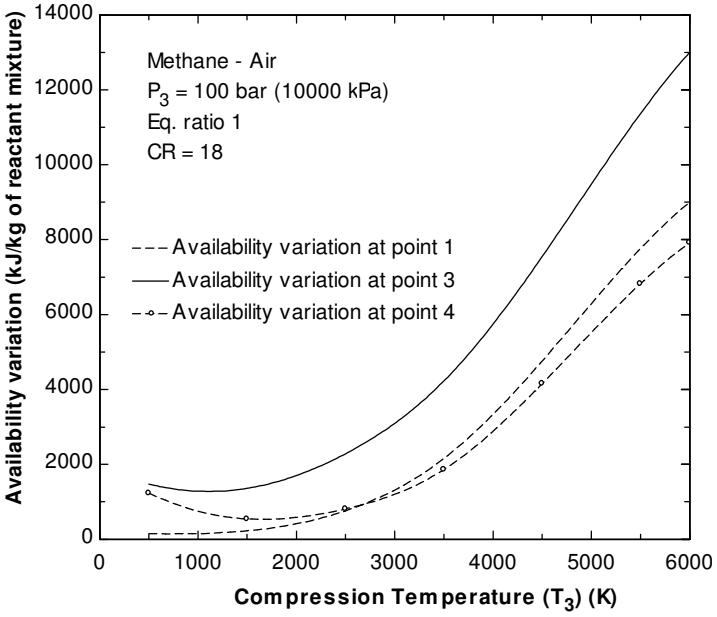

Fig. 138. Availabilities as a function of compression temperature for methane-air at 10000 kPa compression pressure, Φ = 1.0 and CR = 18.

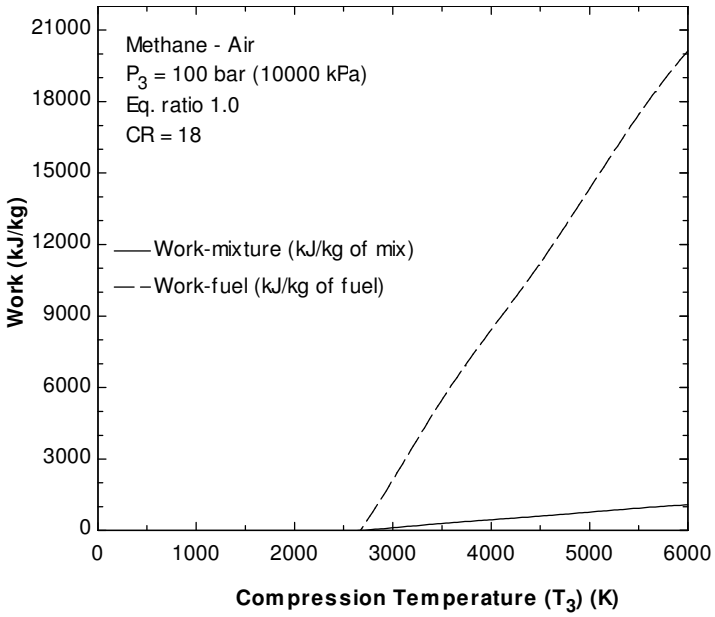

Fig. 139. Work as a function of compression temperature for methane-air at 10000 kPa compression pressure, Φ = 1.0 and CR = 18.

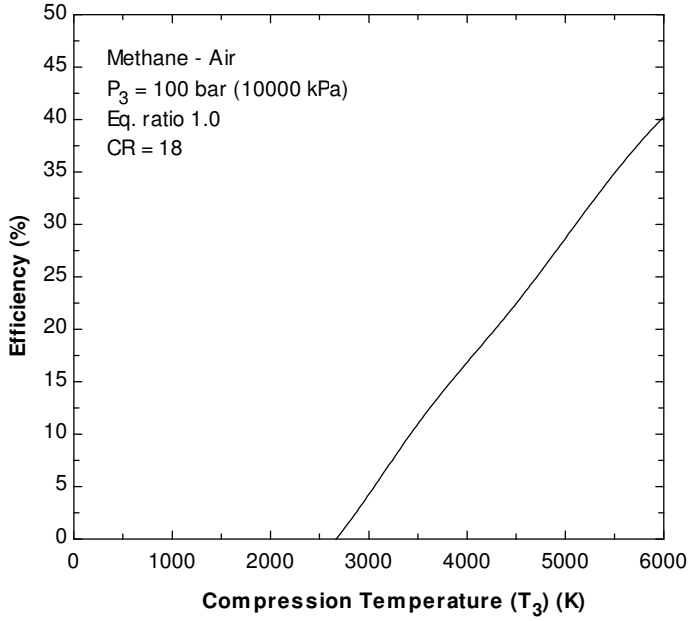

Fig. 140. Percentage efficiency as a function of compression temperature for methane-air at 10000 kPa compression pressure, Φ = 1.0 and CR = 18.

For Propane

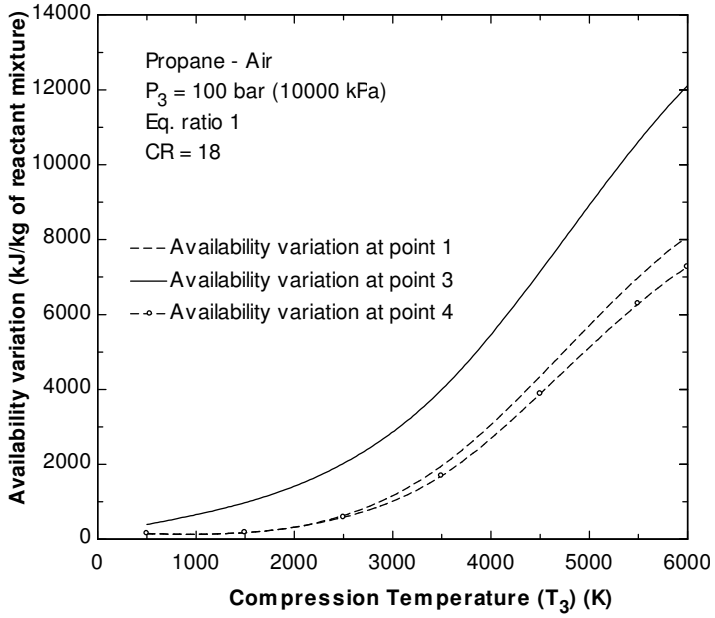

Fig. 141. Availabilities as a function of compression temperature for propane-air at 10000 kPa compression pressure, Φ = 1.0 and CR = 18.

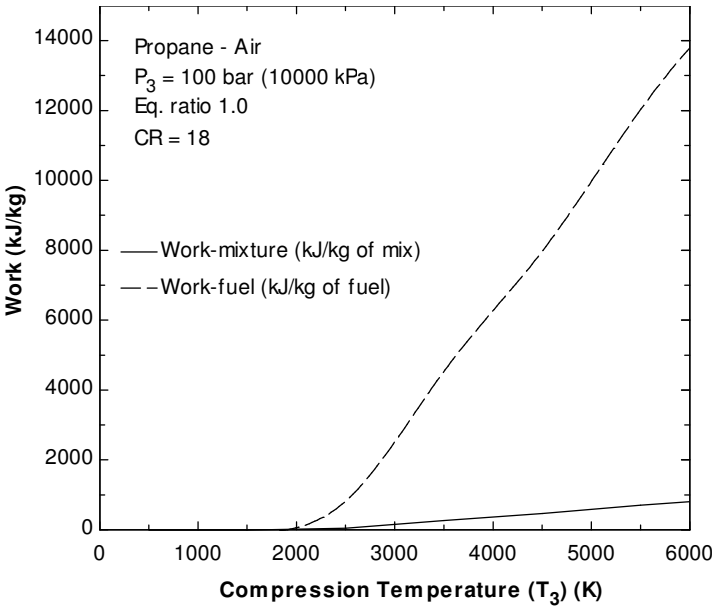

Fig. 142. Work as a function of compression temperature for propane-air at 10000 kPa compression pressure, Φ = 1.0 and CR = 18.

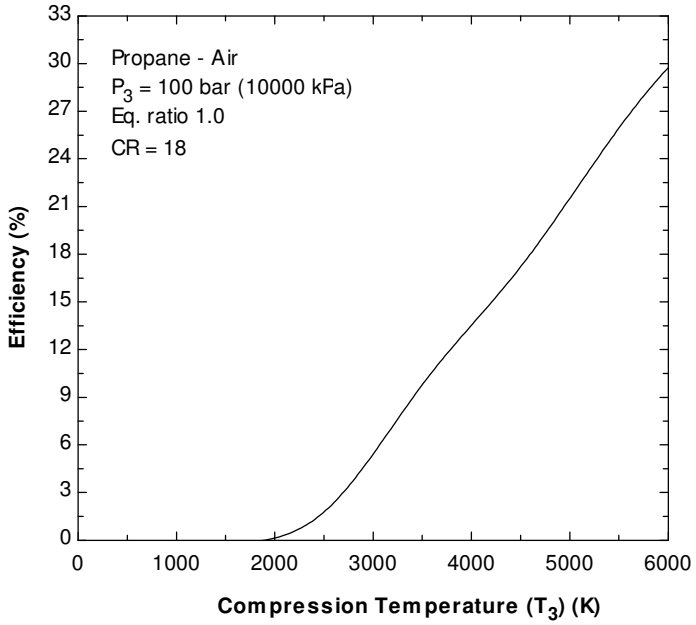

Fig. 143. Percentage efficiency as a function of compression temperature for propane-air at 10000 kPa compression pressure, Φ = 1.0 and CR = 18.

For Methanol

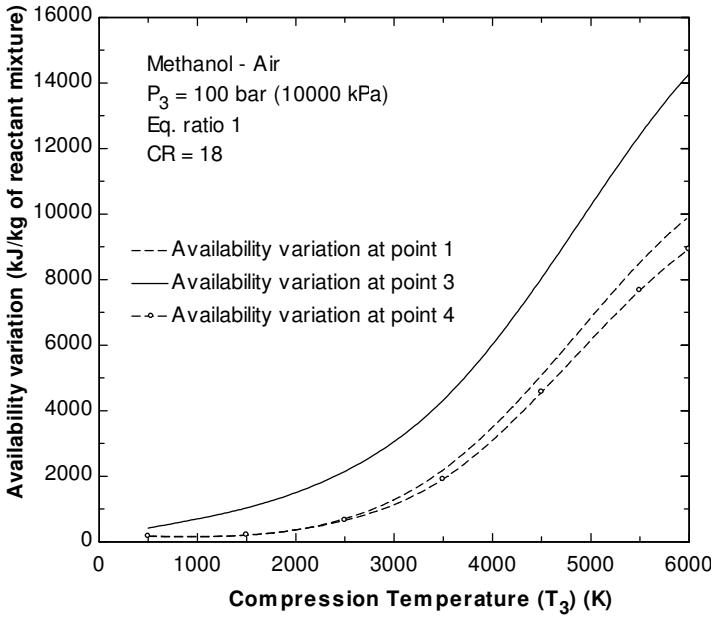

Fig. 144. Availabilities as a function of compression temperature for methanol-air at 10000 kPa compression pressure, Φ = 1.0 and CR = 18.

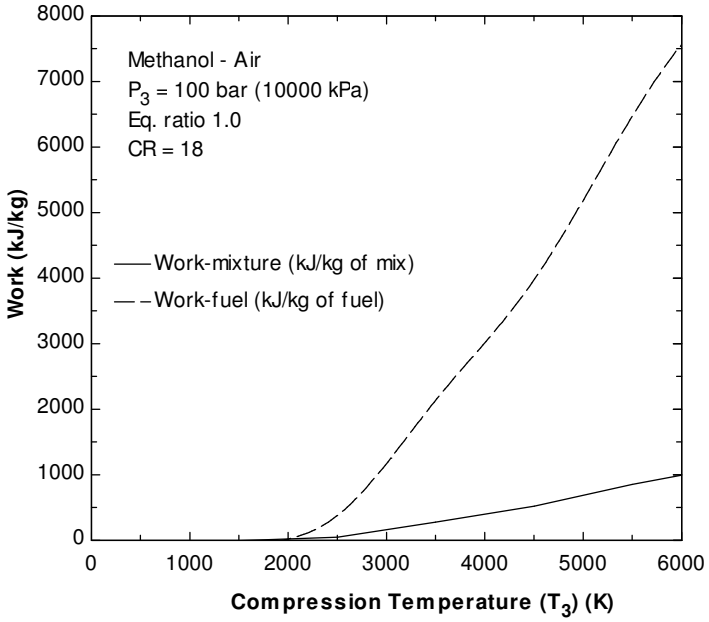

Fig. 145. Work as a function of compression temperature for methanol-air at 10000 kPa compression pressure, Φ = 1.0 and CR = 18.

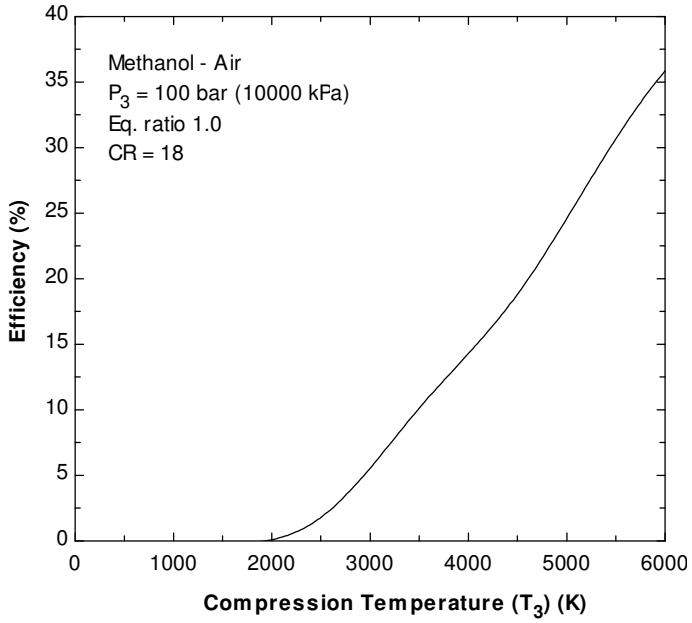

Fig. 146. Percentage efficiency as a function of compression temperature for methanol-air at 10000 kPa compression pressure, Φ = 1.0 and CR = 18.

For Ethanol

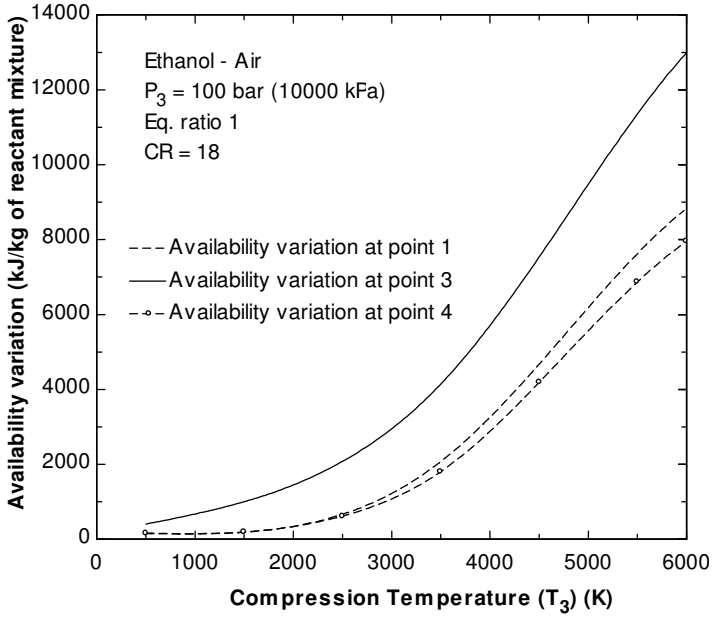

Fig. 147. Availabilities as a function of compression temperature for ethanol-air at 10000 kPa compression pressure, Φ = 1.0 and CR = 18.

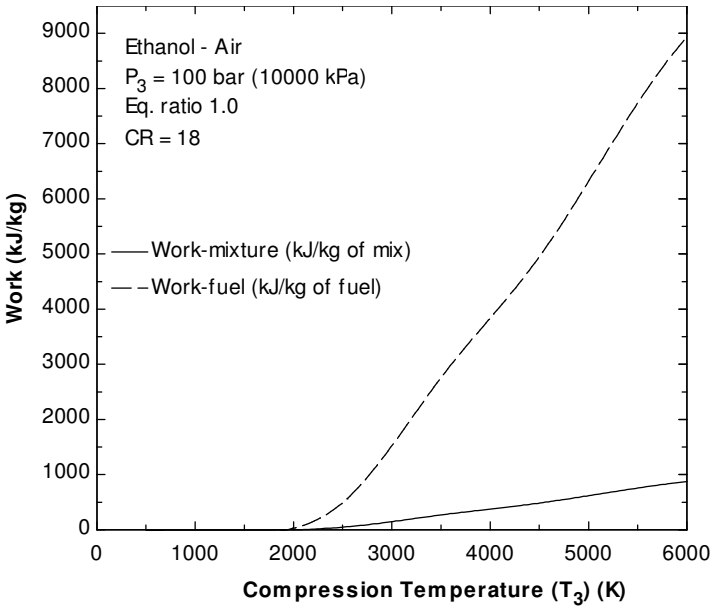

Fig. 148. Work as a function of compression temperature for ethanol-air at 10000 kPa compression pressure, Φ = 1.0 and CR = 18.

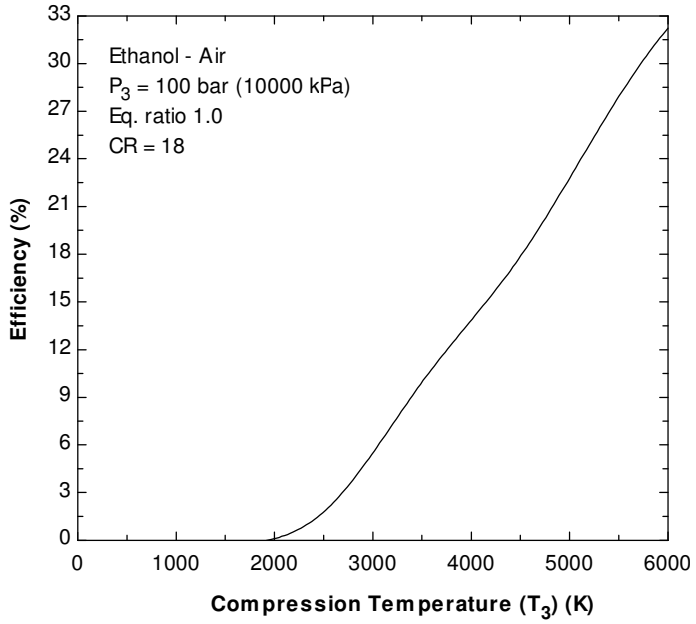

Fig. 149. Percentage efficiency as a function of compression temperature for ethanol-air at 10000 kPa compression pressure, Φ = 1.0 and CR = 18.

For Benzene

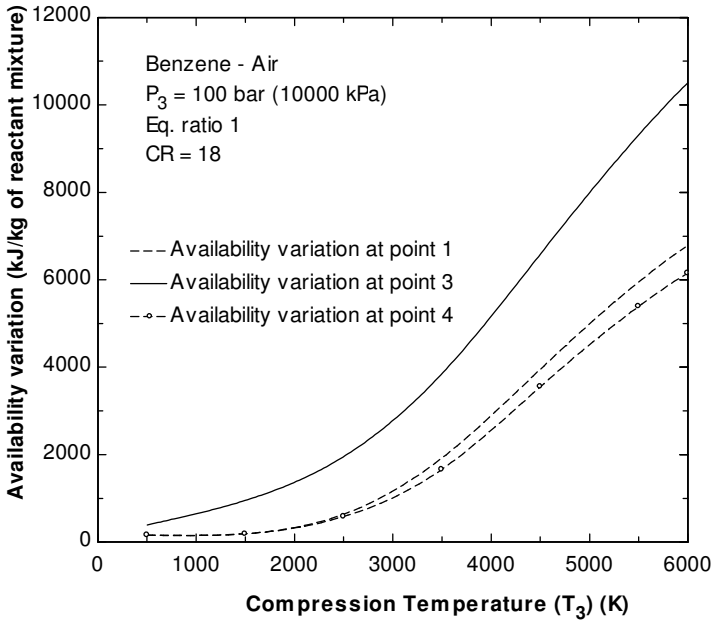

Fig. 150. Availabilities as a function of compression temperature for benzene-air at 10000 kPa compression pressure, Φ = 1.0 and CR = 18.

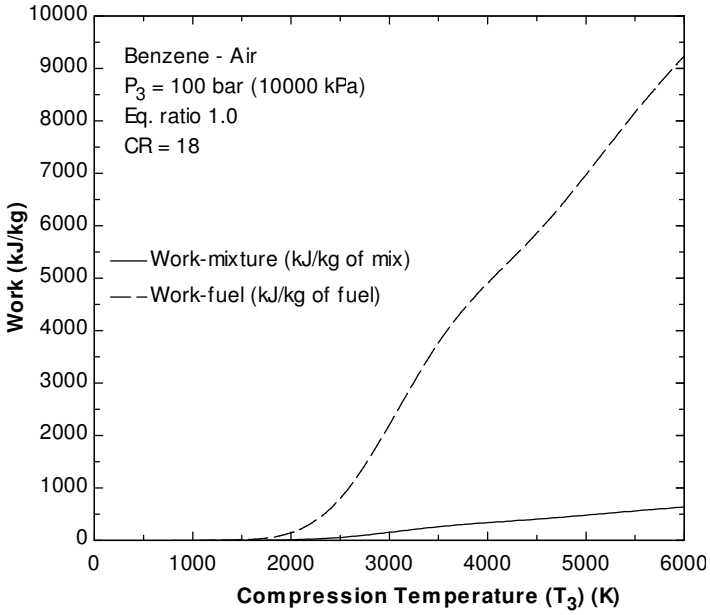

Fig. 151. Work as a function of compression temperature for ethanol-air at 10000 kPa compression pressure, Φ = 1.0 and CR = 18.

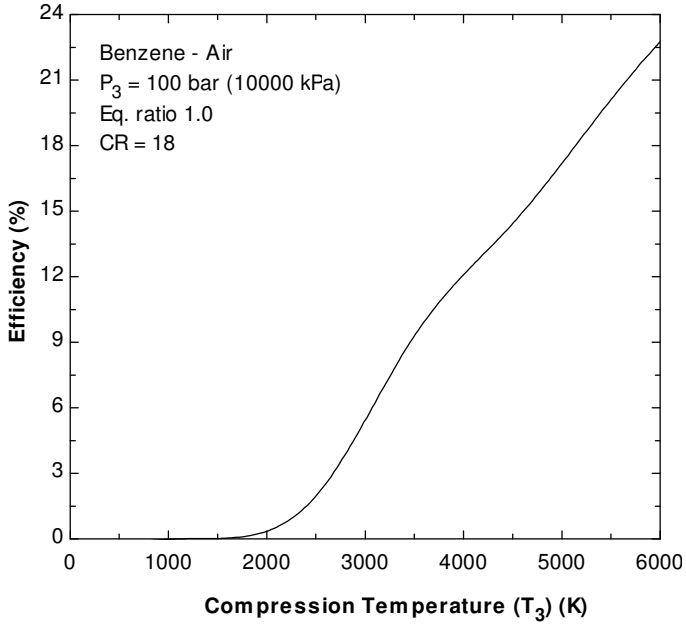

Fig. 152. Percentage efficiency as a function of compression temperature for benzene-air at 10000 kPa compression pressure, Φ = 1.0 and CR = 18.

APPENDIX VI

Detailed description of one case (Compression temperature = 6000 K)

This section provides detailed results of one case. This case is the one that was discussed earlier in the Results and Discussion section, under the subheading Base case study – part II, i.e., for Isooctane-air, a compression temperature of 6000 K, a compression pressure of 10000 KPa, an equivalence ratio of 1.0 and a compression ratio of 18. As shown earlier, fig. 153 shows the variation of the pressure as a function of relative volume for these conditions.

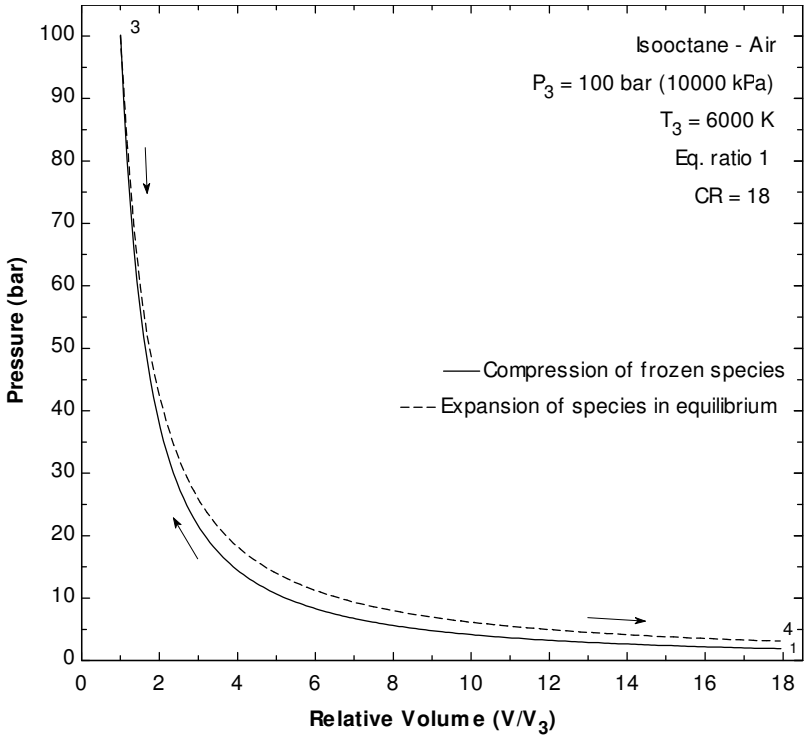

Fig. 153. Pressure as a function of relative volume for isooctane-air at 6000 K compression temperature, 10000 kPa compression pressure, Φ = 1.0 and CR = 18.

Process 1-3 is the isentropic compression of frozen species and process 3-4 is the isentropic expansion of the species in equilibrium. Conventionally, an isentropic process is represented by means of an equation in the form of,

$$PV^{k} = constant \quad \text{(A-1)}$$

where, k is the average ratio of specific heats. For the conditions stated in fig. 153, the equation for the processes 1-3 and 3-4 are,

$$PV^{1.3675} = 10000 \text{ (for process 1-3)} \quad \text{(A-2)}$$

$$PV^{1.1895} = 10000 \text{ (for process 3-4)} \quad \text{(A-3)}$$

where P is in kPa and V is in m^3.

It should be noted that process 1-3 in fig. 153 shows the combined P-V relation during compression of various species. Since the species are compressed in different cylinders, this figure may not be the appropriate way of representing the compression process physically. However, this way of presentation allows the reader to better understand the overall picture of pressure-volume variations. The figure also allows the reader to approximate the net work produced at a glance (as the net work produced is proportional to the area between the compression and expansion curves).

The pressures of the species in the different cylinders as a function of relative volume are shown in fig. 154.

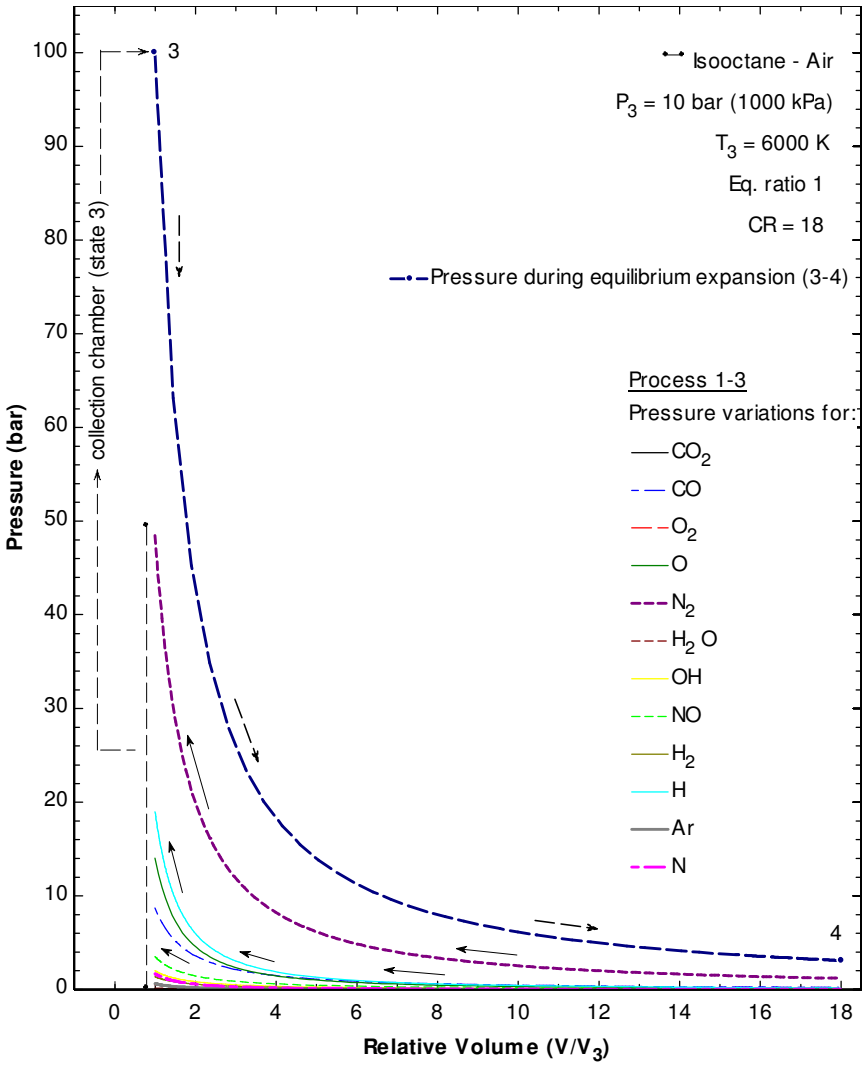

Fig. 154. Pressures during compression and expansion as a function of relative volume for isooctane-air at 6000 K compression temperature, 10000 kPa compression pressure, Φ = 1.0 and CR = 18.

In fig. 154, the individual species that are introduced in different compression cylinders. At the end of compression, the frozen species are collected in the collection chamber where state 3 is achieved. This is followed by expansion of the species (in equilibrium) from state 3 to 4.

Fig. 155 shows the temperature of the species in the different compression cylinders and in the expansion cylinder as a function of relative volume.

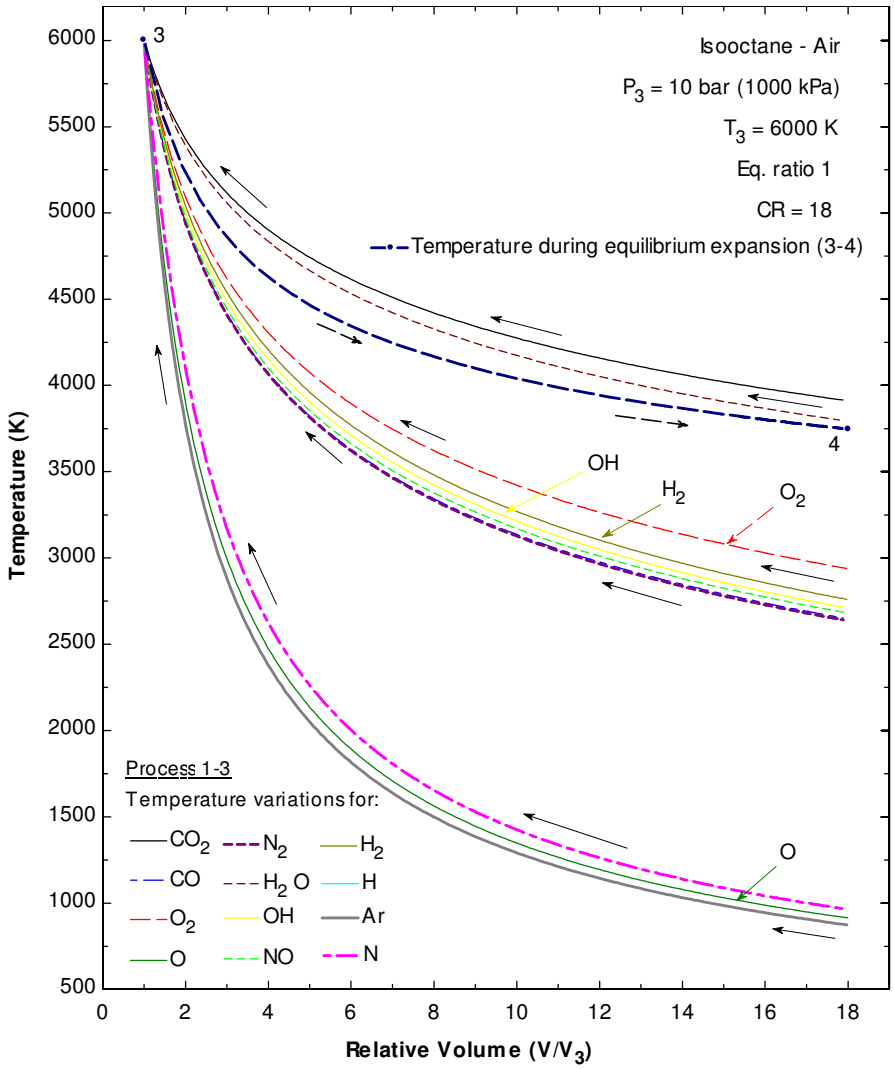

Fig. 155. Temperatures during compression and expansion as a function of relative volume for isooctane-air at 6000 K compression temperature, 10000 kPa compression pressure, Φ = 1.0 and CR = 18.

Due to compression of the frozen species, temperature of each specie increases. At the end of compression, the temperature of all the species is 6000 K which is the preselected compression temperature for this case. As a result, the temperatures of the different species entering the collection chamber is also the same (6000 K), which further allows the species to stay in the equilibrium condition at state 3 without any thermal energy exchange between the species. The species at state 3 are then expanded to state 4 which is shown by a dashed curve (3-4) in fig. 155.

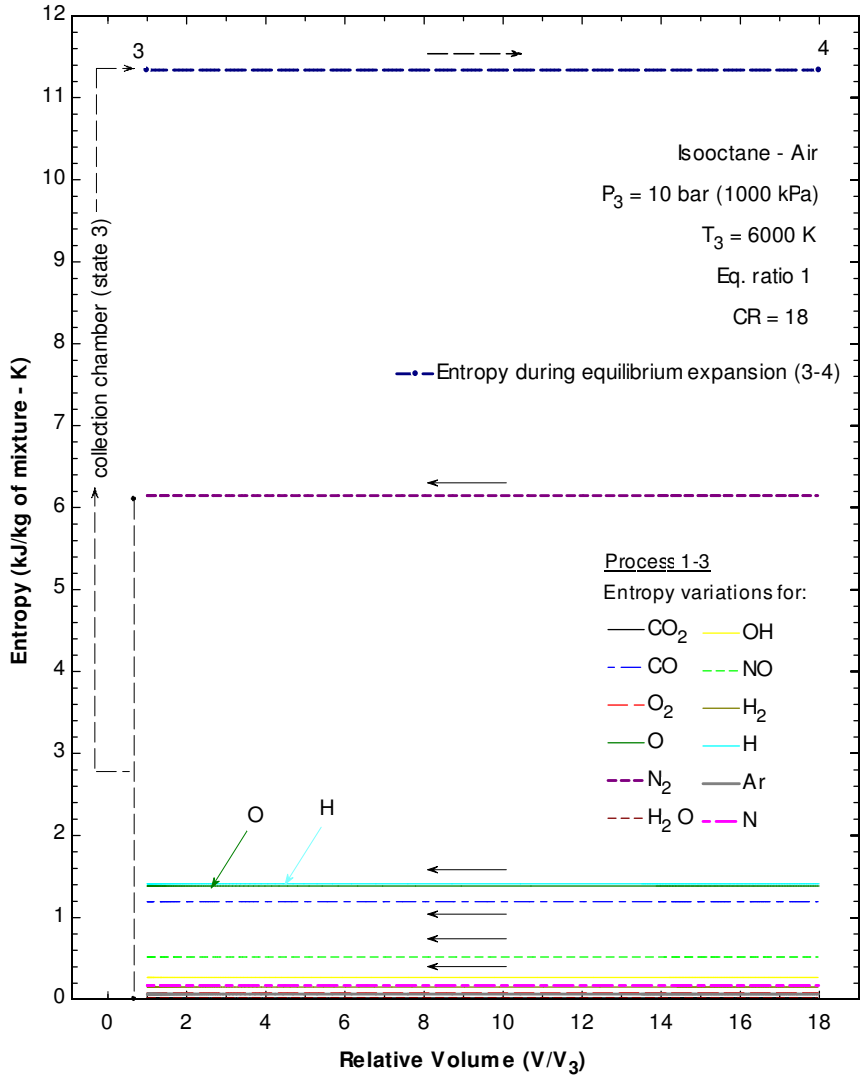

Fig. 156. Entropy during compression and expansion as a function of relative volume for isooctane-air at 6000 K compression temperature, 10000 kPa compression pressure, Φ = 1.0 and CR = 18.

Fig. 156 shows the variation of entropy of the species in the different compression cylinders as a function of the relative volume. The entropy of each of the species remains constant during the individual compression of the species. At the end of compression, when the species are collected in the collection chamber, the total entropy of the species is the same as that at state 3. Again, during the expansion of species in equilibrium, the entropy of the "reactant" mixture remains the same.

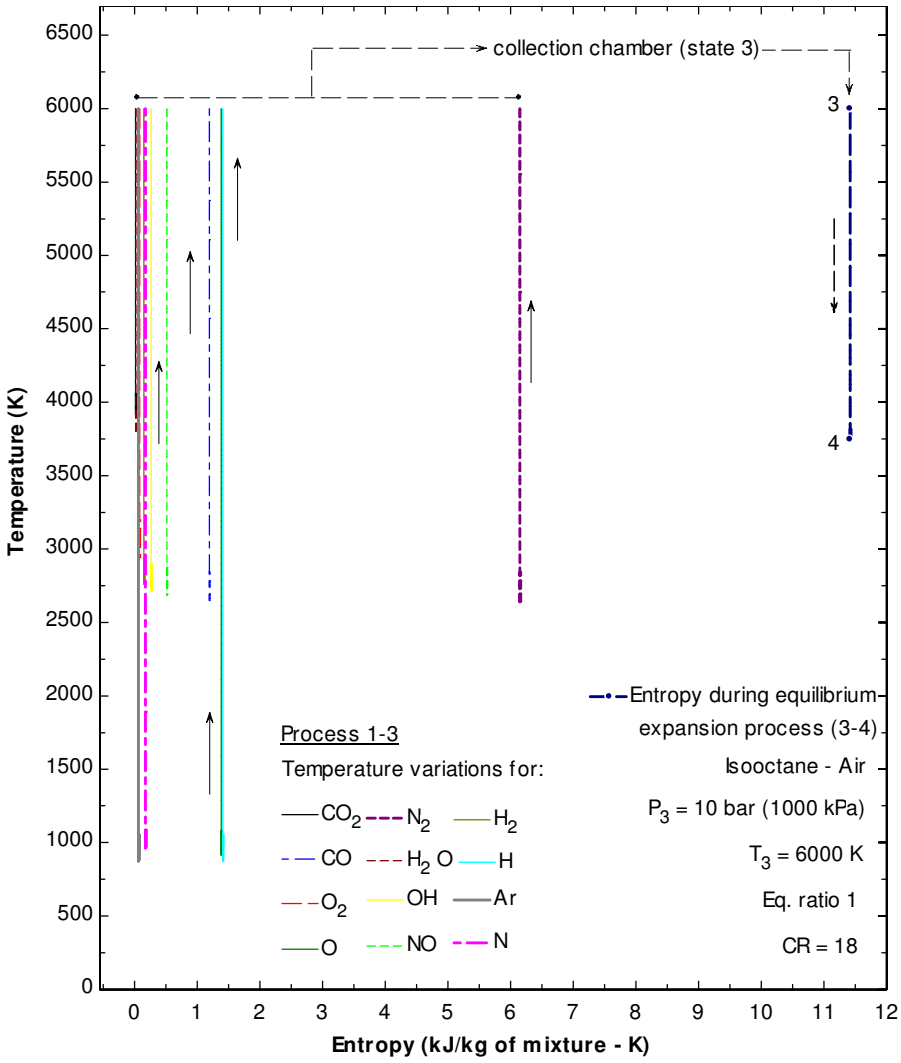

Fig. 157. Temperatures during compression and expansion as a function of entropy for isooctane-air at 6000 K compression temperature, 10000 kPa compression pressure, Φ = 1.0 and CR = 18.

Fig. 157 shows the temperature as a function of entropy for the frozen species during compression and for species in equilibrium during expansion. Consistent with the earlier discussion, the entropy of each of the species remain constant during compression. At the end of compression, the total entropy is same as that at state 3 of the equilibrium composition and the temperature of all the species is 6000 K. The reactant mixture is then expanded in equilibrium, at constant entropy, till the compression ratio of 18 is reached.

The Question of Closing the Cycle

The species enter the system at state 1 and leave the system at point 4. In order to close the cycle, the species at state 4 are to be brought to state 1. The species at state 4 are in equilibrium while at state 1, they are in the dissociated form. To bring the species from the equilibrium state (4) to the dissociated state (1), the species needs to be dissociated to the exact composition that is at state 1 and also the species are to be brought to the correct temperatures and pressures of the individual species of state 1. This can be achieved by first isentropically compressing the species to high temperatures and pressure as that of state 3, to achieve the required dissociation, and then cooling the species through isentropic expansion to reach the conditions as that of state 1. But following these processes is essentially conducting the earlier processes 1-3 and 3-4 in a reverse pattern. Although these processes will bring the system to the initial state 1, the net work will be zero (and the thermal efficiency will be zero).

VITA

Name Kaushik Tanvir Patrawala

Address 203 Nataraj Bldg, Vile Parle (West), Mumbai 400056, India

Education Master of Science, Mechanical Engineering, May 2007
Texas A&M University, College Station, Texas

Bachelor of Engineering, Mechanical Engineering, June 2005
University of Bombay (Mumbai), India

Diploma in Mechanical Engineering, June 2002
Shri Bhagubhai Mafatlal Polyte., Mumbai, India

Experience Graduate Research Assistant (June 2006 – May 2007)
Dept. of Mechanical Engineering, Texas A&M University, College Station, Texas
Examined a reversible combustion concept for reciprocating engine and provided quantified data

Floor Manager (May 2005 – August 2005)
Falls Industries In-Corporation, Mumbai, Maharashtra
Designed specialized fixture for drilling of baffles, developed innovative tube cutting set-up, managed shop floor employees for efficient work flow

Intern (December 2001 – May 2002)
Project Management Group, Larsen & Toubro, Mumbai, Maharashtra
Developed automatic lapping fixture, worked on helixchanger design-analysis and coordinated various activities for base ring templates project

Intern (December 2000 – June 2001)
Quality Control, Larsen & Toubro, Mumbai, Maharashtra
Improved products aesthetic and developed new packing concept to prevent its transit damage, implemented six sigma in product's inspection procedure